ABSTRACT

Title of Dissertation: THE POPULATION BIOLOGY AND ECOSYSTEM EFFECTS OF THE SEA NETTLE, *CHRYSAORA CHESAPEAKEI*

Jacqueline Tay, Doctor of Philosophy, 2020

Dissertation directed by: Professor, Dr. Raleigh Hood
Marine, Estuarine, and Environmental Science

Some of the longest population records of jellyfish are collected from visual shore-based surveys. As surface counting is inexpensive and simple, it is of interest to determine what can be learned from such records as well as the usefulness of the method. A 4-year time series of *Chrysaora chesapeakei* (formerly *quinquecirrha*) medusa counts collected using three sampling methods was analyzed. Medusa abundance was modeled by change points and was highly correlated between the sampling methods. The remaining signal was random, and indices indicated that medusae were aggregated. This study suggests more monitoring from visual shore-based surveys is an effective, low-cost method to increase information on jellyfish.

Data from another long-term visual survey show that *C. chesapeakei* in the Cheasapeake Bay have declined since the 1960s. It is hypothesized that their loss results in a trophic cascade and increases in phytoplankton. However, due to confounding factors, it is not clear that *C. chesapeakei* drives the changes observed. A new 0-dimensional mechanistic model was formulated to include jellyfish. A data assimilation method, Approximate Bayesian Computation, was used to objectively calibrate the model and guide its development. The model fit to observations was improved by the addition of refractory non-living organic materials. Additionally, comments and suggestions related to the model development process are provided.

Using the model, perturbation experiments were conducted to study the effect of changing modeled *C. chesapeakei* (CHRY). Then, sensitivity experiments of the environmental and ecological parameters were conducted to understand the conditions that are important in driving the response. The change in CHRY had the potential to affect every state variable and throughflow but the response did not always conform to the trophic cascade concept and was highly dependent on the parameters. The parameters that were most important in varying the response were related to the energetics of the zooplankton and parameters related to alternative pathways of loss or gains of the state variables. The resulting complexity highlights the far-reaching ecosystem effects of *C. chesapeakei* as well as the need for new frameworks to understand the response of ecosystems to perturbations.

THE POPULATION BIOLOGY AND ECOSYSTEM EFFECTS OF THE SEA NETTLE, *CHRYSAORA CHESAPEAKEI*

by

Jacqueline Tay

Dissertation submitted to the Faculty of the Graduate School of the
University of Maryland, College Park, in partial fulfillment
of the requirements for the degree of
Doctor of Philosophy
2020

Advisory Committee:
Professor Raleigh Hood, Chair
Professor Hongsheng Bi
Professor Victoria Coles
Professor Elizabeth North
Professor James Pierson
Professor Karen Prestegaard, Dean's Representative

Dedication

To Anton, Rebecca, and Gypsy

Acknowledgements

Thank you to Raleigh Hood for giving me the time and the creative space to pursue ideas, while providing constancy and encouragement. Working with Raleigh has provided me with a much better understanding of and approach to a very inspired and happy process of science - which includes remembering to prioritize and to not get derailed by uncertainty. And thank you to all my committee members for their support, patience, and enthusiasm: Elizabeth North for mentorship and providing me with the Scientific Writing TA, which was hugely rewarding and contributed to my development as a writer and teacher; Victoria Coles for the enjoyable scientific (and other) discussions and willingness to help me while I was in the weeds; Hongsheng Bi for excellent guidance in working with messy data in R; and Jamie Pierson for the wonderful opportunity to get on a ship and see real zooplankton.

I want to acknowledge the HPL Education committee for granting me the Horn Point Graduate Fellowship, Teaching Assistantships, and the Bay and Rivers bridge funds.

I also appreciate Anton de la Fuente and Rebecca Tay for their financial support during my PhD. Not to mention, the hours of discussion and amount of care they have provided was invaluable.

Lastly, I owe a great deal of gratitude to people that have helped me specifically through the last year of my PhD: Linda Macri, Cara Snyder, and the Dissertation Success Support Group at the University of Maryland Graduate Writing Center, Tony Huynh, Rachel Wong, Jodie Wong, Stacey Wong, Jennifer Jew, Kate Frei, Charlotte Choi, and Emily Silverman. As well as to people who helped me find my way into graduate school through fostering my interest in science and providing me with many educational opportunities: Jared Young, Lisa Urry, Barbara Bowman, Valerie and Kevin Tay, and Laura Jew.

Table of Contents

List of Tables

List of Figures

Chapter 1: Introduction

Due to flexible, annual life histories, gelatinous zooplankton (also referred to as "jellyfish" herein) populations readily fluctuate in response to climate oscillations (Attrill et al., 2007; Purcell & Decker, 2005), and likewise, to human disturbance. Anthropogenic impacts such as climate change, eutrophication, development, and overfishing tend to favor jellyfish (Purcell et al. 2007, Purcell 2012), leading to the hypothesis that jellyfish have and will continue to increase globally. Due to a lack of long-term monitoring for jellyfish populations worldwide, the answer is thus far inconclusive (Brotz et al., 2012; Condon et al., 2012; Condon et al., 2012). Undoubtedly, there are regions where populations are increasing such as in the East China Sea (Brotz et al., 2012; Dong et al., 2010), likely due to human impacts. Conversely, there are species that are declining, such as the sea nettle, *Chrysaora chesapeakei* (formerly *Chrysaora quinquecirrha*), in the Chesapeake Bay. Their populations have declined since the 1960s, possibly due to overfishing of oysters that reduces the habitat available for the sea nettle's overwintering benthic polyp (Breitberg & Fulford, 2006).

Generally, long-term data on jellyfish populations are lacking in part due to difficulties sampling with net tows (Haddock, 2004) and as a result, some of the longest records of jellyfish are from visual shore-based surveys (Purcell, 2009). One example is the time series of *C. chesapeakei* from the Chesapeake Biological Laboratory pier that started in 1960 in the Patuxent River, a tributary of the Chesapeake Bay (Cargo & King, 1990). This time series has been used to assess

inter-annual variability (Cargo & King, 1990) and long-term change (Breitburg & Fulford, 2006) of *C. chesapeakei* abundance and has also been included in analyses of global jellyfish populations (Brotz et al., 2012; Condon et al., 2012). However, there is a great deal of unexplained high-frequency variability captured in these time series (Decker et al., 2007; Sexton 2012). Because shore-based surveys have been widely used and are the most practical, cost efficient method to collect information on jellyfish, it is of interest to fully understand the information captured by surface counting at a fixed-station. Chapter 1 addresses this problem by using time series analysis to describe the signals of abundance and patchiness that contribute to the patterns in a fixed-station time series and the suitability of surface counts in estimating water column abundance.

In part due to striking changes in jellyfish populations, there has been growing interest in jellyfish, especially considering that they may impart strong control over marine plankton dynamics (Richardson et al., 2009; Robinson et al., 2014). As highly efficient feeders, jellyfish can substantially impact their prey populations by direct predation. Jellyfish anatomy is highly adapted for efficient feeding. Jellyfish are non-visual predators that capture prey by direct contact (using nematocycts or colloblasts in cnidarians and ctenophores, respectively), enabling them to feed in dark or turbid environments. Due to their high water content, jellyfish can grow very quickly, allowing them to capture more food with their large bodies (Acuna et al., 2011). Additionally, jellyfish feeding tends not to saturate at high food

concentrations and thus they will continually consume more at higher prey densities (Purcell & Arai, 2001).

In Chesapeake Bay, both sea nettles and ctenophores can consume high amounts of mesozooplankton and fish eggs and larvae, clearing 13-94% of the copepod standing stocks per day (Purcell, 1997) and 7-32 % and 4-38% of the fish egg and larvae population per day, respectively (Purcell et al., 1994; Purcell, 1997). In the Chesapeake Bay, sea nettles are largely thought to be top predators and also consume ctenophores and can eliminate them within the tributaries (Purcell & Cowan, 1995). Unlike the sea nettle, ctenophores consume oyster larvae and microzooplankton as well (Purcell et al., 1991; Sullivan & Gifford, 2004). These direct pairwise predatory relationships are relatively easy to quantify in feeding experiments, however, indirect effects, or those that emerge in multispecies assemblages are more difficult to study (Wootton, 1994; Wootton, 2002).

Observations suggest that one indirect effect of the decline in sea nettles is a trophic cascade that results in an undesirable ecosystem with low mesozooplankton and high phytoplankton biomass (Feigenbaum & Kelly, 1984; Kimmel et al., 2012; Purcell & Decker, 2005; Testa et al., 2008). Since the decrease in sea nettles in the 1960s, the summertime abundance of the ctenophore has increased (Breitberg & Fulford, 2006) and the dominant crustacean mesozooplankton, *Acartia tonsa*, has declined (Kimmel et al., 2012; Testa et al., 2008), presumably due to increased predation. Indeed, the combined clearance of copepods by gelatinous predators is higher in years with low

sea nettle abundance (Purcell & Decker, 2005). Additionally, the trophic cascade may also reach the level of phytoplankton as long-term monitoring has shown that chlorophyll a has increased over the concomitant time period, despite the reduction of inorganic nutrients (Testa et al., 2008). However, as these are correlations, it is not clear whether declines in the sea nettle are the actual cause of these changes in the lower food web.

Trophic cascades, like all indirect effects, are complex to study (Terbough & Estes, 2010; Wootton, 1994; Wootton, 2002) and difficult to assess solely through experiment or observation. Mechanistic models are an ideal tool to look at the system holistically in order to manipulate components in isolation to establish causal linkages. However, there are no governing equations for ecological systems and the choice of the structure and equations can be rather subjective (as mentioned by Anderson et al., 2015; Fennel & Neumann, 2004; Jopp et al., 2011). The structural complexity of process-based aquatic ecosystem models (also called biogeochemical or nutrient-phytoplankton-zooplankton (NPZ) models) may include between 2 to 90 state variables (Arhonditsis & Brett, 2004) and various combinations of linkages between variables. The functional form of the linkages of the main NPZ processes may be formulated using between 5 to 20 commonly used equations (Tian, 2006).

Once an ecosystem model is formulated, a large number of parameters, which commonly represent process rates, must be assigned values. These parameters are often largely unconstrained (Schartau et al., 2017) due to the difficulty in directly measuring these processes or the differing scales between models and experiments or measurements. In order to specify parameter values, models are most commonly calibrated manually (91.5% of models reviewed in Arhonditsis & Brett, 2004) by changing the parameters values (often one-at-a-time) until the model output reasonably matches the observational data. The problem with manual tuning is that this method does not search the parameter space extensively and is subjective, relying on the modeler's intuition and expertise, and thus doesn't ensure that the resulting parameter value set is optimal.

To ensure that a model is adequate to address ecological problems, it is desirable to objectively calibrate models, which may also reveal problems with the model formulation (Kennedy & O'Hagan, 2001; Spitz et al., 2001; Vallino, 2000). Chapter 2 develops a new model to include jellyfish and uses a Bayesian data assimilation method to enhance objectivity in the calibration stage. With the model developed in Chapter 2, Chapter 3 explores the question of trophic cascades and ecosystem effects imparted by changes in sea nettle populations in the Chesapeake Bay.

References

Acuna, J. L., A. Lopez-Urrutia & S. Colin, 2011. Faking giants: The evolution of high prey clearance rates in jellyfishes. Science 333: 1627–1629.

Anderson, T. R., W. C. Gentleman & A. Yool, 2015. EMPOWER-1.0: an Efficient Model of Planktonic ecOsystems WrittEn in R. Geoscientific Model Development 8: 2231–2262.

Arhonditsis, G. B. & M. T. Brett, 2004. Evaluation of the current state of mechanistic aquatic biogeochemical modeling. Marine Ecology Progress Series 271: 13–26.

Attrill, M. J., J. Wright & M. Edwards, 2007. Climate-related increases in jellyfish frequency suggest a more gelatinous future for the North Sea. Limnology and Oceanography 52: 480–485.

Breitburg, D. L. & R. S. Fulford, 2006. Oyster-sea nettle interdependence and altered control within the Chesapeake Bay ecosystem. Estuaries and Coasts 29: 776–784.

Brotz, L., W. W. L. Cheung, K. Kleisner, E. Pakhomov & D. Pauly, 2012. Increasing jellyfish populations: Trends in large marine ecosystems. Hydrobiologia 690: 1–18.

Cargo, D. G. & D. R. King, 1990. Forecasting the abundance of the sea nettle, *Chrysaora quinquecirrha*, in the Chesapeake Bay. Estuaries 13: 486–491.

Condon, R. H., C. M. Duarte, K. A. Pitt, K. L. Robinson, C. H. Lucas, K. R. Sutherland, H. W. Mianzan, M. Bogeberg, J. E. Purcell, M. B. Decker, S. Uye, L. P. Madin, R. D. Brodeur, S. H. D. Haddock, A. Malej, G. D. Parry, E. Eriksen, J. Quinones, M. Acha, M. Harvey, J. M. Arthur & W. M. Graham, 2012a. Recurrent jellyfish blooms are a consequence of global oscillations. Proceedings of the National Academy of Sciences 110: 1000–1005.

Condon, R. H., W. M. Graham, C. M. Duarte, K. A. Pitt, C. H. Lucas, S. H. D. Haddock, K. R. Sutherland, K. L. Robinson, M. N. Dawson, M. B. Decker, C. E. Mills, J. E. Purcell, A. Malej, H. Mianzan, S. Uye, S. Gelcich & L. P. Madin, 2012b. Questioning the rise of gelatinous zooplankton in the world's oceans. BioScience 62: 160–169.

Decker, M. B., C. W. Brown, R. R. Hood, J. E. Purcell, T. F. Gross, J. C. Matanoski, R. O. Bannon & E. M. Setzler-Hamilton, 2007. Predicting the distribution of

the scyphomedusa *Chrysaora quinquecirrha* in Chesapeake Bay. Marine Ecology Progress Series 329: 99–113.

Dong, Z., D. Liu & J. K. Keesing, 2010. Jellyfish blooms in China: Dominant species, causes and consequences. Marine Pollution Bulletin 60: 954–963.

Feigenbaum, D. & M. Kelly, 1984. Changes in the lower Chesapeake Bay food chain in presence of the sea nettle *Chrysaora quinquecirrha*. Marine Ecology Progress Series 19: 39–47.

Fennel, W. & T. Neumann, 2004. Introduction to the Modelling of Marine Ecosystems. Gulf Professional Publishing.

Haddock, S. H. D., 2004. A golden age of gelata: past and future research on planktonic ctenophores and cnidarians. Hydrobiologia 530: 549–556.

Jopp, F., H. Reuter & B. Breckling (eds), 2011. Modelling Complex Ecological Dynamics. Springer, Heidelberg.

Kennedy, M. C. & A. O'Hagan, 2001. Bayesian calibration of computer models. Journal of the Royal Statistical Society: Series B (Statistical Methodology) 63: 425–464.

Kimmel, D. G., W. R. Boynton & M. R. Roman, 2012. Long-term decline in the calanoid copepod *Acartia tonsa* in central Chesapeake Bay, USA: An indirect effect of eutrophication? Estuarine, Coastal and Shelf Science 101: 76–85.

Purcell, J. E., 1997. Pelagic cnidarians and ctenophores as predators: selective predation, feeding rates, and effects on prey populations. Annales de I'Institut oceanographique 73: 125–137.

Purcell, J. E., 2009. Extension of methods for jellyfish and ctenophore trophic ecology to large-scale research. Hydrobiologia 616: 23–50.

Purcell, J. E., 2012. Jellyfish and ctenophore blooms coincide with human proliferations and environmental perturbations. Annual Review of Marine Science 4: 209–235.

Purcell, J. E. & M. N. Arai, 2001. Interactions of pelagic cnidarians and ctenophores with fish: a review. Hydrobiologia 451: 27–44.

Purcell, J. E. & J. Cowan Jr., 1995. Predation by the scyphomedusan *Chrysaora quinquecirrha* on *Mnemiopsis leidyi* ctenophores. Marine Ecology Progress Series 129: 63–70.

Purcell, J. E., F. P. Cresswell, D. G. Cargo & V. S. Kennedy, 1991. Differential ingestion and digestion of bivalve larvae by the scyphozoan *Chrysaora quinquecirrha* and the ctenophore *Mnemiopsis leidyi*. The Biological Bulletin 180: 103–111.

Purcell, J. E. & M. B. Decker, 2005. Effects of climate on relative predation by scyphomedusae and ctenophores on copepods in Chesapeake Bay during 1987-2000. Limnology and Oceanography 50: 376–387.

Purcell, J. E., D. A. Nemazie, S. E. Dorsey, E. D. Houde & J. C. Gamble, 1994. Predation mortality of bay anchovy *Anchoa mitchilli* eggs and larvae due to scyphomedusae and ctenophores in Chesapeake Bay. Marine Ecology Progress Series 114: 47–58.

Purcell, J., S. Uye & W. Lo, 2007. Anthropogenic causes of jellyfish blooms and their direct consequences for humans: a review. Marine Ecology Progress Series 350: 153–174.

Richardson, A. J., A. Bakun, G. C. Hays & M. J. Gibbons, 2009. The jellyfish joyride: causes, consequences and management responses to a more gelatinous future. Trends in Ecology and Evolution 24: 312–322.

Robinson, K., J. Ruzicka, M. B. Decker, R. Brodeur, F. Hernandez, J. Quiñones, M. Acha, S. Uye, H. Mianzan & W. Graham, 2014. Jellyfish, forage fish, and the world's major fisheries. Oceanography 27: 104–115.

Schartau, M., P. Wallhead, J. Hemmings, U. Löptien, I. Kriest, S. Krishna, B. A. Ward, T. Slawig & A. Oschlies, 2017. Reviews and syntheses: Parameter identification in marine planktonic ecosystem modelling. Biogeosciences 14: 1647–1701.

Sexton, M. A., 2012. Factors influencing appearance, disappearance, and variability of abundance of the sea nettle *Chrysaora quinquecirrha* in Chesapeake Bay. Doctoral dissertation, University of Maryland, College Park, USA.

Spitz, Y. H., J. R. Moisan & M. R. Abbott, 2001. Configuring an ecosystem model using data from the Bermuda Atlantic Time Series (BATS). Deep Sea Research Part II: Topical Studies in Oceanography 48: 1733–1768.

Sullivan, L. J. & D. J. Gifford, 2004. Diet of the larval ctenophore *Mnemiopsis leidyi* A. Agassiz (Ctenophora, Lobata). Journal of Plankton Research 26: 417–431.

Terborgh, J. & J. A. Estes (eds), Trophic Cascades: Predators, Prey, and the Changing Dynamics of Nature. Island Press, Washington DC.

Testa, J. M., W. M. Kemp, W. R. Boynton & J. D. Hagy, 2008. Long-term changes in water quality and productivity in the Patuxent River Estuary: 1985 to 2003. Estuaries and Coasts 31: 1021–1037.

Tian, R. C., 2006. Toward standard parameterizations in marine biological modeling. Ecological Modelling 193: 363–386.

Vallino, J. J., 2000. Improving marine ecosystem models: Use of data assimilation and mesocosm experiments. Journal of Marine Research 58: 117–164.

Wootton, J. T., 1994. The nature and consequences of indirect effects in ecological communities. Annual Review of Ecology and Systematics 25: 443–466.

Wootton, J. T., 2002. Indirect effects in complex ecosystems: Recent progress and future challenges. Journal of Sea Research 48: 157–172.

Chapter 2: Abundance and patchiness of *Chrysaora quinquecirrha* medusae from a high-frequency time series in the Choptank River, Chesapeake Bay *

*Reprinted with minor modifications from "Abundance and patchiness of *Chrysaora quinquecirrha* medusae from a high-frequency time series in the Choptank River, Chesapeake Bay" by Tay, J. T & R. R. Hood, 2017, Hydrobiologia, 792: 227-242. 2016 by Springer International Publishing.

The species name *Chrysaora quinquecirrha* is retained in this chapter for consistency with the published manuscript, which was published prior to the species name change.

Abstract

Despite strong control over marine plankton dynamics and negative impacts on human activities, jellyfish are not well quantified due primarily to sampling difficulties with nets. Therefore, some of the longest records of jellyfish are visual shore-based surveys. As surface counting is inexpensive and simple, it is of interest to determine what can be learned from such records as well as the usefulness of the method. I analyzed a 4-year high-frequency time series of Chrysaora quinquecirrha medusae counts collected using three sampling methods in the Choptank River, Chesapeake Bay. Medusa abundance was modeled by change points and was highly correlated between the sampling methods. The remaining signal was random and indices of aggregation (fit to the Poisson distribution, Taylor's Power Law (TPL) and Morisita's Index) indicated that medusae were aggregated. An idealized conceptualization of the temporal sampling scheme into space suggests that the upper bound of the patch size is on the order of kilometers. TPL indicated that patches grew in the number of individuals as abundance increased. Our results enhance knowledge of local *C. quinquecirrha* abundance and patchiness, alluding to processes that generate these patterns. This study also provides direction for improving population monitoring from visual shore-based surveys.

Introduction

There is growing interest in jellyfish, among the scientific community as well as the general public, as we learn more about their strong control over marine plankton dynamics (Richardson et al., 2009; Robinson et al., 2014) and as their negative impacts on human commercial and recreational activities increase (Purcell et al., 2007; Purcell, 2012). In Chesapeake Bay, the scyphozoan medusa, *Chrysaora quinquecirrha* (Desor, 1848), is a keystone predator that consumes crustacean mesozooplankton, fish eggs and larvae, and ctenophores (Purcell et al., 1994; Purcell, 1997; Feigenbaum & Kelly, 1984; Purcell & Cowan, 1995; Purcell & Decker, 2005), strongly impacting the flow of carbon within the food web (Baird & Ulanowicz, 1989; Libralato et al., 2006). Aside from the consequences for fisheries, *C. quinquecirrha* is a common nuisance to swimmers and watermen and their blooms have even disrupted operations at a nuclear power plant (the Calvert Cliffs Nuclear Power Plant on the western shore of Chesapeake Bay). However, advances in our understanding of the ecological and human impacts of jellyfish have been hampered by the lack of information of jellyfish abundance or biomass (Purcell, 2009; Pauly et al., 2009).

Generally, long-term data on jellyfish populations are lacking in part due to difficulties sampling with net tows (Haddock, 2004) and as a result, some of the longest records of jellyfish are from visual shore-based surveys (Purcell, 2009). One example is the time series of *C. quinquecirrha* from the Chesapeake Biological

Laboratory pier that started in 1960 in the Patuxent River, a tributary of the Chesapeake Bay (Cargo & King, 1990). This time series has been used to assess inter-annual variability (Cargo & King, 1990) and long-term change (Breitburg & Fulford, 2006) of *C. quinquecirrha* abundance and has also been included in analyses of global jellyfish populations (Brotz et al., 2012; Condon et al., 2012). Thus, it is of interest to fully understand the information captured by surface counting at a fixed station. Such methods capture two signals: abundance as well as spatial patchiness. Spatial patchiness may be observed due to behavior of medusae swimming horizontally or vertically into the sampling region but is also due to tidal and estuarine advection that moves different parcels of water in and out of the survey area (Lee & McAlice, 1979).

Jellyfish, like all zooplankton (Haury et al., 1978), exhibit spatial patchiness at multiple scales. *C. quinquecirrha* medusae are heterogeneous at the Bay-wide scale, most likely found in the mesohaline portion of the Bay at salinities between 10 to 16 (Decker et al., 2007). This pattern may be generated by both the salinity requirements of benthic polyps for optimal strobilation (Cargo & Schultz, 1967; Purcell et al., 1999; Black & Webb, 1973), and possibly behaviors that retain medusae in suitable habitat (Kimmerer & McKinnon, 1987; Kimmerer et al., 1998; Albert, 2007). It has also been recognized that *C. quinquecirrha* form smaller-scale aggregations and/or swarms (Hamner & Dawson, 2008; Mayer, 1910), however *C. quinquecirrha* aggregations specifically have not been studied. Previous studies of

jellyfish aggregations have utilized intensive sampling methods, such as blue-water SCUBA (Hamner et al., 1975; Zavodnik, 1987; Costello et al., 1998), plane (Purcell et al., 2000) or acoustic and optical technologies (Graham et al., 2003).

Count data collected from quadrats, such as those collected from a fixed-station, or net tows can also be used to understand patchiness. The most common method is to compare the counts against the null hypothesis of complete spatial randomness (CSR), which is modeled by the Poisson distribution (Krebs, 1999). Many other indices of aggregation have been developed and are widely used in both terrestrial and aquatic studies to detect patchiness. The exponent of Taylor's Power Law (TPL; Taylor, 1961) is also based on deviations from CSR. Because of the ubiquity of TPL (Eisler et al., 2013), there has been a great deal of theoretical work on mechanisms that may generate patchiness that adheres to the scaling law (Taylor & Taylor, 1977; Kilpatrick & Ives, 2003; Hanski, 1980; Perry, 1988; Anderson et al., 1982; Kendal, 1995). Additionally, Morisita's Index (Im; Morisita, 1959) has been championed because, in addition to detecting aggregation, it can also distinguish the degree of aggregation and can be compared across different densities (Hurlbert, 1990; Pinel-Alloul, 1995).

The goal of this work was to describe the signals of abundance and patchiness present in a fixed-station record. I analyzed a 4-year time series of *C. quinquecirrha* medusa counts collected twice per day in the Choptank River, Chesapeake Bay (Sexton, 2012). This time series contains an unprecedented amount of intra-seasonal data for

C. quinquecirrha, ideal for understanding the signal of spatial patchiness in a fixed-station time series. The change in abundance over time was described using a change point model and the fit was analyzed using autocorrelation analysis. Each of the segments was then summarized using indices of aggregation to detect and quantify patchiness. I also compared abundance and patchiness across three sampling methods that sample across two horizontal grains and in the vertical dimension. I used a simple model of tidal and estuarine advection to conceptualize how water moves past the fixed station over time in order to understand the spatial context of the results. These analyses showed that seasonal medusa abundance changed in steps and that the bloom progressed differently year-to-year. The abundance from the three sampling methods were highly correlated, showing that the surface counting methods can be used as an index of local water column abundance. Additionally, medusae are patchy and the aggregations were smaller than the scale of kilometers. This study highlights the benefits and drawbacks to fixed-station sampling and gives recommendations to improve the monitoring of *C. quinquecirrha*.

Materials and Methods

Study area

The Choptank River is a wide, relatively shallow tributary on the eastern side of the Chesapeake Bay, USA (Fig. 2. 1). The surface area is approximately 300 km^2 and mean depth is 3.6 meters (Fisher et al., 2006). The salt-intrusion length is 60-70 km (Fisher et al., 2006) and the median monthly streamflow (Jun-Aug) is 1.25 $m^3 s^{-1}$ (USGS Greensboro, MD), which can drive two-layer estuarine circulation (Goodwin,

2015). The river experiences semi-diurnal tides. Samples were collected from the east side of the Horn Point Laboratory pier, in Cambridge, Maryland, which is on the southeast side of the Choptank River (38° 35.610' N, 76° 7.725' W; Fig. 2. 1 Conceptual diagram of sampling location). The mean, minimum and maximum summer salinity for 2005 was 10.0, 8.1, and 12.3, respectively. The mean depth at the sampling location is 2.3 m.

Data description

The available high-frequency time series counts of *Chrysaora quinquecirrha* medusae spanned the years 2005 to 2008 and were collected by Margaret Sexton (Sexton, 2012). Beginning in 2005, counts were made twice daily at 7 AM and 7 PM until 16 September 2005, when scheduling was changed to sunrise and 20 minutes before sunset in order to control for light conditions and to make observations before dark. Calculated sunrise and sunset times for Cambridge, Maryland, USA were downloaded from the United States Naval Observatory (http://aa.usno.navy.mil/data/docs/RS_OneYear.php). Each year, observations ceased when no medusa had been observed for ten consecutive days.

At each time point, *C. quinquecirrha* medusae were counted using three different sampling methods (Fig. 2. 1). An observer counted the number of medusae visible at the surface within a 183 m^2 area (3 m width x 61 m length, hereinafter referred to as the 'dock count') and a 9 m^2 area (3 m width x 3 m length, hereinafter referred to as the 'visual count'). Additionally, the medusae in the water column were counted

using a 9 m^2 square flat net (0.6 cm nylon mesh; hereinafter referred to as the 'net count') that laid on the bottom at the same location as the visual count and was raised slowly, vertically through the water column. The dock count is a comparable method to how *C. quinquecirrha* have been monitored since the 1960s in the Chesapeake Bay (Cargo & King 1990). The visual and net counts provide information for a smaller horizontal grain and the vertical dimension, respectively. Additionally, medusae were crudely categorized as small (approximately <4 cm), medium (approximately 4-8 cm), or large (approximately >8 cm) using visual estimation.

Software

All analyses were performed in R 3.1.0. Specific packages and arguments are indicated where applicable.

Time series analysis

The purpose of the time series analysis was to describe the abundance change over time. Cursory examination of the time series suggested that the abundance changed in steps, so change point analysis (also called segmentation) was used to detect changes in the time series of dock counts using the Segmentor3IsBack package (Cleynen et al., 2014). The function Segmentor efficiently estimates the optimal breakpoint locations, using the minimal negative log-likelihood, for each segmentation of 1 to K segments. The function SelectModel chose the optimal number of segments (from 1 to K) using oracle penalties (argument: penalty = "oracle"; Cleynen & Lebarbier, 2013). The threshold for the largest complexity

(argument: seuil) was set to n/(2*log(n)) (Arlot & Massart, 2009), where n is the number of data points. The identified change points were used to segment the visual and net count time series as well. Each resulting time series segment was analyzed for temporal autocorrelation to confirm that the model was a good description of the data.

Abundance estimates and comparison

Abundance was estimated as area or volume-weighted mean population density (Craig, 1984; Stehman & Salzer, 2000) in units of number m^{-2} and number m^{-3}, respectively. To calculate area-weighted mean density, $\bar{d}$, the mean count for each time series segment was scaled by the mean area of the relevant sampling method:

$$\bar{d} = \frac{\Sigma area_i d_i}{\Sigma area_i} = \frac{\Sigma count_i}{\Sigma area_i} = \frac{\frac{1}{n}\Sigma count_i}{\frac{1}{n}\Sigma area_i}$$

where $area_i$, d_i, and $count_i$ are the area, medusae density, and count of the ith segment, respectively.

The areas for the dock and visual counts were 183 m^2 and 9 m^2, respectively. To compare the abundance of the net counts, volume-weighted density was calculated for all sampling methods. Net counts were scaled by 9 m^2 * 2.3 m, the surface area multiplied by the average depth of the net haul. Dock and visual surface counts were scaled by their respective volumes, calculated as surface area multiplied by both 0.1 m (diameter of large *C. quinquecirrha* medusae) and 1 m (mean secchi depth for 2005) because the depth to which surface counting methods sample is unknown (Fig.

2. 1). This resulted in a maximum and minimum abundance as measured by the dock and visual counts. Three segments were removed from the comparison between the surface and net counts that corresponded to periods when the methods were known to be incomparable due to cold temperatures that caused medusae to sink to the bottom (Sexton et al., 2010). Abundances for each sampling method were compared by linear regression. The resulting time series were plotted to visualize the intra-annual changes in abundance and the inter-annual differences in bloom progression. The size distribution of medusae for each time series segment was calculated by scaling the number of medusae in each size category by the total number of medusae observed within the respective segment.

Patchiness characterization

To assess whether medusae were aggregated, counts for each data segment were fit by maximum likelihood to both the Poisson distribution, as specified by the null hypothesis of Complete Spatial Randomness (CSR), and Negative Binomial distribution, as a model for aggregation. The fits were assessed using Pearson's chi-square goodness-of-fit (function: chisq.test). Due to small counts in each bin, p-values were computed by Monte Carlo simulation (argument: simulate.p.value = TRUE). Aggregation was also detected using the exponent from Taylor's Power Law (TPL) and Morisita's Index (Im). The power exponent, b, of TPL (variance = $a*mean_b$) was estimated as the slope of the multiple linear regression of the log-transform of both of the variables (log variance ~ sampling method * log mean). Difference in the regression for each of the three sampling methods was determined

by the interaction term in the multiple linear regression (ANCOVA). Im is defined as the probability of sampling two individuals in the same quadrat as compared to that probability as sampled from a population distributed at random:

$Im = n \sum(\frac{x_i}{X})(\frac{x_i - 1}{X - 1})$, where x_i is the count in the ith quadrat, X is the total count, and n is the number of observations. Im was estimated by:

$\widehat{Im} = \frac{s^2 - m}{m^2 - (\frac{s^2}{n})} + 1$, where s^2 is variance, m is mean, and n is as above (Hurlbert, 1990).

Segments with less than 25 data points were removed from the analysis due to negative bias in Im calculated from small samples (Ricklefs & Law, 1980). Three net count segments were removed, corresponding to periods of cold temperatures that cause medusae to sink to the bottom (Sexton et al., 2010), as their aggregation was likely different under these circumstances. Im was compared across mean density and between sampling methods using weighted least squares regression, which corrected for heterogeneity of variance between the sampling methods. Reciprocal of the variance of Im of each sampling method was used as the weights. Tukey post-hoc tests were used to compare between sampling groups using the multcomp package (Hothorn et al., 2008). Non-parametric Kruskal-Wallis tests were also computed, followed by Conover's test for post-hoc pairwise comparisons (PMCMR package; Pohlert, 2014).

Idealized modeling of sampling scheme

The data are a time series but contain spatial information as patches move in and out of the sampling area. In order to better understand the scales of patchiness, I use a conceptual model to describe how the temporal sampling scheme maps onto space. I assume that the surface waters in the Choptank River can be described as a 1-dimensional rigid object that moves past the fixed station due to tides and advection. The distance that any one point at the surface is advected in a given amount of time, x(t), is a function of semi-diurnal tides (A = 5 km for a 10 km tidal extent and = 2pi/12.42 hours) and of downstream residual circulation (s = 0.036 km/hour (0.01 m/s)):

$$x(t) = A * \sin(\omega t) + st.$$

t represents the time lapsed from the time of the first sample and x represents the distance moved in that time. The distance between any two sampling times is $\Delta x = x(t_m) - x(t_n)$, where m and n are different sampling times. Times were taken from the field sampling scheme for 2006, which is representative of any of the years. This simple model shows whether sampling is random or non-random in space and provides order-of-magnitude estimates for the spatial scales of the sampling, such as the distance between samples.

Results

Time series analysis

The high-frequency time series of *C. quinquecirrha* dock counts was well modeled by change points (Fig. 2. 2), demonstrated by the general lack of temporal autocorrelation in each resulting time series segment (Fig. 2. 3). The number of change point segments was different in each of the sampled years: 9 segments in 2005, 6 in 2006 and 2007, and 4 in 2008 (Fig. 2. 2). The median segment length was 26 data points (13 days). The minimum segment length was 9 data points (4.5 days) and the maximum length was 99 data points (45.5 days; Online Resource 1). Although the change points were chosen based on the dock data, similar lack of autocorrelation of the segments suggest that the segmentation was valid for the visual and net counts as well. However, there were some exceptions, as some segments showed temporal autocorrelation. For dock counts, there was significant temporal autocorrelation ($r > .5$) found at a lag of 2 for segment number 2 in 2006 (Fig. 2. 3). A similar pattern was seen in the ACF for the visual and net counts. In addition, for net counts a significant temporal autocorrelation was found in 2005 for segment 9 and in 2006 for segments 5 and 6 (not shown), which started at lag 1 and decreased over time. For visual and net counts, a few other segments showed weak but significant autocorrelation, mostly at lag 1 or 2.

Abundance estimates and comparison

Abundances from both surface counting methods (dock and visual counts) were highly positively related ($r^2(21) = .96$, $p < 2$ e-16) with a slope that was not significantly different from 1 (b = 1.03, 95% CI = 0.93 - 1.12; Fig. 2. 4a), which suggests both methods result in equivalent abundance estimates. Minimum and maximum abundance for each time series segment, calculated from surface counts using maximum (1 m) and minimum (0.1 m) depths, respectively, were also highly correlated to abundance from the net counts (Table 1), however, the regression slopes were not 1 (Fig. 2. 4b, Table 2. 1). The minimum surface counts resulted in estimates that were approximately 1/3 of the net estimates and maximum surface counts resulted in estimates 3.8 times greater than net estimates. Although the range in estimates is wide, the 1:1 line fell between the estimates of minimum abundance and maximum abundance (Fig. 2. 4b).

Due to high correlations between the three abundance estimates (calculated from the dock, visual, and net count sampling methods), the three annual abundance time series generally showed the same patterns. The abundance time series estimated from the dock counts is shown for conciseness (Fig. 2. 5a). The blooms in 2005 and 2006 were large and prolonged. In 2005, the abundance increased to a peak that began on year day 249 and lasted 34 days, after which, abundance declined. However, medusae were observed until year day 319. In 2006, the abundance increased faster, with high abundances beginning on year day 187 that plateaued before

declining. Medusae were observed until year day 302. In 2007, both the peak and the season duration were the shortest of the 4 years; the peak started on year day 234, lasting 6 days before declining, and the last medusa was observed on year day 252. In 2008, there was relatively low abundance throughout the season. The peak abundance was at least 3-4x lower than the 3 previous years and began on year day 222, lasting over 1 month. Medusae were observed until year day 284. The abundance dropped within the season in years 2005 (Segments 4 and 6), 2006 (Segment 3) and 2007 (Segment 3). Every year had a high proportion of small medusae at the beginning of each season, which declined as the season progressed (Fig. 2. 5b). 2005 and 2008 had a second period with an increased proportion of small medusae. Compared to the other years, 2005 had a high and 2006 had a low proportion of small medusae throughout the respective seasons. Un-scaled, the abundance of medium and large medusae generally exceeded that of small medusae at concurrent and previous time segments.

Patchiness characterization

Generally, *C. quinquecirrha* were aggregated as demonstrated by three indices of aggregation (fit to the Poisson, TPL, and Im). Most segments did not fit the Poisson distribution ($p < .05$; Fig. 2. 6), thereby rejecting CSR. Further, the Negative Binomial distribution provided an adequate description of these data, as shown through goodness-of-fit and quantile-quantile plots, suggesting that medusae are clumped rather than random uniform or regularly spaced. However, segments with

low counts (generally less than 5) fit the Poisson distribution and therefore failed to reject CSR. Similarly, the TPL regression line mostly fell above the 1:1 line, suggesting the counts were aggregated, but fell below the 1:1 line at low counts, suggesting TPL failed to reject CSR at low counts (Fig. 2. 7). TPL failed to reject CSR at mean counts less than 1, which was lower than found by distribution fitting. Likewise, most all segments were considered aggregated according to Morisita's Index (Im) (Fig. 2. 8). The mean of Im was 3.06 ± 0.7 s.e., suggesting that two jellyfish are approximately 3 times more likely to be found in the same quadrat than if distributed randomly.

Further analysis of TPL showed that there was significant difference in the slopes of the TPL regression (power exponent) between sampling methods ($F(2,63) = 5.09$, $p = .0089$; Fig. 2. 7a), however, this difference was driven by low means in visual and net counts. The slope for the dock data was 1.92 ± 0.05 s.e. and was not significantly different from 2 (1.80 - 2.04 95% CI). The slopes for the visual and net count data were 1.62 ± 0.075 s.e. and 1.64 ± 0.090 s.e., respectively, and both slopes were significantly less than 2 (1.46 - 1.78 and 1.46 - 1.83 95% CI). Removal of cases with means less than 1 resulted in slopes that were not significantly different between sampling methods ($F(2,43) = 0.71$, $p = .5$; Fig. 2. 7b) and not different from 2 (1.71 – 2.03 95% CI). This demonstrates that low counts, which are captured by the visual and net methods, inflate the variance and lower the TPL slope.

Further comparison of Im revealed that the index did not have a relationship with mean count (beta = 0.001, p = .89) but was different between the three sampling methods (F(2,25) = 4.27, p = .025; Fig. 8). However, individual post-hoc tests failed to detect significant differences between groups, likely due to lack of power in the available dataset. Although insignificant at the .05 level, Im for the net count was 0.6 less than Im for the dock count (t = -2.18, p = .085) and 1.6 less than the visual count (t = 2.23, p = .077), suggesting that the net counts were less aggregated than the counts of the other two methods. Non-parametric tests gave similar results, showing differences in Im between sampling methods (Kruskal-wallis chi-sq(2) = 6.18, p = .045). Non-parametric post-hoc comparisons with Conover's test showed that the Im for the net count was significantly different from the visual count (p = .042), but did not detect significant differences between the other pairwise comparisons.

Idealized modeling

Idealized modeling of tidal and estuarine advection revealed that the temporal sampling procedure resulted in non-random sampling, tracing three patterns in space (Fig. 2. 9). The first pattern was that later time points sample locations that are upstream from the location sampled at the fixed-station at t = 0. This is due to constant downstream estuarine advection in the surface layer. After 28 days (4 weeks), the samples were of water that was approximately 30 km upstream, referenced to t = 0. The second pattern was a sinusoid in space, with a period of approximately 2 weeks, revealing that the samples taken about 14 days apart are

closer in space in relation to their location in the tidal cycle. The third pattern was a day-night pattern in that the location of the sample one morning was closer in space to the sample of the next morning than to the evening in between. Samples taken approximately 24 hours apart were on the order of kilometers apart. The latter two patterns were caused by aliasing due to sampling at a different frequency than the semi-diurnal tides and are not present in a continuous temporal sampling scheme (grey line in Fig. 2. 9).

Discussion

Medusa abundance

Seasonal medusa abundance was well described using a change point model since the resulting segments lacked temporal autocorrelation. This model suggests that abundance was constant and changed as a step change after approximately every 13 days, which was the median segment length. Within-season drops in abundance may have been spuriously generated by the segmentation routine due to some chance of not observing medusae for several consecutive days. It was not a priori evident that the seasonal abundance of medusae should change in steps (Sexton, 2012). I hypothesize that two mechanisms may give rise to this model at a fixed station. First, the constancy in abundance through the duration of each segment may be due to behavior, such as DVM, which retains medusae in the sampling region (Bosch & Taylor, 1973; Kimmerer et al., 2014). Supplementary analysis of the data showed that there was a higher proportion of medusae in the surface in the evening than in the

morning (Fig. 2. 10), demonstrating that *C. quinquecirrha* exhibit DVM in the field, an extension from previous laboratory studies (Schuyler & Sullivan, 1997). Second, the step change in abundance may be due to pulsed strobilation (Cargo & Schultz, 1967; Calder, 1974). Strobilation of *C. quinquecirrha* exhibits semilunar periodicity (Calder, 1974), which is consistent with the median segment length detected by change point analysis. Given that more large than small medusae were observed, it is likely that a high proportion of the medusae are not produced locally but in smaller creeks elsewhere (Feigenbaum & Kelly 1984; Breitburg & Burrell 2014). Together, these mechanisms suggest that the fixed station is sampling a population that is retained by behavior and grows due to pulsed birth over the season.

The seasonal progression of medusa abundance was different for each of the sampled years from 2005 to 2008. The magnitude of the peak was largest in 2005 and 2006 due to recruitment of medusae over the season (Fig. 2. 5a). Relative to the other years, 2005 and 2006 had a higher and lower proportion of small medusae, respectively (Fig. 2. 5b). Differences in the size distribution may reflect differences in sources of medusae and/or growth rate between years. 2007 also had high recruitment and a bloom, but the population declined much earlier than the other three years. The phenomenon of early decline is also observed in the Patuxent River record (Sexton et al., 2010; Sexton 2012) and is preceded by observations of medusae with degenerating oral arms (Doores & Cook, 1976; Sexton et al., 2012). 2008 had low recruitment and the population seemed to plateau. The reasons for this lack of

population growth are not clear; and explanations may include lowered rates of strobilation (Purcell et al., 1999) and/or poor recruitment of ephyrae to the adult stage. The length of the peak lasted from 1 week (2007) to over 1 month (2008) and occurred as early as year day 187 (July 7) in 2006 and as late as year day 249 (Sep 7) in 2005 (Fig. 2. 5a). Past studies of *C. quinquecirrha* have utilized definitions of peak abundance based on fixed dates and/or fixed windows of time (Cargo & King, 1990; Breitburg & Fulford, 2006; Sexton, 2012). Our method extracts the true local peak using change point analysis, which allows for inter-annual variability in the duration and timing of the seasonal cycle of medusae.

The seasonal cycle in 2006 had some anomalies that illustrate that a fixed station provides only a limited view of the *C. quinquecirrha* bloom. Segment 2 in 2006 had temporal autocorrelation at lag 2, approximately 24 hours apart (Fig. 2. 3). This autocorrelation is likely not due to DVM, as it was only detected in this one segment. Instead, at this time, there was extreme streamflow, greater than 56.6 m_3 s_{-1} compared to the 66-year median of less than 1.13 m_3 s_{-1} (USGS Greensboro). Extreme streamflow could have created a large-scale gradient from low to high medusae and could explain the temporal autocorrelation at lag 2. Idealized modeling showed that time points at lag 2 were closest in horizontal space (samples approximately 1 day apart were collected kilometers apart; Fig. 2. 9) and this means that the non-random sampling scheme would alternate sampling within regions of low then high medusae, generating an autocorrelation at this scale. After, the population

appeared to rebound at Segment 4 (Fig. 2. 5), which could be due to medusae moving back upstream or due to new recruitment. If there was new recruitment, then the bloom could be underestimated in this year. This demonstrates that extreme or long-term changes in streamflow can shift the observable population intra- or inter-annually, which could cause patterns in abundance that are the result of observer bias from sampling in only one location.

Although fixed-station sampling may be susceptible to bias, the main advantage is that surface sampling is inexpensive and simple. This study shows that surface counting can provide an index of water column abundance since abundance measured by surface counts and the net haul were highly correlated. Surface counts may be representative of the water column at this station because it is shallow (2.3 m) and the water is generally well mixed, without a distinct pycnocline. However, surface counts may not reflect water column abundance when measured in deeper waters of Chesapeake Bay, especially where there is a distinct pycnocline that may aggregate or restrict the vertical distribution of medusae (Graham et al., 2003; Suzuki et al., 2016; Moriarty et al., 2012; Rakow & Graham, 2006). As fixed-stations are generally located in shallow waters, increasing these stations could help increase the amount of Bay-wide information on medusae abundance and variability. Additionally, abundance measured by the two surface counting methods, dock and visual counts, are highly related. It has been noted that different sampling grains can often lead to similar abundance estimates (Dungan et al., 2002). The small sampling grain (3 x 3

m) is conducive to a citizen science project and may provide a feasible way to increase spatial sampling of *C. quinquecirrha* medusae.

Patchiness of Medusae

Fit to a change point model made separating the signal of abundance and patchiness straightforward; indices of aggregation were used to summarize the patchiness signal within each of the time series segments. The indices of aggregation (lack of fit to Poisson, power exponent of TPL, and Im) all generally showed that the spatial structure of *C. quinquecirrha* medusae was patchy, which was expected as they, like most scyphozoans, form conspicuous aggregations (Mayer, 1910; Hamner & Dawson, 2008). Two medusae are on average 3 times more likely to be found in the same quadrat than if distributed randomly, according to the interpretation of Im. Goodness-of-fit tests had some difficulty detecting aggregation in segments with low counts. The data fit both the Poisson or Negative Binomial distributions when counts were less than 5 because the distributions are very similar at low densities (Fig. 2. 6f). TPL and Im were more sensitive at detecting aggregation at low densities, but they also indicated lack of aggregation at the lowest densities (Taylor, 1961; Taylor et al., 1978). With one exception, these non-aggregated cases occurred in the visual count during the beginning or end of a season. This suggests that at low-density periods, patches were larger than the scale of the visual count area (individuals were spaced greater than 3 m apart) because aggregation was detected in the dock and net count methods at these times.

As these data were a time series, I used idealized modeling to infer the patch size. Idealized modeling showed that the closest samples were collected at scales of kilometers apart (at lag 2; Fig. 2. 9), thus, lack of autocorrelation at lag 2 implies that regions on the order of kilometers apart are uncorrelated and patches should be smaller than this scale. Kilometer scales are the upper bound on patch size because that is the scale of the minimum distance between samples and we cannot determine if the lack of autocorrelation is due to smaller-scale variability. There may be patchiness at the scale of 1-10 meters due to similarity of Im between the dock and visual counts, which may suggest nested patchiness (patches within patches) at these scales. Indeed, jellyfish have generally been observed in fine-scaled aggregations (10-100 meters; Miyao et al., 2014; Purcell et al., 2000). Small-scale patchiness is predominately generated by behavioral processes (reviewed in Pinel-Alloul, 1995). Medusae behave in response to a wide range of physical (Graham et al., 2001; Costello et al., 1998; Rakow & Graham, 2006; Magome et al., 2007; Fossette et al., 2015), chemical (Albert, 2011) and biological (Matanoski et al., 2001; Hamner et al., 1994) stimuli that may generate aggregations. The observed scales of *C. quinquecirrha* patchiness are smaller than the 10s of kilometer-scale patchiness observed for crustacean mesozooplankton in Chesapeake Bay (Zhang et al., 2006). This difference may be expected since medusae are stronger swimmers and less abundant than mesozooplankton.

Results from TPL allude to the dynamics of medusae aggregations. The TPL exponent was found to be 2 (Fig. 2. 7), which results if, as the population grows, aggregations have proportionally more individuals as opposed to the spatial distribution becoming more uniformly random or evenly dispersed. Numerous studies have considered the processes that may generate the TPL relationship (Taylor & Taylor, 1977; Kilpatrick & Ives, 2003; Hanski, 1980; Perry, 1988; Anderson et al., 1982; Kendal, 1995). However, many of these models consider patchiness due to population dynamic processes, such as variability in birth, death, and immigration. However, the mechanisms that generate patchiness depend on the time and space scales of sampling (Soberón & Loevinsohn, 1987) as well as the species' life history. Aggregations of *C. quinquecirrha* do not grow due to reproduction of medusae within patches because *C. quinquecirrha* has a bipartite lifecycle. Instead, aggregations are formed due to medusae that "find" each other after benthic strobilation of ephyrae. Kendall (1995) proposed a probabilistic model for TPL in which small patches of organisms migrate randomly through their environment until they become associated with larger groups, which may provide a good description of how aggregations of medusae grow across the season. Behavior is likely important in maintaining cohesion between individuals.

Conclusions

This work extends previous efforts that monitor *C. quinquecirrha* in the Chesapeake Bay (Cargo & King, 1990; Breitburg & Fulford, 2006; Sexton et al., 2010; Sexton,

2012). I found that a change point model was a good description of seasonal abundance at a fixed-station. This model suggests that the fixed-station is sampling a local population that is retained by behavior and that grows due to pulsed birth over the season. Thus, sampling at a fixed station is likely not representative of the larger Chesapeake Bay population and may be affected by bias. However, high-frequency surface sampling, even within a small area (3 x 3 m), can provide an index for water-column abundance. Using citizen scientists may allow increased spatial sampling of *C. quinquecirrha* medusae across Chesapeake Bay and other Atlantic estuaries (Mayer, 1910). Ideally, this work will encourage increased spatial sampling of medusae to improve our understanding of seasonal and long-term changes of *C. quinquecirrha* as they respond rapidly to natural and anthropogenic perturbations (Purcell et al., 2007; Purcell, 2012). Additionally, improved Bay-wide abundance estimates will allow for the inclusion of keystone gelatinous predators in ecosystem-based fisheries management models (Purcell, 2009; Pauly et al., 2009).

This is the first known attempt to quantify aggregation of *C. quinquecirrha* medusae in Chesapeake Bay. Lack of fit to the Poisson distribution and the indices, Im and TPL, suggest that medusae are aggregated. Understanding patchiness is important for accurately assessing abundance (Haury et al., 1978), and in fact, attention to this "nuisance" signal led us to choose the change point model. Additionally, quantifying patterns of patchiness is the first step towards understanding the processes that drive it. Further experimental work and individual-based modeling studies will help

elucidate the behaviors that generate and maintain aggregation. Furthermore, studying patchiness is of interest for fully understanding the effect of gelatinous predators on ecosystem dynamics, diversity, and stability (Wiens, 2000; Levin, 1994; Steele, 1974). While coarse-scale patterns (Decker et al., 2007) determine the range of *C. quinquecirrha* influence on plankton dynamics, smaller scale aggregations can affect the magnitude of this influence. The TPL relationship determined in this study can be used in modeling studies to specify medusae patchiness across a range of mean densities in order to understand the impact of spatial variability of keystone predators on ecosystem dynamics.

Acknowledgments

I thank Margaret Sexton for collecting and sharing the medusa time series data. This work was supported by the Horn Point Laboratory Education Committee and a National Oceanographic and Atmospheric Administration grant to R. Hood. This paper represents UMCES contribution number 5278.

References

Albert, D. J., 2007. *Aurelia labiata* medusae (Scyphozoa) in Roscoe Bay avoid tidal dispersion by vertical migration. Journal of Sea Research 57: 281–287.

Albert, D. J., 2011. What's on the mind of a jellyfish? A review of behavioural observations on *Aurelia sp.* jellyfish. Neuroscience & Biobehavioral Reviews 35: 474–482.

Anderson, R. M., D. M. Gordon, M. J. Crawley, & M. P. Hassell, 1982. Variability in the abundance of animal and plant species. Nature 296: 245–248.

Arlot, S., & P. Massart, 2009. Data-driven calibration of penalties for least-squares regression. The Journal of Machine Learning Research 10: 245–279.

Baird, D., & R. E. Ulanowicz, 1989. The Seasonal Dynamics of The Chesapeake Bay Ecosystem. Ecological Monographs 59: 329–364.

Black, R., & K. Webb, 1973. Metabolism of 131I in relation to strobilation of *Chrysaora quinquecirrha*. Comp. Biochem. Physiol. 45a: 1023–1029.

Bosch, H. F., & R. R. Taylor, 1973. Diurnal vertical migration of an estuarine cladoceran, *Podon polyphemoides*, in the Chesapeake Bay. Marine Biology 19: 172–181.

Breitburg, D., & R. Burrell, 2014. Predator-mediated landscape structure: seasonal patterns of spatial expansion and prey control by *Chrysaora quinquecirrha* and *Mnemiopsis leidyi*. Marine Ecology Progress Series 510: 183–200.

Breitburg, D. L., & R. S. Fulford, 2006. Oyster-sea nettle interdependence and altered control within the Chesapeake Bay ecosystem. Estuaries and Coasts 29: 776–784.

Brotz, L., W. W. L. Cheung, K. Kleisner, E. Pakhomov, & D. Pauly, 2012. Increasing jellyfish populations: trends in Large Marine Ecosystems. Hydrobiologia 690: 1–18.

Calder, D., 1974. Strobilation of the sea nettle, *Chrysaora quinquecirrha*, under field conditions. Biological Bulletin 146: 326–334.

Cargo, D. G., & D. R. King, 1990. Forecasting the abundance of the sea nettle, *Chrysaora quinquecirrha*, in the Chesapeake Bay. Estuaries 13: 486–491.

Cargo, D. G., & L. P. Schultz, 1967. Further observations on the biology of the sea nettle and jellyfishes in Chesapeake Bay. Chesapeake Science 8: 209–220.

Cleynen, A., M. Koskas, E. Lebarbier, G. Rigaill, & S. Robin, 2014. Segmentor3IsBack: an R package for the fast and exact segmentation of Seq-data. Algorithms for Molecular Biology 9: 6.

Cleynen, A., & E. Lebarbier, 2013. Segmentation of the Poisson and negative binomial rate models: a penalized estimator. arXiv preprint arXiv:1301.2534 , http://arxiv.org/abs/1301.2534.

Condon, R. H., C. M. Duarte, K. A. Pitt, K. L. Robinson, C. H. Lucas, K. R. Sutherland, H. W. Mianzan, M. Bogeberg, J. E. Purcell, M. B. Decker, S. Uye, L. P. Madin, R. D. Brodeur, S. H. D. Haddock, A. Malej, G. D. Parry, E. Eriksen, J. Quinones, M. Acha, M. Harvey, J. M. Arthur, & W. M. Graham, 2012. Recurrent jellyfish blooms are a consequence of global oscillations. Proceedings of the National Academy of Sciences 110: 1000–1005.

Costello, J. H., E. Klos, & M. Ford, 1998. In situ time budgets of the scyphomedusae *Aurelia aurita*, *Cyanea sp*., and *Chrysaora quinquecirrha*. Journal of Plankton Research 20: 383–391.

Craig, J., 1984. Averaging Population Density. Demography 21: 405.

Decker, M. B., C. W. Brown, R. R. Hood, J. E. Purcell, T. F. Gross, J. C. Matanoski, R. O. Bannon, & E. M. Setzler-Hamilton, 2007. Predicting the distribution of the scyphomedusa *Chrysaora quinquecirrha* in Chesapeake Bay. Marine Ecology Progress Series 329: 99–113.

Doores, S., & T. M. Cook, 1976. Occurrence of *Vibrio* and Other Bacteria on the Sea Nettle, *Chrysaora quinquecirrha*. Microbial Ecology 3: 31–40.

Dungan, J. L., J. N. Perry, M. R. T. Dale, P. Legendre, S. Citron-Pousty, M. J. Fortin, A. Jakomulska, M. Miritit, & M. S. Rosenberg, 2002. A balanced view of scale in spatial statistical analysis. Ecography 25: 626–640.

Eisler, Z., I. Bartos, & J. Kertesz, 2008. Fluctuation scaling in complex systems: Taylor's law and beyond. Advances in Physics 57: 89–142.

Feigenbaum, D., & M. Kelly, 1984. Changes in the lower Chesapeake Bay food chain in presence of the sea nettle *Chrysaora quinquecirrha*. Marine Ecology Progress Series 19: 39–47.

Fisher, T. R., J. D. Hagy Iii, W. R. Boynton, & M. R. Williams, 2006. Cultural eutrophication in the Choptank and Patuxent estuaries of Chesapeake Bay. Limnology and Oceanography 435–447.

Fossette, S., A. C. Gleiss, J. Chalumeau, T. Bastian, C. D. Armstrong, S. Vandenabeele, M. Karpytchev, & G. C. Hays, 2015. Current-Oriented Swimming by Jellyfish and Its Role in Bloom Maintenance. Current Biology 25: 342–347.

Goodwin, J. D., 2015. Integrating automated imaging and a novel identification technique to estimate mortality and identify factors that influence the vertical distribution of *Crassostrea virginica* larvae. PhD dissertation. University of Maryland College Park, MD.

Graham, W. M., D. L. Martin, & J. C. Martin, 2003. In situ quantification and analysis of large jellyfish using a novel video profiler. Marine Ecology Progress Series 254: 129–140.

Graham, W. M., F. Pages, & W. M. Hamner, 2001. A physical context for gelatinous zooplankton aggregations: a review. Hydrobiologia 451: 199–212.

Haddock, S. H. D., 2004. A golden age of gelata: past and future research on planktonic ctenophores and cnidarians. Hydrobiologia 530: 549–556.

Hamner, W. M., & M. N. Dawson, 2008. A review and synthesis on the systematics and evolution of jellyfish blooms: advantageous aggregations and adaptive assemblages. Hydrobiologia 616: 161–191.

Hamner, W. M., P. P. Hamner, & S. W. Strand, 1994. Sun-compass migration by *Aurelia aurita* (Scyphozoa): population retention and reproduction in Saanich Inlet, British Columbia. Marine Biology 119: 347–356.

Hamner, W. M., L. P. Madin, A. L. Alldredge, R. W. Gilmer, & P. P. Hamner, 1975. Underwater observations of gelatinous zooplankton: sampling problems, feeding biology, and behavior. Limnology and Oceanography 907–917.

Hanski, I., 1980. Spatial Patterns and Movements in Coprophagous Beetles. Oikos 34: 293.

Haury, L. R., J. A. McGowan, & P. H. Wiebe, 1978. Patterns and processes in the time-space scales of plankton distributions Spatial Pattern in Plankton Communities. Plenum Press, N.Y.: 277–327.

Hothorn, T., F. Bretz, & P. Westfall, 2008. Simultaneous inference in general parametric models. Biometrical Journal 50: 346–363.

Hurlbert, S. H., 1990. Spatial Distribution of the Montane Unicorn. Oikos 58: 257–271.

Kendal, W. S., 1995. A probabilistic model for the variance to mean power law in ecology. Ecological Modelling 80: 293–297.

Kilpatrick, A. M., & A. R. Ives, 2003. Species interactions can explain Taylor's power law for ecological time series. Nature 422: 65–68.

Kimmerer, W. J., J. R. Burau, & W. A. Bennett, 1998. Tidally oriented vertical migration and position maintenance of zooplankton in a temperate estuary. Limnology and Oceanography 43: 1697–1709.

Kimmerer, W. J., E. S. Gross, & M. L. MacWilliams, 2014. Tidal migration and retention of estuarine zooplankton investigated using a particle-tracking model. Limnology and Oceanography 59: 901–916.

Kimmerer, W., & A. McKinnon, 1987. Zooplankton in a marine bay II. Vertical migration to maintain horizontal distributions. Marine Ecology Progress Series 41: 53–60.

Krebs, C. J., 1999. Ecological Methodology. Benjamin Cummings, Menlo Park, CA.

Lee, W. Y., & B. J. McAlice, 1979. Sampling variability of marine zooplankton in a tidal estuary. Estuarine and Coastal Marine Science 8: 565–582.

Levin, S. A., 1994. Patchiness in Marine and Terrestrial Systems: From Individuals to Populations. Philosophical Transactions of the Royal Society of London. Series B: Biological Sciences 343: 99–103.

Libralato, S., V. Christensen, & D. Pauly, 2006. A method for identifying keystone species in food web models. Ecological Modelling 195: 153–171.

Magome, S., T. Yamashita, T. Kohama, A. Kaneda, Y. Hayami, S. Takahashi, & H. Takeoka, 2007. Jellyfish patch formation investigated by aerial photography and drifter experiment. Journal of Oceanography 63: 761–773.

Matanoski J., Hood R., & Purcell J., 2001. Characterizing the effect of prey on swimming and feeding efficiency of the scyphomedusa *Chrysaora quinquecirrha*. Marine Biology 139: 191–200.

Mayer, A. G., 1910. Medusae of the World. Carnegie Institution of Washington, Washington D.C.

Miyao, Y., A. Isobe, & S. Kako, 2014. An Application of Low-altitude Remote Sensing Using a Vessel-towed Balloon for Monitoring Jellyfish Patchiness in Coastal Waters. Journal of the Remote Sensing Society of Japan 34: 113–120.

Moriarty, P., K. Andrews, C. Harvey, & M. Kawase, 2012. Vertical and horizontal movement patterns of scyphozoan jellyfish in a fjord-like estuary. Marine Ecology Progress Series 455: 1–12.

Morisita, M., 1959. Measuring of the dispersion of individuals and analysis of the distributional patterns. Memoirs of the Faculty of Science, Kyushu University, Series E (Biology) 2: 215–235.

Pauly, D., W. M. Graham, L. Morissette, & M. L. D. Palomares, 2009. Jellyfish in ecosystems, online databases, and ecosystem models. Hydrobiologia 616: 67–85.

Perry, J. N., 1988. Some Models for Spatial Variability of Animal Species. Oikos 51: 124.

Pinel-Alloul, P., 1995. Spatial heterogeneity as a multiscale characteristic of zooplankton community. Hydrobiologia 300: 17–42.

Pohlert, T., 2014. The pairwise multiple comparison of mean ranks package (PMCMR). , http://CRAN.R-project.org/package=PMCMR.

Purcell, J., & M. Decker, 2005. Effects of climate on relative predation by scyphomedusae and ctenophores on copepods in Chesapeake Bay during 1987-2000. Limnology and Oceanography 376–387.

Purcell, J. E., 1997. Pelagic cnidarians and ctenophores as predators: selective predation, feeding rates, and effects on prey populations. Annales de l'Institut oceanographique 73: 125–137.

Purcell, J. E., 2009. Extension of methods for jellyfish and ctenophore trophic ecology to large-scale research. Hydrobiologia 616: 23–50.

Purcell, J. E., 2012. Jellyfish and ctenophore blooms coincide with human proliferations and environmental perturbations. Annual Review of Marine Science 4: 209–235.

Purcell, J. E., E. D. Brown, K. D. E. Stokesbury, L. H. Haldorson, & T. C. Shirley, 2000. Aggregations of the jellyfish *Aurelia labiata*: abundance, distribution, association with age-0 walleye pollock, and behaviors promoting aggregation in Prince William Sound, Alaska, USA. Marine Ecology Progress Series 195: 145–158.

Purcell, J. E., & J. Cowan Jr., 1995. Predation by the scyphomedusan *Chrysaora quinquecirrha* on *Mnemiopsis leidyi* ctenophores. Marine Ecology Progress Series 129: 63–70.

Purcell, J. E., D. A. Nemazie, S. E. Dorsey, E. D. Houde, & J. C. Gamble, 1994. Predation mortality of bay anchovy *Anchoa mitchilli* eggs and larvae due to scyphomedusae and ctenophores in Chesapeake Bay. Marine Ecology Progress Series 114: 47–58.

Purcell, J. E., J. R. White, D. A. Nemazie, & D. A. Wright, 1999. Temperature, salinity and food effects on asexual reproduction and abundance of the scyphozoan *Chrysaora quinquecirrha*. Marine Ecology Progress Series 180: 187–196.

Purcell, J., S. Uye, & W. Lo, 2007. Anthropogenic causes of jellyfish blooms and their direct consequences for humans: a review. Marine Ecology Progress Series 350: 153–174.

Rakow, K. C., & W. M. Graham, 2006. Orientation and swimming mechanics by the scyphomedusa *Aurelia sp*. in shear flow. Limnology and Oceanography 51: 1097–1106.

Richardson, A. J., A. Bakun, G. C. Hays, & M. J. Gibbons, 2009. The jellyfish joyride: causes, consequences and management responses to a more gelatinous future. Trends in Ecology and Evolution 24: 312–322.

Ricklefs, R. E., & M. Lau, 1980. Bias and Dispersion of Overlap Indices: Results of Some Monte Carlo Simulations. Ecology 61: 1019.

Robinson, K., J. Ruzicka, M. B. Decker, R. Brodeur, F. Hernandez, J. Quiñones, M. Acha, S. Uye, H. Mianzan, & W. Graham, 2014. Jellyfish, Forage Fish, and the World's Major Fisheries. Oceanography 27: 104–115.

Schuyler, Q., & B. K. Sullivan, 1997. Light responses and diel migration of the scyphomedusa *Chrysaora quinquecirrha* in mesocosms. Journal of Plankton Research 19: 1417.

Sexton, M. A., 2012. Factors influencing appearance, disappearance, and variability of abundance of the sea nettle, *Chrysaora quinquecirrha* in Chesapeake Bay. University of Maryland for Environmental Science.

Sexton, M. A., R. R. Hood, J. Sarkodee-adoo, & A. M. Liss, 2010. Response of *Chrysaora quinquecirrha* medusae to low temperature. Hydrobiologia 645: 125–133.

Soberón, J., & M. Loevinsohn, 1987. Patterns of Variations in the Numbers of Animal Populations and the Biological Foundations of Taylor's Law of the Mean. Oikos 48: 249.

Steele, J. H., 1974. The structure of marine ecosystems. Harvard University Press, Cambridge.

Stehman, S. V., & D. W. Salzer, 2000. Estimating density from surveys employing unequal-area belt transects. Wetlands 20: 512–519.

Suzuki, K. S., A. Yasuda, Y. Murata, E. Kumakura, S. Yamada, N. Endo, & Y. Nogata, 2016. Quantitative effects of pycnocline and dissolved oxygen on vertical distribution of moon jellyfish *Aurelia aurita* s.l.: a case study of Mikawa Bay, Japan. Hydrobiologia 766: 151–163.

Taylor, L. R., 1961. Aggregation, variance and the mean. Nature 189: 732–735.

Taylor, L. R., & R. A. J. Taylor, 1977. Aggregation, migration and population mechanics. Nature 265: 415–421.

Taylor, L. R., I. P. Woiwod, & J. N. Perry, 1978. The Density-Dependence of Spatial Behaviour and the Rarity of Randomness. The Journal of Animal Ecology 47: 383.

Wiens, J. A., 1989. Spatial Scaling in Ecology. Functional Ecology 3: 385.

Zavodnik, D., 1987. Spatial aggregations of the swarming jellyfish *Pelagia noctiluca* (Scyphozoa). Marine Biology 94: 265–269.

Zhang, X., M. Roman, D. Kimmel, C. McGilliard, & W. Boicourt, 2006. Spatial variability in plankton biomass and hydrographic variables along an axial transect in Chesapeake Bay. Journal of Geophysical Research 111: C05S11.

Table 2. 1 Regression of abundance measured by surface counting and net haul methods

Regression between abundances collected by	Slope	r^2	*P* value
Max Dock ~ Net	3.84	.91	<1e−6
Max Visual ~ Net	3.88	.82	<1e−6
Min Dock ~ Net	0.384	.91	<1e−6
Min Visual ~ Net	0.388	.82	<1e−6

Maximum and minimum abundances were calculated for surface counting methods due to uncertainty in the depth to which these methods sample. Maximum and minimum abundances were calculated using 0.1-m and 1-m visual depths, respectively

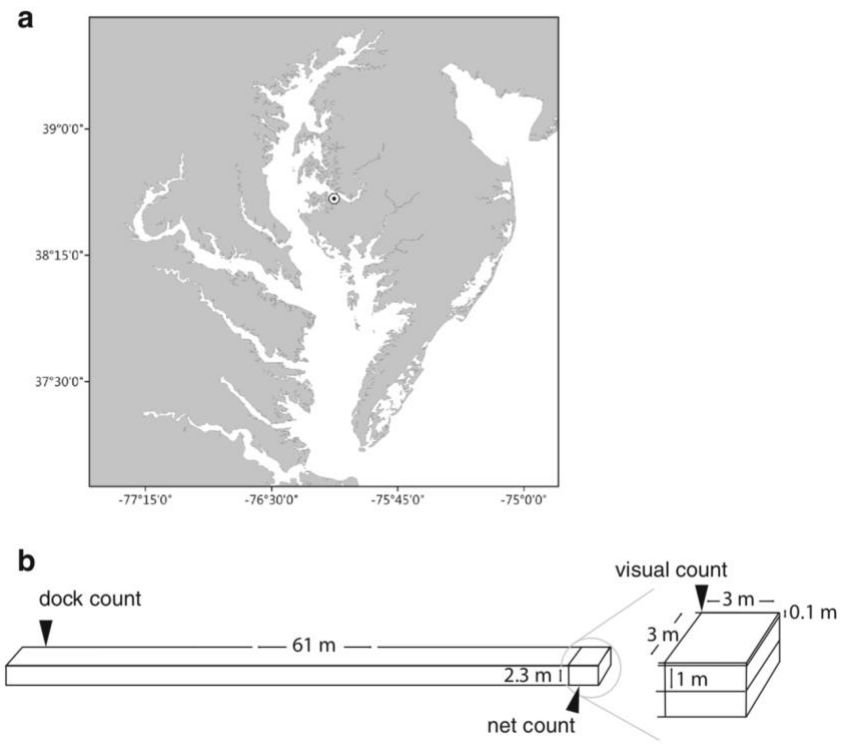

Fig. 2. 1 Conceptual diagram of sampling location

a. Chesapeake Bay, USA with the sampling location at Horn Point Laboratory (HPL) in the Choptank River denoted by the dot b. Counts of medusae were collected using three sampling methods - two surface counting (dock and visual) methods and a vertical net haul (net). The values reflect the dimensions that are sampled by each of the methods. To compare the abundances sampled by surface (dock and visual) counts with those sampled by net counts, a minimum, 0.1 m, and maximum, 1 m, depth was used to calculate maximum and minimum abundance, respectively

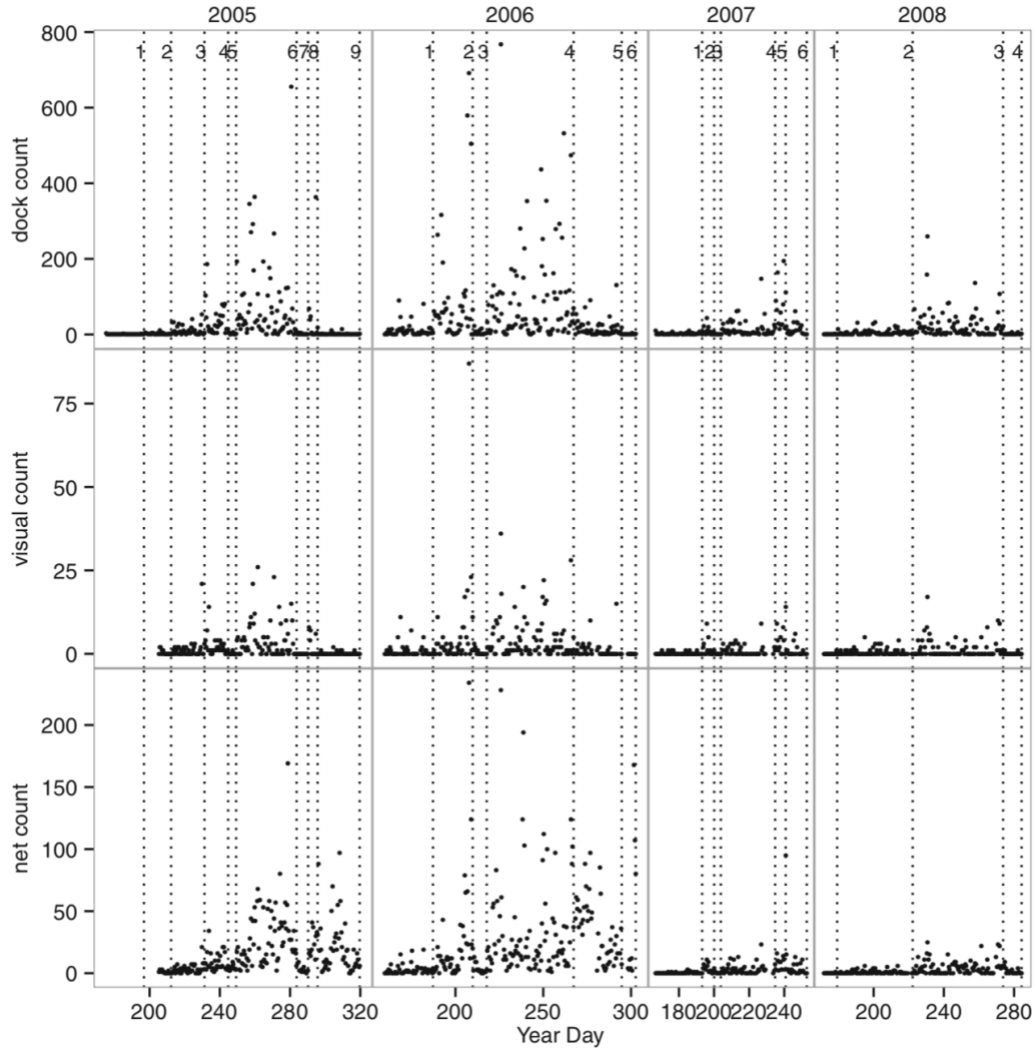

Fig. 2. 2 Twice daily *Chrysaora quinquecirrha* medusa counts for three different sampling methods (dock, visual, net)

Counts collected at Horn Point Laboratory from 2005 to 2008 for three different sampling methods Dotted vertical lines represent change points detected using the Segmentor3IsBack package (Cleynen et al., 2014) in R. Numbers refer to segment numbers

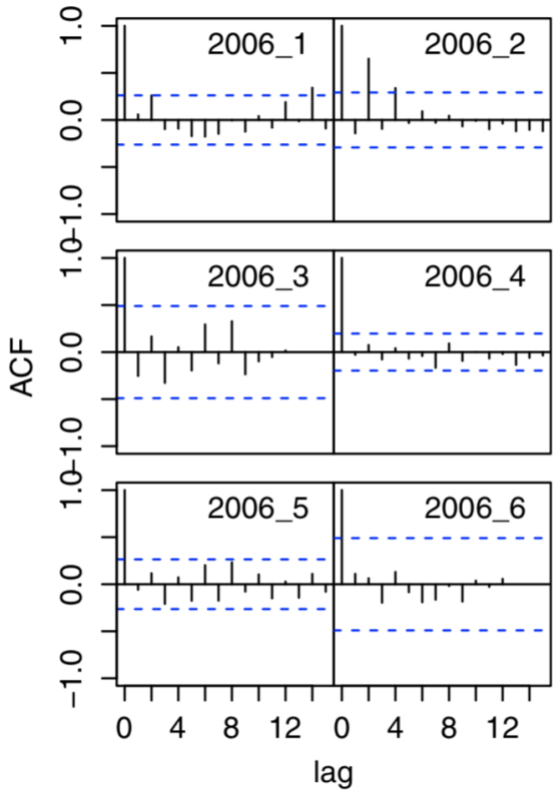

Fig. 2. 3 Autocorrelation function for each 2006 segment for dock counts

Lag is in units of sampling points (2 sampling points per day). Blue dashed lines denote significance (p = .05). Most segments had no significant autocorrelation. Segment 2 in 2006 was an exception and showed high correlation at lag 2

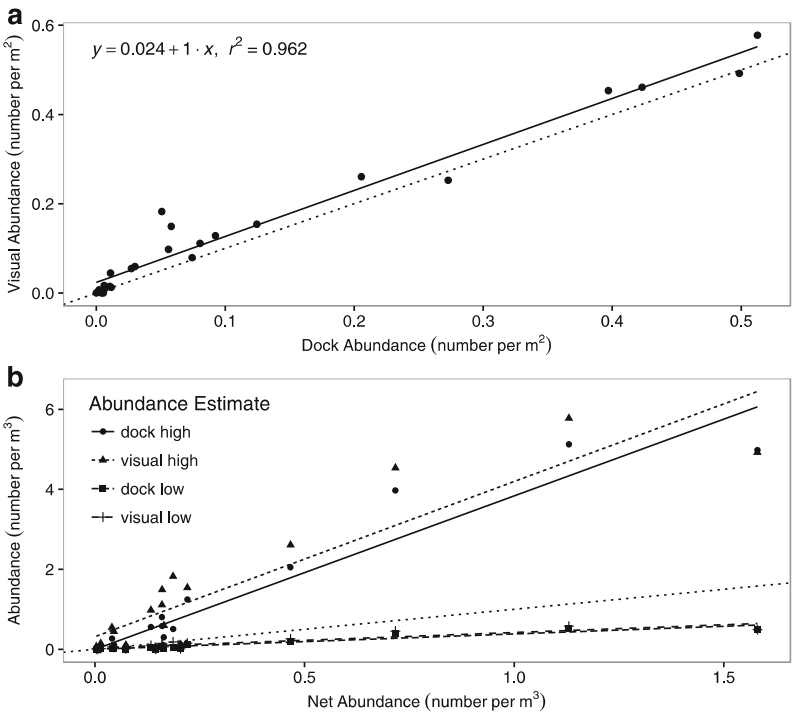

Fig. 2. 4 Linear regressions of abundance as collected by different sampling methods

Dotted line represents 1:1 line that is expected if two methods give the same estimate of abundance. a. Regression between abundances in number m^{-2} collected by the two surface counting methods. The slope was not significantly different from 1. b. Regression between the abundances in number m^{-3} collected by the net count and the surface counting methods. Because the depth to which medusae were observed from surface counting was ambiguous, a minimum, 0.1 m, and maximum, 1 m, depth were used to calculate a maximum (high) and minimum (low) abundance, respectively, for the two surface counting methods. The abundances were significantly related (see text)

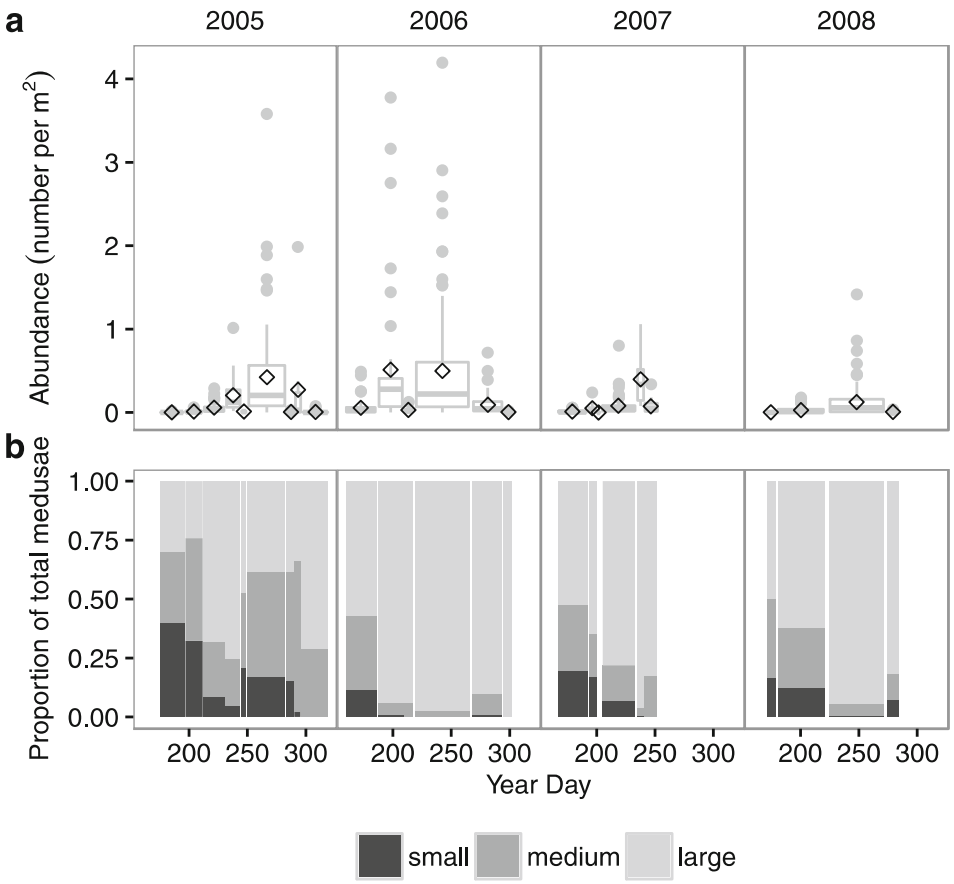

Fig. 2. 5 Abundance and size distribution of medusae

a. Abundance medusae per square meter as measured by dock counts. The abundance for each segment is denoted by diamonds. Grey boxplots show median, interquartile range, and extreme values of abundances collected during each time series segment. b. Proportion of total medusae that fall within each size category for each segment as measured by dock counts. Medusae were categorized as small (<4 cm), medium (4-8 cm), or large (>8 cm) using visual estimation. Width of the boxplot denotes the duration of the segment for both panels

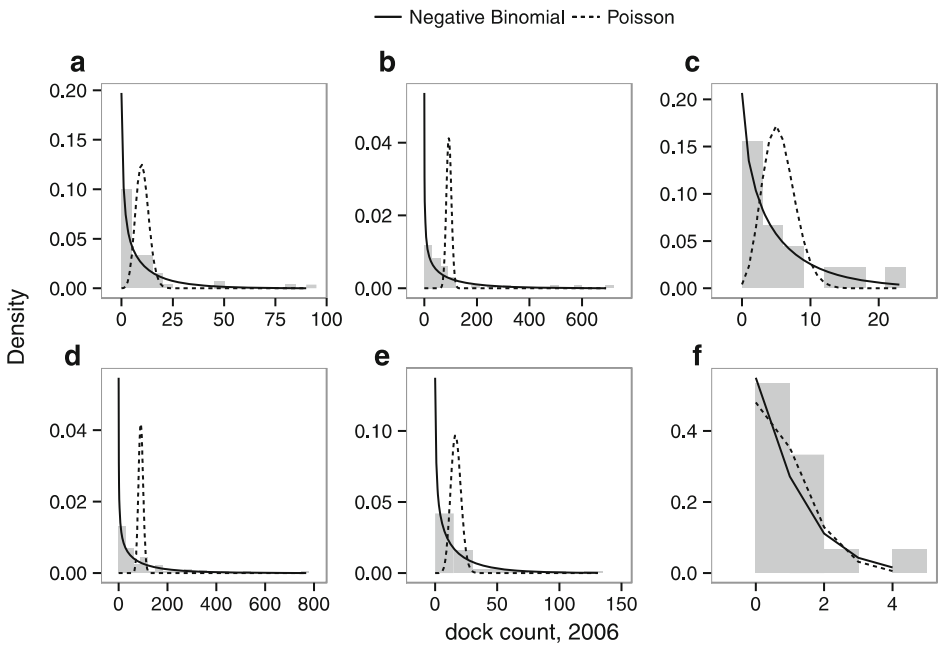

Fig. 2. 6 Histograms for each 2006 segment for dock counts and maximum likelihood fits to both the Poisson (dotted line) and Negative Binomial (solid line) distributions

Units of density are probability per count. a-f represent Segments 1-6, respectively

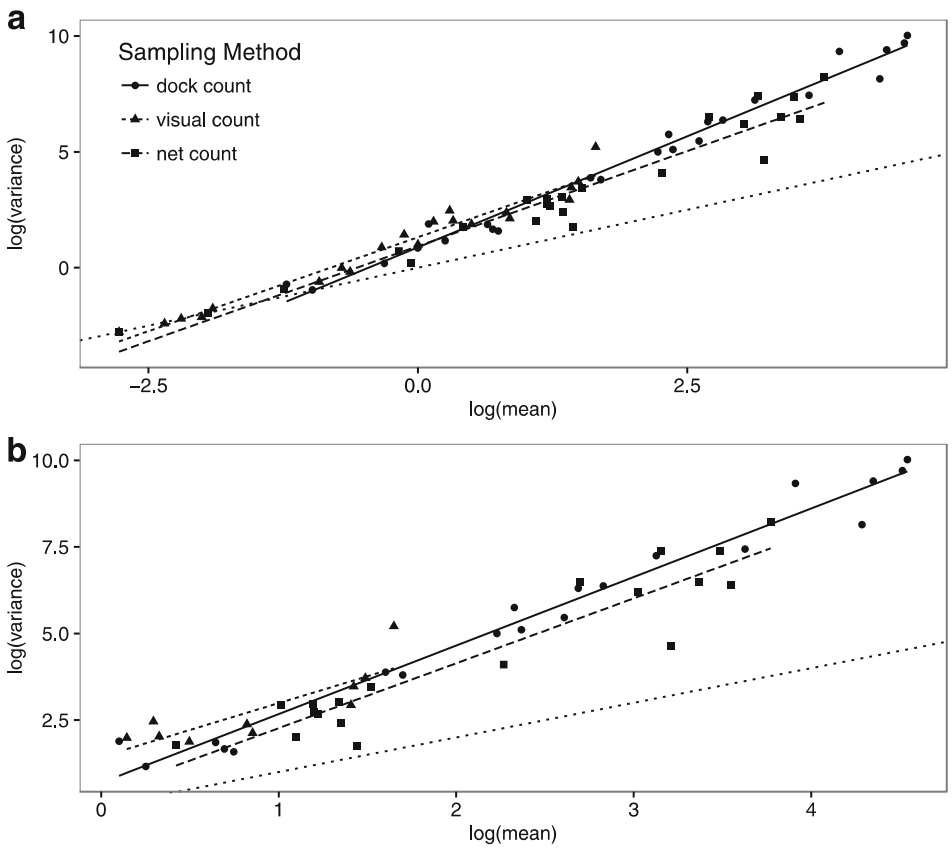

Fig. 2. 7 Taylor's Power Law (TPL) for *Chrysaora quinquecirrha* medusae

Each point is the relationship between the log(mean) and log(variance) of one segment. a. TPL for all data b. TPL with low counts (log(mean) less than 0 removed). The power exponent (slope) was 2 ($F(2,43) = .71$, $p = .5$, 1.71 – 2.03 95% CI)

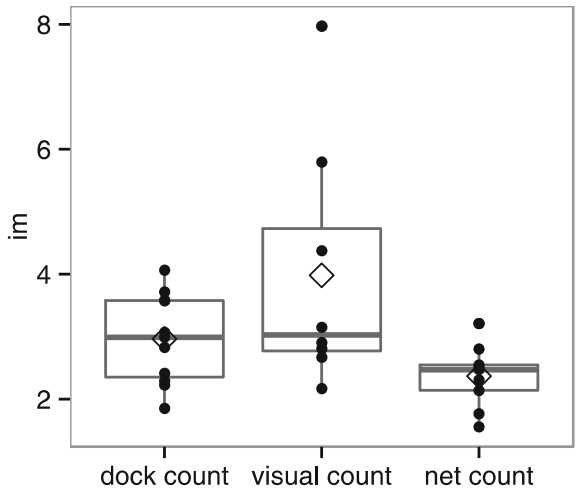

Fig. 2. 8 Morisita's Index (Im) for each sampling method

Points represent Im for individual segments. Boxplots show median and interquartile range. Diamonds represent the mean. Im is different between sampling methods as shown through weighted-least squares regression and Kruskal-wallis ($F(2,25) = 4.27$, $p = .025$, Kruskal-wallis chi-sq(2) = 6.18, $p = .045$). Conover's test shows that Im for the net count was significantly different from the visual count ($p = .042$), but other post-hoc pairwise comparisons failed to detect differences

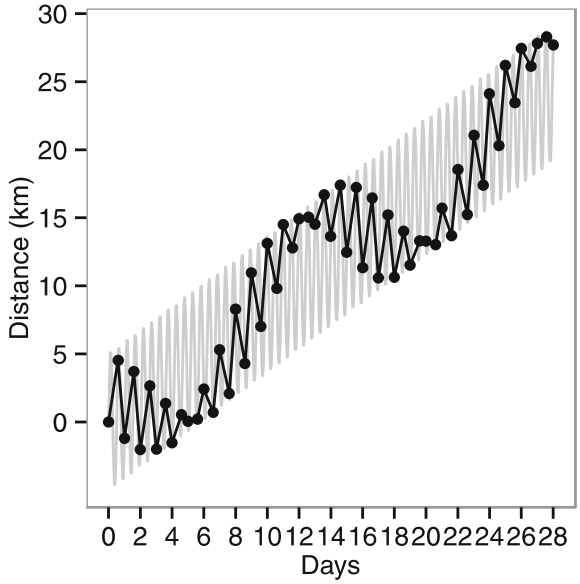

Fig. 2. 9 Conceptual diagram showing how the temporal sampling scheme maps onto space assuming simple 1-dimensional motion of surface water due to advection and tides

The distance from x0 (the sampling location at time 0) is plotted over time. Grey lines show continuous sampling and black points show actual sampling. Three non-random spatial patterns are traced by the sampling scheme: downstream advection and two patterns generated by aliasing in which samples collected 1 and 14 days apart are closer with respect to their location in the tidal extent

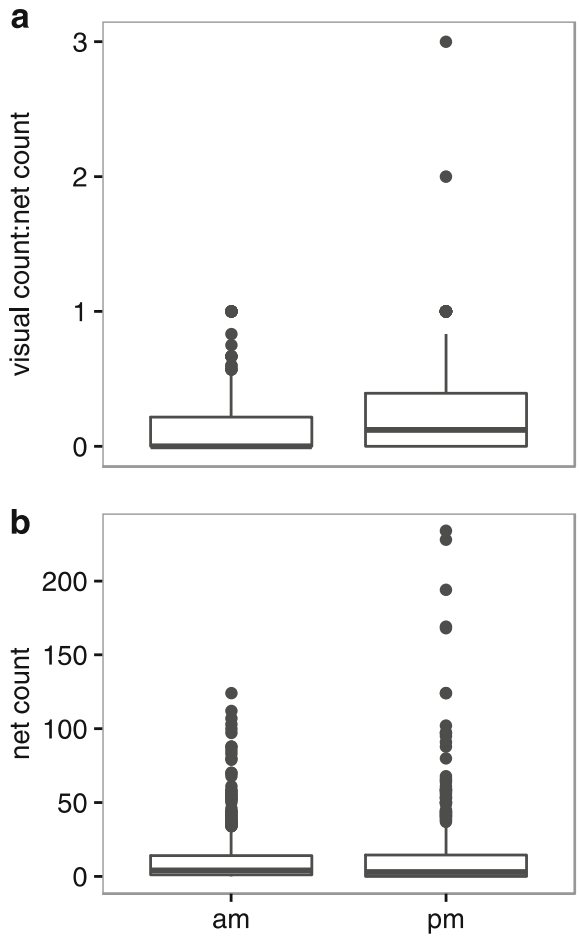

Fig. 2. 10 Comparison of medusae counts between morning and evening

a. Ratio of medusa numbers sampled from the visual and net count methods separated into morning and evening samples. A higher proportion of medusae are found in the surface in the evening than in the morning (Wilcox = 40610, p = 1.92 e-05). b. Medusae counts sampled by the net, showing that the difference in a. is not due to difference in water column counts between the morning and evening (Wilcox = 90102, p = 0.67). Boxplots for both panels show median, interquartile range, and extreme values

Chapter 3: Model development and calibration using Approximate Bayesian Computation: An estuarine ecosystem model with jellyfish as an example

Abstract

Ecological models are not based on fundamental governing laws, but rather rely on the knowledge and judgement of the modeler. Data assimilation may help calibrate the model more objectively, which would highlight inadequacies in the model formulation. Therefore, I use a data assimilation method, Approximate Bayesian Computation, to calibrate and guide the development of a process-based aquatic ecosystem model, specifically to represent gelatinous top predators in the Chesapeake Bay, USA. Using the development workflow, the model fidelity to observations was improved by the addition of refractory non-living organic materials. I found the form of the cost function and the metrics of skill assessment should be carefully considered. Additionally, improvements in documentation of both structure and process would be helpful to improve model transparency and assessment. Overall, these issues highlight the need for continued improvements in understanding the uncertainty and adequacy of models.

Introduction

Numerical models are important for understanding and, increasingly, predicting the dynamics of nature, however there are no fundamental governing laws for ecological systems. Therefore, model developers must use their judgement and intuition in choosing model complexity and structure, equations, and parameters. One large class of ecological models are process-based aquatic ecosystem models (also called biogeochemical or nutrient-phytoplankton-zooplankton (NPZ) models). Model

complexity may be between 2 to 90 state variables (Arhonditsis & Brett, 2004) with various combinations of fluxes. The main NPZ processes may be formulated using between 5 to 20 commonly used equations (Tian, 2006). Lastly, there are often a large number of process rate parameters, which must be assigned values. These parameters are often largely unconstrained or unidentifiable (Schartau et al., 2017) due the difficulty in directly measuring these processes, the differing scales between models and experiments or measurements, and/or insufficient data.

Furthermore, the evidence is overwhelming that small changes in model complexity, structure, equations, and parameters can fundamentally alter the response of the model system to external forcing, leading to different results and conclusions (e.g. Anderson et al., 2010; Davidson, 1996; Edwards, 2001; Gentleman et al., 2003; Keohane et al., 2019; Lignell et al., 2013; Löptien, 2011; Mitra, 2009; Mitra et al., 2014; Spitz et al., 2001; Steele & Henderson, 1992; Steele & Henderson, 1995; Taucher & Oschlies, 2011). Ultimately, the modeler and other users want to be assured that the model is adequate to address the questions of interest and to ascertain the uncertainty in the results. Both adequacy and uncertainty are often assessed by calculating model-observation error through a metric(s) of model skill, and ideally, using data that is independent from that used to calibrate the model. Poor model skill results from inadequacies in the model formulation (defined here as the complexity or number of state variables, the structure or linkages between state variables, and the

equations) as well as poor parameter choice (described in Vallino, 2000; Beven, 2005).

It has been proposed that formulation and parameter error can be separated by using data assimilation (Kennedy & O'Hagan, 2001; Vallino, 2000; Spitz et al., 2001). As opposed to the typical method of manual tuning, which relies on modelers' intuition and expertise, data assimilation should objectively select the parameters that result in the best fit to observations (described in Arhonditsis & Brett, 2004; Rothstein et al., 2006). Because the parameter space is well searched, any lack of fit between the model and observations is less likely to be a problem with the parameters and more likely to be inadequacy in the model formulation. The model can then be reformulated to better represent the system (Kawamiya, 2002; Kennedy & O'Hagan 2001; Spitz et al., 2001).

While several data assimilation schemes exist (Dowd et al., 2014; Vallino, 2000), Bayesian approaches do not search for a single optimum parameter value, but instead return the posterior distribution of the parameter, which is the probability of the parameter given the model and the data. Having this distribution of parameters is beneficial in that it has the potential to take into account the uncertainty in the calibration data. Additionally, returning a suite of parameter sets takes into account the problem of parameter identifiability, when the parameters cannot be constrained to a unique set by the available data. Of the Bayesian parameter estimation methods, Approximate Bayesian Computation (ABC) has gained recent attention and is being

used in diverse fields (Beaumont, 2010; Csillery et al., 2010; Lintusaari et al., 2016; Toni et al., 2009). ABC is a method that should approximate the posterior distribution when the distance between the observed and predicted data is small and converges to the posterior distribution as the difference approaches zero. ABC is useful when models are complex and the evaluation of the likelihood is computationally prohibitive. There are several ABC algorithms, and the ABC-rejection scheme is the simplest to implement.

While data assimilation has been used to guide model development (Spitz et al., 2001) and Bayesian methods have been used for calibration (Arhonditsis et al., 2011), to my knowledge, Bayesian methods have not yet been used in a workflow to calibrate and guide the development of an ecological model. Therefore, my goal was to use Bayesian methods (the ABC-rejection scheme) for objective calibration that would isolate structural inadequacies and guide a workflow to develop a suitable model for the given question. The structure of this paper deviates slightly from many other modeling papers in that the model description is presented in the results, as the model formulation was a result of the workflow laid forth in the methods section. The discussion comments on both the model formulation as well as the development workflow more generally.

Methods

Our goal was to use Approximate Bayesian Computation (ABC) to calibrate parameters and guide the development of a mechanistic ecosystem model. Existing

model development workflows (Jakeman et al., 2006; Jorgensen & Fath, 2011; Soetaert & Herman, 2009) contain four main steps that are iterated through until the model adequately represents the observations: defining the problem of interest, conceptualizing and formulating the model, calibration, and skill assessment.

Step 0: Define the problem

The modeling workflow began with defining the problem of interest and specifying the available data resources.

Step 1: Conceptualize and formulate model

The initial model formulation was chosen based on past observational and modeling studies in the region. The ranges for each parameter in the model were determined through a search of the literature. For parameters with highly uncertain bounds, the range was set to span at least 1 order of magnitude.

The models were written in Fortran and numerically solved using the function "ode" from the R (version 3.4.1) package deSolve (Soetaert & Herman, 2009). The function ode was set to use the solver method lsoda, which switches between stiff and non-stiff methods automatically. The minimum and maximum value of the integration step size (parameter: hmin and hmax) were set to 0 and 1e-3 days, respectively. The absolute and relative error tolerances (parameters atol and rtol) were set to 1e-8. The maximum number of steps per output interval (maxsteps) was set to 400,000 steps.

All simulations were run to steady state. Simulations that were oscillating or did not reach steady state were removed from the analysis.

Step 2: Calibration using ABC

The ABC-rejection scheme was used to calibrate the model. First, Monte Carlo model simulations were generated from 1e6 randomly-generated parameter sets. To develop parameter sets, each parameter was sampled independently from a uniform or a log distribution, and the latter was chosen if the parameter's range spanned several orders of magnitude to most efficiently sample the parameter space. Second, in the rejection step, the steady state model results were compared to the observations and the parameter sets with the lowest total cost were accepted. To understand the effect of cost function choice, two cost functions were used: the squared percentage error (SPE):

$$SPE = \sum_{i}^{N} \left(\frac{predicted_i - observed_i}{observed_i}\right)^2$$

and the Reliability Index (RI; Leggett & Williams, 1981; Stow et al., 2009):

$$RI = \sum_{i}^{N} log\left(\frac{predicted_i}{observed_i}\right)^2,$$

,where i represents the state variable and N represents the total number of observations. In order to assess the effect of the acceptance threshold on the results,

the 10, 100, and 1000 parameter sets with lowest total cost were selected for each cost function.

Step 3: Assess skill

In order to assess whether the model was capturing the properties of the system, plots comparing the simulated steady state biomasses and observations were examined. The model structure was deemed inadequate if the range of the predictions did not fall within the region of the observed mean +/- 1 S.D. (also referred to herein as the observed range or range of observations). The mismatch represents the inability of the model to capture processes in the observations. And ideally, for an adequate model, the median of the predictions, which represent the most likely result, would fall within the observed error. Skill was assessed using the observations used for calibration as well as an independent set of observations.

Step 4: Go back to step 1 (reconceptualize and reformulate the model) or Stop when model is satisfactory

In order to improve model behavior, hypotheses were made about the causes of the mismatch and the experimental, observational, and modeling literature was surveyed to look for guidance and solutions. Once a new model was conceptualized and formulated, the calibration step was repeated. This process was iterated with the goal of obtaining an adequate model as described in the skill assessment (Step 3).

Results

Step 0: Define the problem

The model in this paper was developed to explore the role of the gelatinous top predator, *Chrysaora chesapeakei* (the sea nettle), in the Chesapeake Bay. *C. chesapeakei* populations have decreased since the 1960s (Breitburg & Fulford, 2006). It is hypothesized that their decline in the mesohaline mainstem of the Bay triggers a trophic cascade that results in an undesirable planktonic ecosystem with low mesozooplankton (Feigenbaum & Kelly, 1994; Purcell & Decker, 2005) and high phytoplankton biomass (Kimmel et al., 2012; Testa et al., 2008). This hypothesis is based on field observations, where other confounding factors are changing simultaneously, making it unclear whether the changes are solely due to declines in sea nettles. Furthermore, the complexity in the Chesapeake Bay planktonic food web, including microzooplankton and microbes, may alter or minimize the effects of changes in *C. chesapeakei*. Due to the time (interannual) and spatial (Chesapeake Bay mainstem) scales and complexity (the planktonic ecosystem), a model is an ideal tool to isolate and study the effect of changes in the population of the top predator.

Data from the Chesapeake Bay Program (CBP) Water Quality and Plankton Monitoring Program for the years 1990-2000 were available to force as well as calibrate and assess the skill of the model. Water quality parameters included: nitrate and nitrite, ammonium, dissolved and particulate organic nitrogen (in mmol N m^{-3}), chlorophyll (ug l^{-1}), total suspended solids (mg l^{-1}), and salinity. Plankton

observations included: mesozooplankton and microzooplankton (individuals per m^{-3}). All zooplankton were converted to nitrogen units. Mesozooplankton observations were separated into 3 biomass pools: large zooplankton (LZ; which consisted of the copepod taxa Acartia and Eurytemora), Mnemiopsis (MNE), and Chrysaora (CHRY). A biomass pool named small zooplankton (SZ) was calculated from the three dominant taxa in the microzooplankton observations (ciliophora, rotifera, and copepoda nauplii). Additionally, as heterotrophic microflagellates were not sampled by the monitoring program, their biomass was included using a statistical relationship between heterotrophic microflagellates and ciliates (Dolan & Coats, 1990). All observed quantities were averaged for the summer (days 182-273) either for the bottom layer or the surface layer and above pycnocline locations. Data from Station CB2.2, representing the oligohaline boundary, and CB4.3C, representing the mesohaline region of the mainstem of Chesapeake Bay, were used to force and calibrate the model, respectively.

Step 1: Conceptualize and formulate the model

As the features of interest were gelatinous predators as well as the complexity of the food web, the initial iteration of the model formulation (Fig. 3. 1 Visual adjacency matrices of the initial (left), final (middle), and difference between the two versions model of the summer mesohaline Chesapeake Bay planktonic food web, which includes gelatinous predatorsleft) was based on models with similar state variables and levels of complexity:

Oguz et al. 2001, which includes five zooplankton state variables, including two gelatinous zooplankton, and bacteria; Keller and Hood 2011, which includes two zooplankton compartments, DON and bacteria; and Fasham et al. 1990, which contains DON and bacteria. The resulting 11-state variable model tracks nitrogen mass in units of mmol N m^{-3} (equivalent to umol N l^{-1}). Six state variables represent living functional groups or species: phytoplankton (P), bacteria (B), microzooplankton (SZ), mesozooplankton (LZ), *Mnemiopsis* (MNE), and *Chrysaora* (CHRY). Three state variables represent nutrients: dissolved inorganic nitrogen (NH4 and NO3) and labile dissolved organic nitrogen (DON). The final two state variables represent solids: organic detritus (DET) and inorganic suspended solids (ISS). ISS (mg L^{-1}) is not a nitrogen-based state variable and does not directly interact with the other state variables but is included to modulate the light field.

While the Chesapeake Bay is a physically dynamic system, the focus of the research is on ecological processes, thus physical processes are represented simply as flows in and out of the system. The 0-dimensional model was implemented similarly to Keller and Hood 2011, Kemp et al. 2001, Stickney et al. 1999, Keohane et al. 2019. However, the flows were calculated using a 2-D box model of a salt wedge estuary (Officer 1980; Pritchard, 1969) and include cross-pycnocline exchange.

For brevity, only the representation of the zooplankton are described in detail here. The Supplemental Materials contains the full set of model equations.

Grazing

Small and large zooplankton graze on multiple prey types according to:

$$Grazing_j^i = \frac{p_{i,j} * g_{max,j} * N_j N_i}{k+R} \; ; \; R = \sum_{r=1}^{n} p_{r,j} N_r \; ;$$

where N_j represents the predator (LZ or SZ), N_i represents the resource, N_r is the resource available to N_j, $p_{i,j}$ is the preference of j on i, $g_{max,j}$ is the maximum grazing rate of j, R is weighted available resource density (as in Gentleman et al., 2003; Keller & Hood, 2011). This is an extension of the single-resource Michaelis-Menten functional form where preference for a given prey type is fixed (no switching) and the half saturation coefficients (k) for all prey types are the same (Class 1A; Gentleman et al., 2003). This formulation assumes that predators attack and handle only one resource at a time and that there is no dependence of the handling time and attack rate success due to density (Gentleman et al., 2003). Small zooplankton graze on B, P, SZ (cannibalism/ intraguild predation), and DET. Large zooplankton graze on P, SZ, LZ, and DET.

MNE and CHRY also graze on multiple prey types, however, their functional response is linear (Class 1D; Gentleman et al., 2003), as jellyfish tend not to saturate in grazing under natural prey conditions (Clifford & Cargo, 1978):

$$Grazing_j^i = \frac{p_{i,j} * g_{max,j} * N_j N_i}{p_{tot}}$$

Where N_j represents the biomass of MNE or CHRY, N_i represents the resource, $g_{max,j}$ is the maximum grazing rate of j, p_{tot} is used to scale the preferences to 1. Their prey preference is also fixed (no switching). The preferences are scaled such that $\sum p_i = 1$ in order for the parameter for (max) grazing rate to be the same for all prey types and as such, more easily interpretable. MNE graze on SZ, LZ and DET. CHRY graze on SZ, LZ, MNE and DET.

The grazed material has two fates: to increase zooplankton biomass due to growth or to move to non-living pools due to egestion and sloppy feeding. This fate is partitioned using one parameter for assimilation efficiency for each of the grazers.

Mortality and excretion

The 4 zooplankton compartments are lost due to non-predatory mortality that is modeled as a linear loss (Oguz et al., 2001). Each zooplankton excretes NH4 waste, which is also modeled as a linear loss.

Step 2: Calibration using ABC

The ranges for each parameter in the model were determined through a search of the literature and are fully documented in the Supplemental Materials. The model was calibrated using an ABC-rejection scheme with two different cost functions and three thresholds for acceptance. The two cost functions resulted in different predictions for the state variables (Fig. 3. 2, Fig. 3. 3), which will be described in more detail in the next section on assessing skill. Generally, the predictions from SPE had less

variability than those from RI for a given year. Additionally, the number of parameter sets accepted did not drastically alter the predictions of the state variables. As expected, the widest acceptance (1000 parameter sets) resulted in the widest variance in the predictions.

Steps 3: Assess skill

In the initial version of the model, the predictions of zooplankton (SZ, LZ, MNE, and CHRY) were systematically lower than the observations regardless of the cost function used to select parameter sets and the threshold of acceptance (Fig. 3. 2). For both cost functions, the predictions of NH4 and NO3 fell within the range of observations (except NO3 for 1990, which was under-predicted). CHLA was well-predicted for some years but over-predicted for others, and was better for more years for the RI compared to SPE. PON and TSS were also predicted well in some years for RI but were mostly under-predicted for SPE. DON was over-predicted for both cost functions. However for RI, the range of DON predictions selected using the larger tolerance did overlap with the observed range.

Step 4: Reconceptualize and reformulate model

Through iterations, I implemented many changes ranging from adding or removing state variables, connections, and modification of the flux equations (which included adding new parameters to the formulation). Based on the variability between models in the literature, most of my attempts were related to changing the structure (linkages) or the form of the equations. I attempted to keep the model as simple as possible and

chose to keep only the modifications that either improved the simulations substantially or were processes that I deemed were overlooked during the initial formulation of the model (such as fish predation). I built the simplest model based on the pragmatic recognition that the ability to understand why the model behaves as it does is greater for reduced dimensionality (not on the belief that nature must be simple).

End: Stop when the model is satisfactory

The final version of the model, which contains representation of refractory detritus and DON (Fig. 3. 1), made predictions for the tuned state variables that fell within the range of observed uncertainty (Fig. 3. 3). Notably, the zooplankton predictions overlapped with the range of observations. The median of the predictions was more likely to fall within the range for the RI compared to SPE, which systematically under-predicted the zooplankton observations. CLHA, PON, and TSS were predicted well for most years and both cost functions, however, for some years, the median was predicted to be lower than the observed range. DON was captured well across years and cost functions. I concluded that the model was adequate as the range of observations was captured across state variables, especially using the RI. Additionally, the final version also performed better than the initial version of the model for years that were not used in the calibration stage (1995-2000; Fig. 3. 4a).

Although the predictions for many of the calibrated (non-zooplankton) state variables were relatively comparable between the initial and final versions of the model, there

were large differences between the predictions made for variables that weren't used in the tuning process, such as bacteria and gross primary productivity (Fig. 3. 4b). DON and B were several times higher and lower, respectively, in the final versus initial version of the model. Additionally, gross primary production was about an order of magnitude lower for the final compared to the first version.

Discussion

The expectation was to use ABC to systematically search the parameter space in order to minimize errors due to poor parameter choice as well as provide uncertainty in the parameters. This would allow us to detect problems with model formulation that could then be improved upon (Kennedy & O'Hagan, 2001; Spitz et al., 2001; Vallino, 2000). However, there were different predictions between cost functions (Fig. 3. 2 and Fig. 3. 3) that may suggest that the results were not converging to the posterior distribution, making it somewhat more difficult to isolate the problems due to formulation inadequacies. Nonetheless, the structured approach to model calibration helped us to develop a model formulation that predicted the observations better than the initial version of the model, which was based on previously established formulations. Additionally, we encountered other issues in the model development process that should be further considered in order to improve model development and understanding of model uncertainty. I discuss the resulting model and then comment briefly on each of the model development steps.

Model of Chesapeake Bay planktonic food web in the summertime

The model's ability to predict the observations was improved by adding refractory non-living organic matter (DETR and DONR; Fig. 3. 1). The initial model without refractory pools had high levels of primary production (compared to both observations and the final version), likely leading to high top-level predation by CHRY which kept the zooplankton at low biomass compared to the observations. The final version of the model with refractory pools captured observed zooplankton biomass and had more realistic predictions of primary productivity. However, refractory matter is relatively uncommon in aquatic biogeochemical models as they often only carry labile DON and DET pools, as established in Fasham et al., 1990. Modeling the refractory components may be important for properly capturing nutrient cycling and rates in ecosystem models. This result is concordant with the importance and large size of non-living organic matter in ecosystems (Lindeman, 1942).

Step 1: Conceptualize and formulate the model

I used equations and structure based on other modeling studies that included processes relevant to my questions, which is common practice. To compare and understand the full set of model equations from even a select number of papers was time consuming. Some problems included that equations were not always fully or clearly documented (reviewed in Anderson et al., 2015) and notation and symbols differ between papers. In this paper, I displayed the model complexity and structure

using a visual interpretation of the adjacency matrix (Fig. 3. 1), which I have not yet seen used to document ecological models. This documentation is simple, with the minimum amount of data needed being an adjacency matrix (the state variable names and the presence of linkages). Additionally, the plot is easy to generate, interpret, and helps to make comparisons across models. This is one simple approach to improve documentation, which is needed for transparency and to facilitate communication between researchers (Benz & Knorrenschild, 1997; Benz et al., 2001; Crosier et al., 2003; Grimm et al., 2006; Hoch et al., 1998; Martinez-Moyano, 2012).

Step 2: Calibration using ABC

The goal was to use ABC to objectively calibrate the model in order to separate the error due to parameter misspecification versus formulation deficiencies. However, I found that separating error to be less-straightforward because the predictions depended on the choice of the cost function (there was uncertainty between the cost functions). For the initial version of the model, neither cost function predicted zooplankton within the observed range (Fig. 3. 2), making it simple to conclude that there were structural issues. However, for the final version of the model, while the difference-based cost function (SPE) under-estimated the value of zooplankton, the log-based cost function (RI) was able to better capture the zooplankton observations (Fig. 3. 3). It was not immediately clear how to assess adequacy of the model structure if one cost function deemed the model acceptable, while the other did

not. While it was obvious that the cost functions have different forms, which generated more "correct" results?

In attempting to address this question, I came across two different but likely overlapping perspectives related to cost functions. The first perspective is that there is no objectively "correct" cost function, but that cost functions are metrics that translate a researchers' informal and subjective interest into the formal language of mathematics (Hennig & Kutlukaya, 2007). The SPE fails to penalize errors between 0 and the observed value (Fig. 3. 5a, c), which may lead to errors of the zooplankton state variables, which are small in magnitude, to be mostly ignored. Conversely, the RI will penalize the errors in both directions of the observed values equally (Fig. 3. 5b, d), which may make it more appropriate when calibrating using data that spans several orders of magnitude and includes very small values.

The second issue is from the lens that the difference in between the cost functions is due to deficiencies in ABC to return a proper posterior distribution. ABC may fail because of the information loss in a cost function, also known as insufficiency of summary statistics. This idea is likely related to the idea discussed above. Another reason ABC may fail is due to the prior distribution and how the cost function interacts with the prior. For this model, the distribution of the full set of unfiltered results, which is driven by the random parameter input and the model equations, was not uniform but were right skewed and underestimated the observed zooplankton biomass (Fig. 3. 6). This skew together with the tendency for the SPE to under-

penalize small values may be leading to systematic under prediction in the accepted simulations.

Despite some difficulties assuming that the ABC-rejection method returns results with rigorous Bayesian statistical properties of a proper posterior distribution, this method is still deemed useful in detecting structural issues. The systematic search of the parameter space is more repeatable, and more comprehensive and complete, than manual tuning. Additionally, the task of setting a cost function is a mathematical formalization of modelers' project goals and the resulting model strengths and weaknesses. Furthermore, using several cost functions helped increase the confidence that the error was due to the model misspecification when both cost functions failed to find good agreement between the model and the observations.

Step 3: Assess skill or Stop

Skill was assessed using two cost functions (goodness-of-fit) but also by a more qualitative assessment of the predictions' ability to overlap with the range of the observations (Fig. 3. 2 and Fig. 3. 3). Many quantitative and qualitative assessments exist (Jakeman et al., 2006; Jorgensen & Fath, 2011; Olsen et al., 2016; Stow et al., 2009) and multiple metrics are likely required to describe different aspects of the model's ability to capture different features of the system. In this study, skill was assessed using 10 variables, including zooplankton, which is not the norm. In fact, often there may only be observations for nutrients and CHLA, and if these were the only variables in the assessment, the initial version of the model may have been

deemed adequate (Fig. 3. 2). Therefore, assessment is limited by data availability. Furthermore, models are impossible to fully evaluate or "validate" due to unknown processes as well as the inability to close natural systems (Beven, 2002; Oreskes et al., 1994). Some solutions to addressing this model uncertainty have been to assess the process by which a model is produced (described in Jakeman et al., 2006; Ravetz, 1997) or to compare different models (perhaps that differ in their first principles) (Beven, 2002; Journel, 1997). Methods and philosophies for understanding model structural error and adequacy is an area in need of continued study (Beven, 2002).

Step 4: Reconceptualize and reformulate the model

Through many iterations, I implemented changes ranging from adding or removing state variables, connections, and modification of the flux equations (which included adding new parameters to the formulation). Based on the type of variability between models in the literature, most of my attempts were related to changing the structure (linkages) or the form of the equations (Anderson et al., 2010; Gentleman et al., 2003; Keohane et al., 2019; Mitra, 2009; Mitra et al., 2014; Steele & Henderson 1992; Steele & Henderson, 1995). However, changing the model complexity (adding DETR and DONR) was more effective in improving the results. The addition of detritus has previously been shown to alter model behavior (Edwards, 2001), but this finding could also reflect a more general principle regarding the importance of complexity versus equation form in driving model variability.

Initially, I assumed that by finding structural deficiencies, it would be clear which changes would need to be made to improve the representation of the system. I quickly realized that there was no rational unbiased method for choosing how to solve the structural problems and we defaulted to trial-and-error, making changes based on intuition, discussion with colleagues, and searches through the observational, experimental, and modeling literature for suggestions. In retrospect, I see the use of keeping and publishing a modeling log that entails the formulations tried during development. Each "failed" model represents a hypothesis that was rejected (Anderson & Mitra 2010; Franks, 2009), which is useful for further understanding how we model natural processes. Additionally, a log would make the model building process more reproducible (similar to efforts to improve the literature review process; Wolfswinkel et al., 2013) and also capture the immense amount of modeling effort and expertise that is largely undocumented.

Conclusions

This work documents the development of an adequate aquatic ecosystem model to address questions related to gelatinous top predators. The model fidelity to observations was improved by the addition of refractory non-living organic materials. The primary thrust was to use Approximate Bayesian Calibration as a data assimilation method to minimize error due to parameter choice and separate out formulation inadequacy. I found the form of the cost function and the metrics of skill assessment should be carefully considered. Additionally, improvements in

documentation of both structure and process would be helpful to improve model transparency and assessment. Overall, these issues highlight the need for continued improvement related to understanding the uncertainty and adequacy of models.

References

Anderson, T. R., 2010. Progress in marine ecosystem modelling and the "unreasonable effectiveness of mathematics." Journal of Marine Systems 81: 4–11.

Anderson, T. R., W. C. Gentleman & B. Sinha, 2010. Influence of grazing formulations on the emergent properties of a complex ecosystem model in a global ocean general circulation model. Progress in Oceanography 87: 201–213.

Anderson, T. R., W. C. Gentleman & A. Yool, 2015. EMPOWER-1.0: an Efficient Model of Planktonic ecOsystems WrittEn in R. Geoscientific Model Development 8: 2231–2262.

Anderson, T. R. & A. Mitra, 2010. Dysfunctionality in ecosystem models: An underrated pitfall? Progress in Oceanography 84: 66–68.

Arhonditsis, G. B. & M. T. Brett, 2004. Evaluation of the current state of mechanistic aquatic biogeochemical modeling. Marine Ecology Progress Series 271: 13–26.

Arhonditsis, G., S. Stremilov, A. Gudimov, M. Ramin & W. Zhang, 2011. Integration of bayesian inference techniques with mathematical modeling. Treatise on Estuarine and Coastal Science. 9: 173–192.

Beaumont, M. A., 2010. Approximate bayesian computation in evolution and ecology. Annual Review of Ecology, Evolution, and Systematics 41: 379–406.

Benz, J., R. Hoch & T. Legović, 2001. ECOBAS – modelling and documentation. Ecological Modelling 138: 3–15.

Benz, J. & M. Knorrenschild, 1997. Call for a common model documentation etiquette. Ecological Modelling 97: 141-143.

Beven, K., 2002. Towards a coherent philosophy for modelling the environment. Proceedings of the Royal Society of London. Series A: Mathematical, Physical and Engineering Sciences 458: 2465–2484.

Beven, K., 2005. On the concept of model structural error. Water Science and Technology 52: 167–175.

Breitburg, D. L. & R. S. Fulford, 2006. Oyster-sea nettle interdependence and altered control within the Chesapeake Bay ecosystem. Estuaries and Coasts 29: 776–784.

Clifford, H. C. & D. G. Cargo, 1978. Feeding rates of the sea nettle, *Chrysaora quinquecirrha*, under laboratory conditions. Estuaries 1: 58–61.

Crosier, S. J., M. F. Goodchild, L. L. Hill & T. R. Smith, 2003. Developing an infrastructure for sharing environmental models. Environment and Planning B: Planning and Design 30: 487–501.

Csilléry, K., M. G. B. Blum, O. E. Gaggiotti & O. François, 2010a. Approximate Bayesian Computation (ABC) in practice. Trends in Ecology & Evolution 25: 410–418.

Davidson, K., 1996. Modelling micobial food webs. Marine Ecology Progress Series 145: 279–296.

Dolan, J. R. & D. Wayne Coats, 1990. Seasonal abundances of planktonic ciliates and microflagellates in mesohaline Chesapeake Bay waters. Estuarine, Coastal and Shelf Science 31: 157–175.

Dowd, M., E. Jones & J. Parslow, 2014. A statistical overview and perspectives on data assimilation for marine biogeochemical models: Overview of marine biogeochemical data assimilation. Environmetrics 25: 203–213.

Edwards, A. M., 2001. Adding detritus to a nutrient-phytoplankton-zooplankton model: A dynamical-systems approach. Journal of Plankton Research 23: 389–413.

Feigenbaum, D. & M. Kelly, 1984. Changes in the lower Chesapeake Bay food chain in presence of the sea nettle *Chrysaora quinquecirrha*. Marine Ecology Progress Series 19: 39–47.

Franks, P. J. S., 2009. Planktonic ecosystem models: perplexing parameterizations and a failure to fail. Journal of Plankton Research 31: 1299–1306.

Gentleman, W., A. Leising, B. Frost, S. Strom & J. Murray, 2003. Functional responses for zooplankton feeding on multiple resources: a review of assumptions and biological dynamics. Deep Sea Research Part II: Topical Studies in Oceanography 50: 2847–2875.

Grimm, V., U. Berger, F. Bastiansen, S. Eliassen, V. Ginot, J. Giske, J. Goss-Custard, T. Grand, S. K. Heinz, G. Huse, A. Huth, J. U. Jepsen, C. Jørgensen, W. M. Mooij, B. Müller, G. Pe'er, C. Piou, S. F. Railsback, A. M. Robbins, M. M.

Robbins, E. Rossmanith, N. Rüger, E. Strand, S. Souissi, R. A. Stillman, R. Vabø, U. Visser & D. L. DeAngelis, 2006. A standard protocol for describing individual-based and agent-based models. Ecological Modelling 198: 115–126.

Hennig, C. & M. Kutlukaya, 2007. Some thoughts about the design of loss functions. REVSTAT - Statistical Journal 5: 19–39.

Hoch, R., T. Gabele,& J. Benz, 1998. Towards a standard for documentation of mathematical models in ecology. Ecological Modelling 113: 3–12.

Jakeman, A. J., R. A. Letcher & J. P. Norton, 2006. Ten iterative steps in development and evaluation of environmental models. Environmental Modelling & Software 21: 602–614.

Jorgensen, S. E. & B. D. Fath, 2011. Fundamentals of Ecological Modelling: Applications in Environmental Management and Research. Elsevier, Netherlands.

Journel, A. G., 1997. The abuse of principles in model building and the quest for objectivity. In Baafi, E. Y. & N.A. Schofield (eds), Geostatistics Wollongong `96. Kluwer Academic Publishers, Netherlands: 3–14.

Kawamiya, M., 2002. Numerical model approaches to address recent problems on pelagic ecosystems. Journal of Oceanography 58: 365–378.

Keller, D. P. & R. R. Hood, 2011. Modeling the seasonal autochthonous sources of dissolved organic carbon and nitrogen in the upper Chesapeake Bay. Ecological Modelling 222: 1139–1162.

Kennedy, M. C. & A. O'Hagan, 2001. Bayesian calibration of computer models. Journal of the Royal Statistical Society: Series B (Statistical Methodology) 63: 425–464.

Keohane, I. P., J. Tay, R. K. Gawde & R. R. Hood, 2019. Sensitivity of a biogeochemical model to the formulation of oyster filtration. Ecological Modelling 403: 70–84.

Kimmel, D. G., W. R. Boynton & M. R. Roman, 2012. Long-term decline in the calanoid copepod *Acartia tonsa* in central Chesapeake Bay, USA: An indirect effect of eutrophication? Estuarine, Coastal and Shelf Science 101: 76–85.

Leggett, R. W. & L. R. Williams, 1981. A reliability index for models. Ecological Modelling 13: 303–312.

Lignell, R., H. Haario, M. Laine & T. F. Thingstad, 2013. Getting the "right" parameter values for models of the pelagic microbial food web. Limnology and Oceanography 58: 301–313.

Lindeman, R., 1942. The trophic-dynamic aspect of ecology. Ecology 23: 399-417.

Lintusaari, J., M. U. Gutmann, R. Dutta, S. Kaski & J. Corander, 2016. Fundamentals and recent developments in approximate bayesian computation. Systematic Biology 66: 66-82.

Löptien, U., 2011. Steady states and sensitivities of commonly used pelagic ecosystem model components. Ecological Modelling 222: 1376–1386.

Martinez-Moyano, I. J., 2012. Documentation for model transparency. System Dynamics Review 28: 199–208.

Mitra, A., 2009. Are closure terms appropriate or necessary descriptors of zooplankton loss in nutrient–phytoplankton–zooplankton type models? Ecological Modelling 220: 611–620.

Mitra, A., C. Castellani, W. C. Gentleman, S. H. Jónasdóttir, K. J. Flynn, A. Bode, C. Halsband, P. Kuhn, P. Licandro, M. D. Agersted, A. Calbet, P. K. Lindeque, R. Koppelmann, E. F. Møller, A. Gislason, T. G. Nielsen & M. St. John, 2014. Bridging the gap between marine biogeochemical and fisheries sciences; configuring the zooplankton link. Progress in Oceanography 129: 176–199.

Officer, C. B., 1980. Box models revisited. In Hamilton, P. & K. B. Macdonald (eds), Estuarine and Wetland Processes. Springer, Boston: 65–114.

Oguz, T., H. W. Ducklow, J. E. Purcell & P. Malanotte-Rizzoli, 2001. Modeling the response of top-down control exerted by gelatinous carnivores on the Black Sea pelagic food web. Journal of Geophysical Research: Oceans 106: 4543–4564.

Olsen, E., G. Fay, S. Gaichas, R. Gamble, S. Lucey & J. S. Link, 2016. Ecosystem model skill assessment. Yes we can! PLoS One 11: e0146467.

Oreskes, N., K. Shrader-Frechette & K. Belitz, 1994. Verification, validation, and confirmation of numerical models in the earth sciences. Science 263: 641–646.

Pritchard, D. W., 1969. Dispersion and flushing of pollutants in estuaries. Journal of the Hydraulics Division 95: 115–124.

Purcell, J. E. & M. B. Decker, 2005. Effects of climate on relative predation by scyphomedusae and ctenophores on copepods in Chesapeake Bay during 1987-2000. Limnology and Oceanography 376–387.

Ravetz, J. R., 1997. Integrated environmental assessment forum: Developing guidelines for "good practice". Darmstadt University of Technology, ULYSSES Project.

Rothstein, L., J. Cullen, M. Abbott, E. Chassignet, K. Denman, S. Doney, H. Ducklow, K. Fennel, M. Follows, D. Haidvogel, E. Hofmann, D. Karl, J. Kindle, I. Lima, M. Maltrud, C. McClain, D. McGillicuddy, M. J. Olascoaga, Y. Spitz, J. Wiggert & J. Yoder, 2006. Modeling ocean ecosystems: The PARADIGM program. Oceanography 19: 22–51.

Schartau, M., P. Wallhead, J. Hemmings, U. Löptien, I. Kriest, S. Krishna, B. A. Ward, T. Slawig & A. Oschlies, 2017. Reviews and syntheses: parameter identification in marine planktonic ecosystem modelling. Biogeosciences 14: 1647–1701.

Sisson, S. A., Y. Fan & M. Beaumont, 2018. Overview of ABC. In Sisson, S. A., Y. Fan & M. Beaumont (eds), Handbook of Approximate Bayesian Computation. CRC Press, Boca Raton: 3–54.

Soetaert, K. & P. M. J. Herman, 2009. A Practical Guide to Ecological Modelling: Using R as a Simulation Platform. Springer, Dordrecht.

Spitz, Y. H., J. R. Moisan & M. R. Abbott, 2001. Configuring an ecosystem model using data from the Bermuda Atlantic Time Series (BATS). Deep Sea Research Part II: Topical Studies in Oceanography 48: 1733–1768.

Steele, J. H. & E. W. Henderson, 1992. The role of predation in plankton models. Journal of Plankton Research 14: 157–172.

Steele, J. H. & E. W. Henderson, 1995. Predation control of plankton demography: III. Food chain control. ICES Journal of Marine Science: Journal du Conseil 52: 565–573.

Stow, C. A., J. Jolliff, D. J. McGillicuddy, S. C. Doney, J. I. Allen, M. A. M. Friedrichs, K. A. Rose & P. Wallhead, 2009. Skill assessment for coupled biological/physical models of marine systems. Journal of Marine Systems 76: 4–15.

Taucher, J. & A. Oschlies, 2011. Can we predict the direction of marine primary production change under global warming? Geophysical Research Letters 38: L02603, doi: 10.1029/2010GL045934

Testa, J. M., W. M. Kemp, W. R. Boynton & J. D. Hagy, 2008. Long-term changes in water quality and productivity in the Patuxent River Estuary: 1985 to 2003. Estuaries and Coasts 31: 1021–1037.

Tian, R. C., 2006. Toward standard parameterizations in marine biological modeling. Ecological Modelling 193: 363–386.

Toni, T., D. Welch, N. Strelkowa, A. Ipsen & M. P. H. Stumpf, 2009. Approximate bayesian computation scheme for parameter inference and model selection in dynamical systems. Journal of The Royal Society Interface 6: 187–202.

Vallino, J. J., 2000. Improving marine ecosystem models: Use of data assimilation and mesocosm experiments. Journal of Marine Research 58: 117–164.

Wolfswinkel, J. F., E. Furtmueller & C. P. M. Wilderom, 2013. Using grounded theory as a method for rigorously reviewing literature. European Journal of Information Systems 22: 45–55.

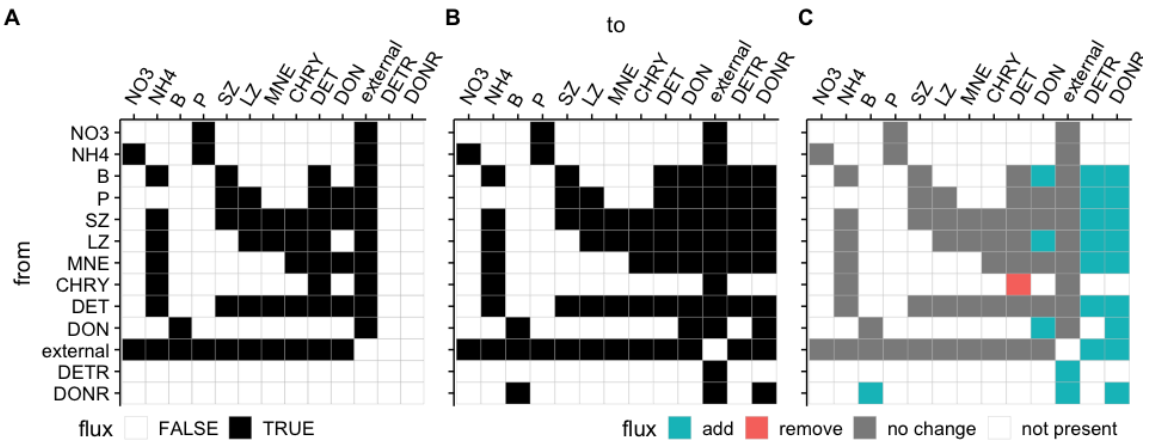

Fig. 3. 1 Visual adjacency matrices of the initial (left), final (middle), and difference between the two versions model of the summer mesohaline Chesapeake Bay planktonic food web, which includes gelatinous predators

Filled boxes represent the receivers (x axis) of flow from donors (y axis). Unfilled boxes represent no flow between the two compartments. The model currency is nitrogen (NO3, NH4) and contains four zooplankton (SZ, LZ, MNE, and CHRY) state variables, bacteria and two non-living organic compartments (DET, DON). The final version also includes refractory detritus and DON (DETR and DONR), which were added state variables that allowed this version to better capture observed zooplankton biomass than the initial version. "External" represents flows forcing into or outflow from the model domain

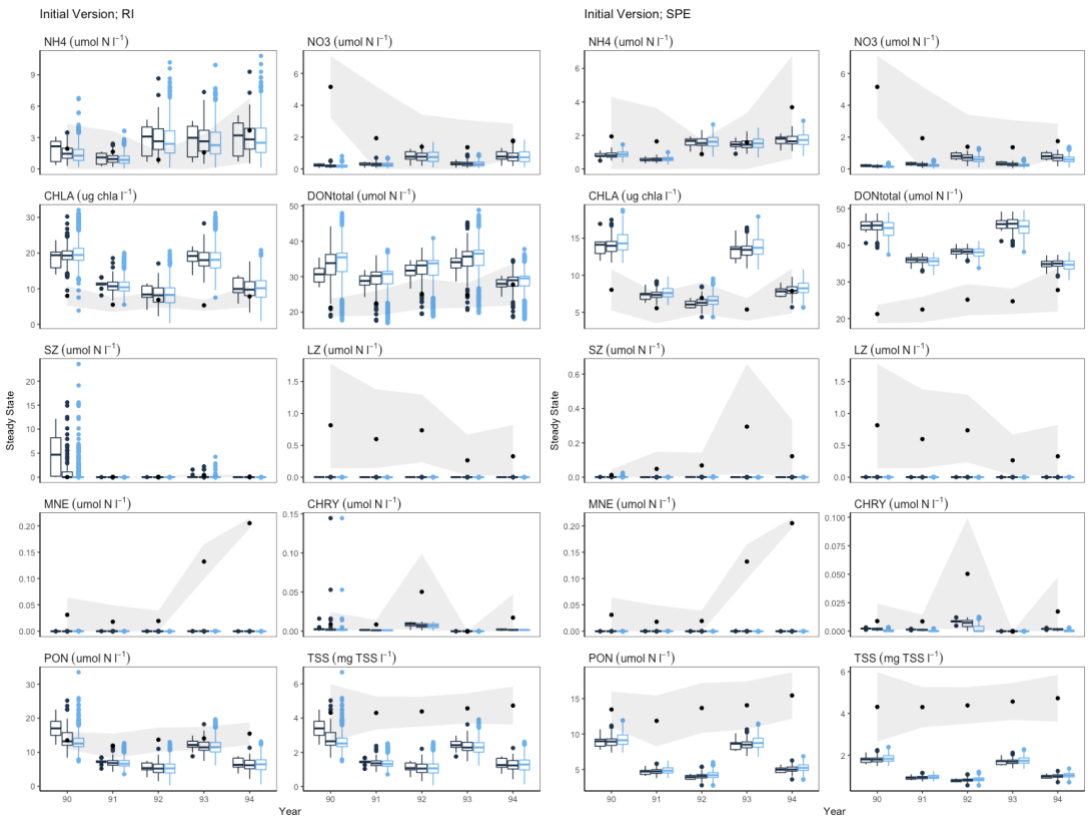

Fig. 3. 2 Steady state predictions (boxplots) from the initial version of the model using the Reliability Index (RI) and squared percentage error (SPE) as cost functions compared to the observations

The colors represent 10, 100, and 1000 accepted parameter sets for each of the cost functions. The observation mean is represented by the black point and the grey ribbon represents +/- 1 S.D. from the mean

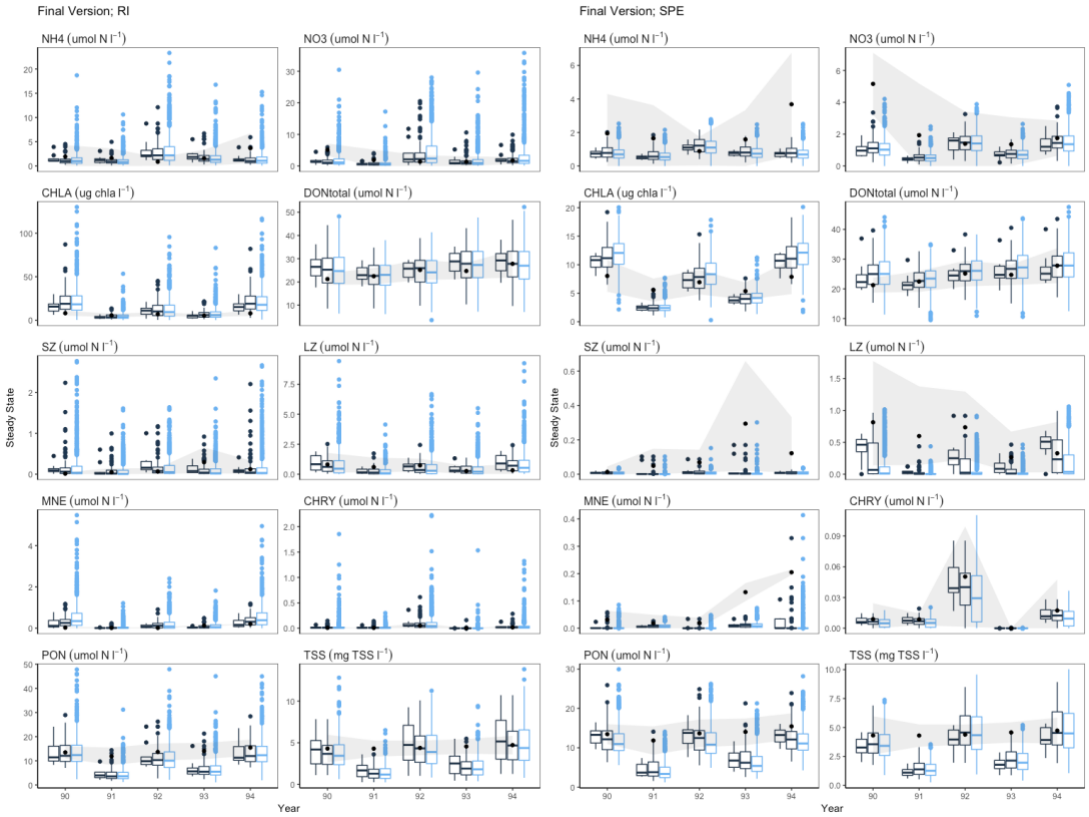

Fig. 3. 3 Steady state predictions (boxplots) from the final version of the model using the Reliability Index (RI) and squared percentage error (SPE) as cost functions compared to the observations

The colors represent 10, 100, and 1000 accepted parameter sets for each of the cost functions. The observation mean is represented by the black point and the grey ribbon represents +/- 1 S.D. from the mean

a

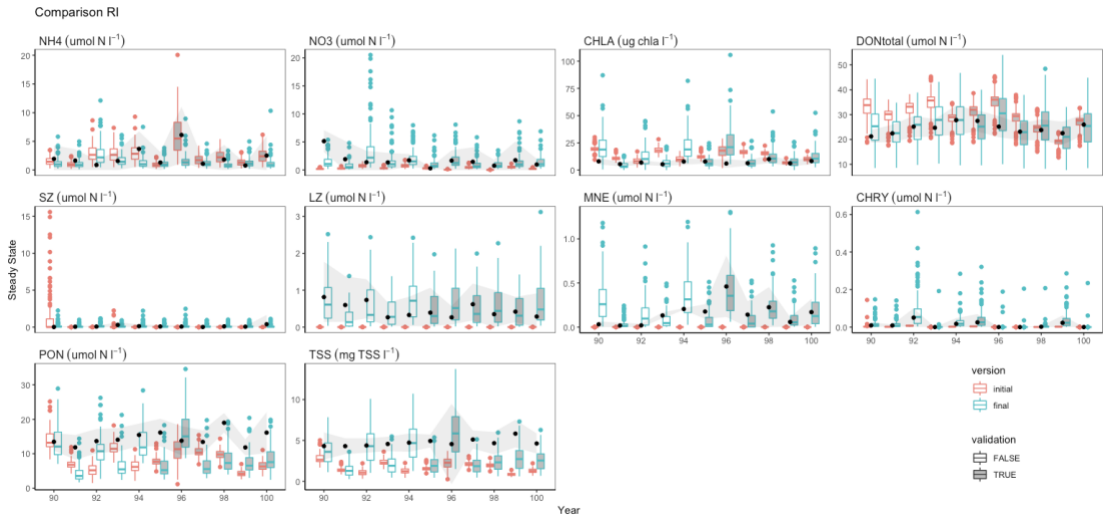

b

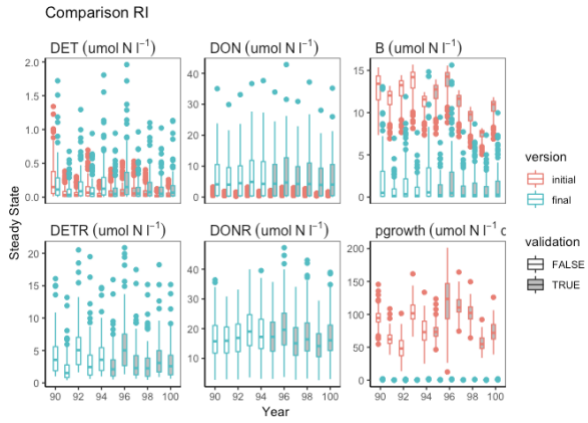

Fig. 3. 4 Comparison between the predictions of the first and final model versions (represented by color) for the variables with calibration observations (a) and those without (b).

The predictions are for the best 100 parameter sets selected by the Reliability Index (RI). The observation mean (in a) is represented by the black point and the grey ribbon represents +/- 1 S.D. from the mean. Boxplots with no fill were used in the

calibration stage and those with grey fill were used for model assessment only (validation = TRUE).

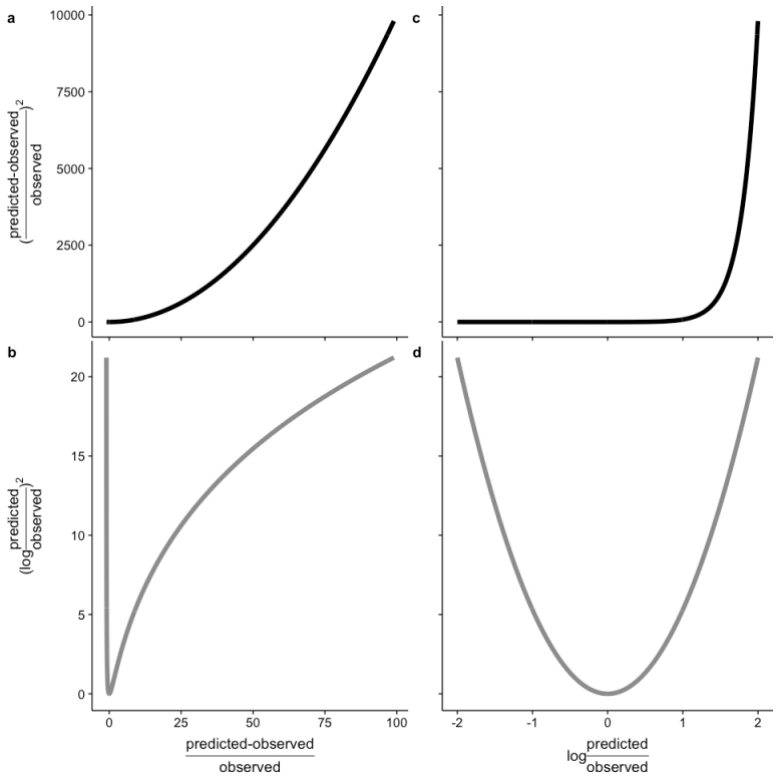

Fig. 3. 5 The cost (y-axis) for the squared percentage error (SPE; top) compared to the Reliability Index (RI; bottom).

The error (x-axis) is displayed in terms of difference (left) compared to the log ratio (right).

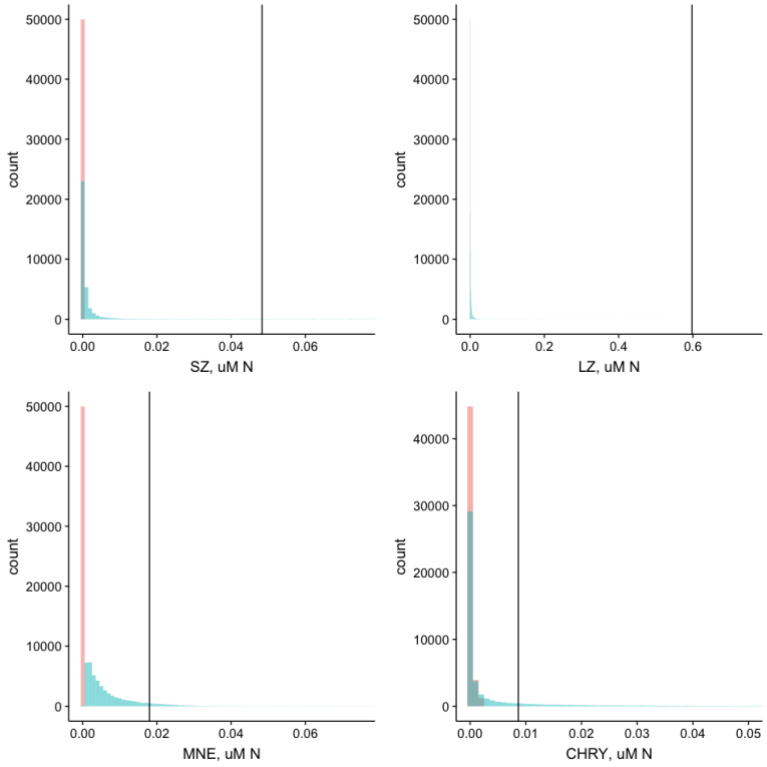

Fig. 3. 6 Histogram of steady state biomass results of the runs prior to rejection for the first (red) and final (blue) versions of the model

For ease of plotting, only 5% of 1e6 simulations for each model and the year 1991 are shown. The vertical black line represents the observed mean.

ODEs

$$\frac{\mathrm{dNO_3}}{\mathrm{dt}} = \mathrm{Nitrification} - \mathrm{No3\_uptake} + \mathrm{External_{NO_3}}$$

$$\frac{\mathrm{dNH_4}}{\mathrm{dt}} = \mathrm{Det\_remin_{nh4}} + \sum_{\mathrm{i}=1}^{\mathrm{N}} \mathrm{Excretion_i} - \mathrm{Nitrification} - \mathrm{Nh4\_uptake} + \mathrm{External_{NH_4}}$$

$$\frac{\mathrm{dP}}{\mathrm{dt}} = \sum_{\mathrm{i}} \mathrm{N\_uptake_i} - \sum_{\mathrm{j}} \mathrm{Grazing_{j,P}} - \mathrm{Mortality_P} - \mathrm{Exudation} + \mathrm{External_P}$$

$$\frac{\mathrm{dSV_i}}{\mathrm{dt}} = \sum_{\mathrm{j}} \mathrm{Growth_{i,j}} - \mathrm{Excretion_i} - \sum_{\mathrm{j}} \mathrm{Grazing_{j,i}} + \mathrm{External_i} \quad \text{,where i = B, SZ, LZ, MNE, or CHRY}$$

$$\frac{\mathrm{dD_i}}{\mathrm{dt}} = \sum_{\mathrm{k}} \sum_{\mathrm{j}} \mathrm{split_{j,i}} \cdot \mathrm{Egestion_{k,j}} + \sum_{\mathrm{j}} \mathrm{split_{j,i}} \cdot \mathrm{Mortality_j} + \mathrm{split_{i,P}} \cdot \mathrm{Exudation_P} + \mathrm{Det\_remin_i} - \sum_{\mathrm{j}} \mathrm{Grazing_{j,i}} - \delta_{\mathrm{i,DET}} \cdot \mathrm{Det\_remin} + \mathrm{External_i}$$

$$\frac{\mathrm{dISS}}{\mathrm{dt}} = \mathrm{External_{ISS}}$$

Zooplankton Terms

$$\mathrm{Excretion_i} = \begin{cases} excret\_rate_i \cdot \mathrm{SV_i} & \text{if i = B, SZ, LZ, MNE, or CHRY} \\ excret_i \cdot fish\_graze\_lz & \text{if i = Fish} \end{cases}$$

$$\mathrm{Mortality_i} = mort\_rate_i \cdot \mathrm{SV_i}$$

$$\mathrm{Grazing_{i,j}} = \begin{cases} \frac{pref_{i,j} \cdot graze\_rate_i \cdot \mathrm{SV_i} \cdot \mathrm{SV_j}}{\mathrm{Omega_i}} & \text{if i = SZ, LZ, MNE, or CHRY} \\ \frac{max\_fish\_pred \cdot \mathrm{LZ}}{\mathrm{LZ} + half\_sat_{Fish,LZ}} & \text{if i = Fish and j = LZ} \end{cases}$$

$$\mathrm{Omega_i} = \begin{cases} \sum_j pref_{i,j} \cdot \mathrm{SV_j} + half\_sat_{i,j} & \text{if i = B, SZ or LZ} \\ \sum_j pref_{i,j} & \text{if i = MNE or CHRY} \end{cases}$$

$$\mathrm{Growth_{i,j}} = assim_{i,j} \cdot \mathrm{Grazing_{i,j}}$$

$$\mathrm{Egestion_{i,j}} = (1 - assim_{i,j}) \cdot \mathrm{Grazing_{i,j}}$$

Other loss

$$\mathrm{External_i} = \mathrm{In_i} - \mathrm{Out_i} - \mathrm{Sinking_i} - \delta_{\mathrm{i,CHRY}} \cdot \mathrm{Mortality_{CHRY}}$$

$$\mathrm{In_i} = \begin{cases} qm_1 \cdot inflow_i + (qvm + evm) \cdot inflow_{i,bottom} & \\ chry\_inflowrate \cdot inflow_i & \text{if i = CHRY} \end{cases}$$

$$\mathrm{Out_i} = (qm + evm) \cdot \mathrm{SV_i}$$

$qvm = evm = 0$ for swimming state variables (SZ, LZ, MNE, CHRY)

$$\mathrm{Sinking_i} = \frac{sinking\_velocity_i}{depth} \cdot \mathrm{SV_i} \text{ for i = DET, DETR, P (and ISS)}$$

Phytoplankton terms

Uptake

$$\mathrm{N_i uptake} = \mathrm{primary\_production} \cdot \mathrm{n\_limitation_i}$$

$$\mathrm{primary\_production} = \frac{\mathrm{a} \cdot \mathrm{P}}{\mathrm{light\_atten}}$$

$$\mathrm{a} = \mathrm{maxgrowthrate_T} \cdot \frac{frac\_day\_sun}{depth} \cdot (\mathrm{plattsathy\_fn5(I_{star})} - \mathrm{plattsathy\_fn5}(\mathrm{I_{star}} e^{-\mathrm{lightatten} \cdot depth}))$$

$$\mathrm{maxgrowthrate_T} = Vp0 \cdot \log(2.00) \cdot 1.066^{temp}$$

$$\mathrm{light\_atten} = keb + a_{iss}(\mathrm{ISS}) + b_{oss}(\mathrm{OSS}) + c_{don}(\mathrm{DON} + \mathrm{DONR})$$

$$\mathrm{I_{star}} = I\_noon\_surf \cdot \frac{PhyIS}{Vp0}$$

$$\mathrm{PON} = \mathrm{P} + \mathrm{SZ} + \mathrm{SZ} + \mathrm{DET} + \mathrm{DETR}$$

$$\mathrm{OSS} = \frac{pon2oss \cdot \mathrm{PON} \cdot 12.00}{1000.00}$$

$$\mathrm{n\_limitation_{NH4}} = \frac{\mathrm{NH4}}{kNH4 + \mathrm{NH4}}$$

$$\mathrm{n\_limitation_{NO3}} = \frac{\mathrm{NO3}}{kNO3 + \mathrm{NO3}} \frac{1}{1 + \frac{\mathrm{NH4}}{kNH4}}$$

Photosynthesis integration (Edwards 1997)

$$\mathrm{plattsathy\_fn5(x)} = 0.61035 \cdot \mathrm{x} - 8.9251\mathrm{e}-02 \cdot \mathrm{x}^2 + 8.1477\mathrm{e}-03 \cdot \mathrm{x}^3 - 3.7427\mathrm{e}-04 \cdot \mathrm{x}^4 + 6.6103\mathrm{e}-06 \cdot \mathrm{x}^5$$

P loss terms

$$\mathrm{Exudation} = PhyEP \cdot \sum_{\mathrm{j}} \mathrm{Growth_{i,j}}$$

$$\mathrm{Mortality_P} = PhyMR \cdot \max(\mathrm{P} - PhyMin, 0)$$

Nutrient terms

$$\mathrm{Nitrification} = NitriR \cdot \mathrm{NH4}$$

$$\mathrm{Det\_remin} = \mathrm{remin_T} \cdot (detr \cdot \mathrm{DET})$$

$$\mathrm{remin_T} = \mathrm{e}^{0.086(temp - 30.0)}$$

$$\mathrm{Det\_remin_i} = \mathrm{split\_DET_i} \cdot \mathrm{Det\_remin}$$

Partition detritus remineralization into non-living pools

$$\mathrm{split\_DET_{NH4}} = split\_remin_{DET,labile} \cdot split\_remin_{DET,NH4}$$

$$\mathrm{split\_DET_{DON}} = split\_remin_{DET,labile} \cdot (1 - split\_remin_{DET,NH4})$$

$$\mathrm{split\_DET_{DETR}} = (1 - split\_remin_{DET,labile}) \cdot split\_remin_{DET,DETR}$$

$$\mathrm{split\_DET_{DONR}} = (1 - split\_remin_{DET,labile}) \cdot (1 - split\_remin_{DET,DETR})$$

Partition egestion, mortality into non-living pools

$$\text{split}_{\text{i,DET}} = split\_par_{i,solid} \cdot split\_par_{i\_solid,DET}$$

$$\text{split}_{\text{i,DETR}} = split\_par_{i,solid} \cdot (1 - split\_par_{i\_solid,DET})$$

$$\text{split}_{\text{i,DON}} = (1 - split\_par_{i,solid}) \cdot split\_par_{i\_dissolved,DON}$$

$$\text{split}_{\text{i,DONR}} = (1 - split\_par_{i,solid}) \cdot (1 - split\_par_{i\_dissolved,DON})$$

Table S 1 Parameter ranges used for calibration of the final version of the model.

The parameter names are given as in the body of the manuscript and the indexed names are to correspond to the notation in the ODEs in the supplemental materials

Parameter Names, indexed (equations)	Parameter Names (plots)	Minimum	Maximum	Reference	Units
NitriR	NitriR	1e-03	1e-01	Fennel et al. 2006	d^{-1}
Vp0	Vp0	1e-02	4	Harding et al. 1986, Fennel et al. 2006	d^{-1}
PhyIS	PhyIS	1e-02	1e-01	Harding et al. 1986, Fennel et al. 2006	$(Wm^{-2})^{-1}$ d^{-1}
kNO3	kNO3	2	10	Fisher et al. 1988	mmol N m^{-3}
kNH4	kNH4	2	10	Fisher et al. 1988	mmol N m^{-3}
PhyEP	PhyEP	1e-03	4e-01	Bronk et al. 1994	nd
PhyMR	PhyMR	1e-03	2e-01	Fennel et al. 2006	d^{-1}
PhyMin	PhyMin	1e-04	1e-02		mmol N m^{-3}
$graze\_rate_B$	maxBgraze	1e-01	4	Bronk et al. 1998 from urea uptake, and assuming 4uM of bacterial biomass	d^{-1}
$graze\_rate_{LZ}$	maxLZgraze	1e-01	2	Houde and Roman 1987, Stoecker and Egloff 1987, Kiorboe et al. 1985	d^{-1}
$graze\_rate_{SZ}$	maxSZgraze	1e-01	4	Gallegos 1989, Johnson et al. 2003, McManus and Ederington-Cantrell 1992	d^{-1}
$graze\_rate_{MNE}$	maxMNEgraze	1e-02	2	Kremer and Reeve 1989	m^3 (mmol $N)^{-1}$ d^{-1}
$graze\_rate_{CHRY}$	maxCHRYgraze	1e-02	2	Purcell 1992, Clifford and	m^3 (mmol

				Cargo 1978	$N)^{-1}$ d^{-1}
fish_graze_lz	maxFISHpred	1e-02	1	Wang and Houde 1995	mmol N m^{-3} d^{-1}
$pref_{B,DONR}$	bprefdonr	0	1e-02	max constrained	nd
$pref_{LZ,SZ}$	lzprefsz	1e-01	1	max constrained	nd
$pref_{LZ,LZ}$	lzpreflz	1e-01	1	max constrained	nd
$pref_{LZ,DET}$	lzprefdet	1e-01	1	max constrained	nd
$pref_{SZ,B}$	szprefb	1e-01	1	max constrained	nd
$pref_{SZ,P}$	szprefp	1e-01	1	max constrained	nd
$pref_{SZ,SZ}$	szprefsz	1e-01	1	max constrained	nd
$pref_{SZ,DET}$	szprefdet	1e-01	1	max constrained	nd
$pref_{MNE,LZ}$	mnepreflz	1e-01	1	max constrained	nd
$pref_{MNE,SZ}$	mneprefsz	1e-01	1	max constrained	nd
$pref_{MNE,DET}$	mneprefdet	1e-01	1	max constrained	nd
$pref_{CHRY,LZ}$	chrypreflz	1e-01	1	max constrained	nd
$pref_{CHRY,SZ}$	chryprefsz	1e-01	1	max constrained	nd
$pref_{CHRY,MNE}$	chryprefmne	1e-01	1	max constrained	nd
$pref_{CHRY,DET}$	chryprefdet	1e-01	1	max constrained	nd
$assim_{B,i}$	bassim	1e-01	1	max constrained	nd
$assim_{SZ,living}$	szassim	1e-01	1	max constrained	nd
$assim_{MNE,living}$	mneassim	1e-01	1	max constrained	nd
$assim_{CHRY,living}$	chryassim	1e-01	1	max constrained	nd
$assim_{LZ,DET}$	szassimdet	0	1	max constrained	nd

$assim_{SZ,DET}$	lzassimdet	0	1	max constrained	nd
$assim_{MNE,DET}$	mneassimdet	0	1	max constrained	nd
$assim_{CHRY,DET}$	chryassimdet	0	1	max constrained	nd
$mort\_rate_{B}$	bmortrate	1e-02	1e-01		d^{-1}
$mort\_rate_{LZ}$	lzmortrate	1e-03	1e-01	Elliot and Tang 2011	d^{-1}
$mort\_rate_{SZ}$	szmortrate	1e-03	1e-01	based on lzmortrate and Oguz et al. 2001	d^{-1}
$mort\_rate_{MNE}$	mnemortrate	1e-03	1e-01	based on lzmortrate and Oguz et al. 2001	d^{-1}
$mort\_rate_{CHRY}$	chrymortrate	1e-03	1e-01	based on lzmortrate and Oguz et al. 2001	d^{-1}
$excret\_rate_{B}$	bexcretrate	1e-02	8	Glibert 1982	d^{-1}
$excret\_rate_{LZ}$	lzexcretrate	1e-02	5e-01	Kiorboe et al. 1985	d^{-1}
$excret\_rate_{SZ}$	szexcretrate	1e-02	8	Glibert 1982, Verity 1985, Sherr et al. 1983	d^{-1}
$excret\_rate_{MNE}$	mneexcretrate	1e-02	5e-01	Kremer and Reeve 1989	d^{-1}
$excret\_rate_{CHRY}$	chryexcretrate	1e-02	5e-01	Purcell 1992	d^{-1}
$excret_{Fish}$	splitfishpred2nh4	1e-01	7e-01	Luo and Brandt 1993, Fasham et al. 1990	nd
$half\_sat_{B,DON}$	bhalfsatgrazing	1e-01	10	based on szhalfsatgrazing	mmol N m^{-3}
$half\_sat_{B,DONR}$	bhalfsatgrazingdonr	1e-01	10	based on bhalfsatgrazing	mmol N m^{-3}
$half\_sat_{SZ,j}$	szhalfsatgrazing	1e-01	10	Chen et al. 2014	mmol N m^{-3}
				Steele and Henderson	

$half\_sat_{LZ,j}$	lzhalfsatgrazing	1e-01	5	1992, Kiorboe et al. 1985, Houde and Roman 1987	mmol N m^{-3}
$half\_sat_{Fish,LZ}$	fishhalfsatgrazing	1e-02	1	Politikos et al. 2011	mmol N m^{-3}
detrr	detrr	1e-02	8	based on bexcretrate, Fennel et al. 2006	d^{-1}
$split\_par_{i\_dissolved,DON}$	splitexmo2don	0	1	max constrained	nd
$split\_par_{i,solid}$	splitegmo2solid	0	1	max constrained	nd
$split\_par_{i\_solid,DET}$	splitegmosolid2lab	0	1	max constrained	nd
$split\_par_{i\_dissolved,DON}$	splitegmodis2lab	0	1	max constrained	nd
$split\_par_{DET,solid}$	splitegdet2solid	0	1	max constrained	nd
$split\_par_{DET\_solid,DET}$	splitegdetsolid2lab	0	1	max constrained	nd
$split\_par_{DET\_dissolved,DON}$	splitegdetdis2lab	0	1	max constrained	nd
$split\_remin_{DET,labile}$	splitdetremin2lab	0	1	max constrained	nd
$split\_remin_{DET\_labile,NH4}$	splitdetreminlab2nh4	0	1	max constrained	nd
$split\_remin_{DET\_refractory,DETR}$	splitdetreminr2detr	0	1	max constrained	nd
splitdonextracell2don	splitdonextracell2don	0	1	max constrained	nd
chry_inflowrate	chryinflowrate	1e-06	1		d^{-1}
cchla	cchla	15	50	Geider et al. 1997	g C: g CHLA
pon2oss	pon2oss	6.625	20	assume redfield and 1mgOSS:mgC; assume 8 molC:molN and 2.5OSS:mgC	(mmol C)(mg OSS) (mmol N) $^{-1}$ (mg C)$^{-1}$
keb	keb	1e-03	7e-01	Cerco and Meyers 2000	m^{-1}

a_iss	a_iss	1e-03	1	Cerco and Meyers 2000	$m^2\ g^{-1}$
b_oss	b_oss	1e-03	2e-01	Cerco and Meyers 2000	$m^2\ g^{-1}$
c_don	c_don	1e-03	2e-01		m^2 mmol N^{-1}
$sinking\_velocity_{ISS}$	ISSsinkingvelocity	1e-01	10	Fennel et al. 2006	$m\ d^{-1}$
$sinking\_velocity_{DET}$	detsinkingvelocity	1e-01	10	Fennel et al. 2006, Fasham et al. 1990	$m\ d^{-1}$
$sinking\_velocity_{DETR}$	detrsinkingvelocity	0	1	Fennel et al. 2006	$m\ d^{-1}$
$sinking\_velocity_{P}$	psinkingvelocity	0	1	Fennel et al. 2006	$m\ d^{-1}$
splitdetinflow2det	splitdetinflow2det	0	1	max constrained	nd
splitDONinflow1	splitDONinflow1	0	1	max constrained	nd
splitDONinflow2	splitDONinflow2	0	1	max constrained	nd

References

Bronk, D. A., P. M. Glibert, T. C. Malone, S. Banahan, & E. Sahlsten, 1998. Inorganic and organic nitrogen cycling in Chesapeake Bay: autotrophic versus heterotrophic processes and relationships to carbon flux. Aquatic Microbial Ecology 15: 177–189.

Bronk, D. A., P. M. Glibert, & B. B. Ward, 1994. Nitrogen uptake, dissolved organic nitrogen release, and new production. Science 265: 1843–1846.

Cerco, C. F., & M. Meyers, 2000. Tributary refinements to Chesapeake Bay model. Journal of Environmental Engineering 126: 164–174.

Chen, B., E. A. Laws, H. Liu, & B. Huang, 2014. Estimating microzooplankton grazing half-saturation constants from dilution experiments with nonlinear feeding kinetics. Limnology and Oceanography 59: 639–644.

Clifford, H. C., & D. G. Cargo, 1978. Feeding rates of the sea nettle, *Chrysaora quinquecirrha*, under laboratory conditions. Estuaries 1: 58–61.

Elliott, D., & K. Tang, 2011. Influence of carcass abundance on estimates of mortality and assessment of population dynamics in *Acartia tonsa*. Marine Ecology Progress Series 427: 1–12.

Fasham, M. J. R., H. W. Ducklow, & S. M. McKelvie, 1990. A nitrogen-based model of plankton dynamics in the oceanic mixed layer. Journal of Marine Research 48: 591–639.

Fennel, K., J. Wilkin, J. Levin, J. Moisan, J. O'Reilly, & D. Haidvogel, 2006. Nitrogen cycling in the Middle Atlantic Bight: Results from a three-dimensional model and implications for the North Atlantic nitrogen budget. Global Biogeochemical Cycles 20: GB3007.

Fisher, T. R., L. W. Harding, D. W. Stanley, L. G. Ward, & others, 1988. Phytoplankton, nutrients, and turbidity in the Chesapeake, Delaware, and Hudson estuaries. Estuarine, Coastal and Shelf Science 27: 61–93.

Gallegos, C. L., 1989. Microzooplankton grazing on phytoplankton in the Rhode River, Maryland: Nonlinear feeding kinetics. Marine Ecology Progress Series 57: 23–33.

Geider, R. J., H. L. MacIntyre, & T. M. Kana, 1997. Dynamic model of phytoplankton growth and acclimation: responses of the balanced growth rate and the chlorophyll a: carbon ratio to light, nutrient-limitation and temperature. Marine Ecology Progress Series 148: 187–200.

Glibert, P. M., 1982. Regional studies of daily, seasonal and size fraction variability in ammonium remineralization. Marine Biology 70: 209–222.

Harding, L. W., B. W. Meeson, & T. R. Fisher, 1986. Phytoplankton production in two east coast estuaries: photosynthesis-light functions and patterns of carbon assimilation in Chesapeake and Delaware Bays. Estuarine, Coastal and Shelf Science 23: 773–806.

Houde, S. E. L., & M. R. Roman, 1987. Effects of food quality on the functional ingestion response of the copepod *Acartia tonsa*. Marine Ecology Progress Series 40: 69–77.

Johnson, M. D., M. Rome, & D. K. Stoecker, 2003. Microzooplankton grazing on *Prorocentrum minimum* and *Karlodinium micrum* in Chesapeake Bay. Limnology and Oceanography 48: 238–248.

Kiørboe, T., F. Møhlenberg, & K. Hamburger, 1985. Bioenergetics of the planktonic copepod *Acartia tonsa*: relation between feeding, egg production and respiration, and composition of specific dynamic action. Marine Ecology Progress Series 26: 85–97.

Kremer, P., & M. R. Reeve, 1989. Growth dynamics of a ctenophore (*Mnemiopsis*) in relation to variable food supply. II. Carbon budgets and growth model. Journal of Plankton Research 11: 553–574.

Luo, J., & S. B. Brandt, 1993. Bay anchovy *Anchoa mitchilli* production and consumption in mid-Chesapeake Bay based on a bioenergetics model and acoustic measures of fish abundance. Marine Ecology Progress Series 98: 223–236.

McManus, G. B., & M. C. Ederington-Cantrell, 1992. Phytoplankton pigments and growth rates, and microzooplankton grazing in a large temperate estuary. Marine Ecology Progress Series 87: 77–85.

Oguz, T., H. W. Ducklow, J. E. Purcell, & P. Malanotte-Rizzoli, 2001. Modeling the response of top-down control exerted by gelatinous carnivores on the Black Sea pelagic food web. Journal of Geophysical Research: Oceans 106: 4543–4564.

Politikos, D. V., G. Triantafyllou, G. Petihakis, K. Tsiaras, S. Somarakis, S.-I. Ito, & B. A. Megrey, 2011. Application of a bioenergetics growth model for European anchovy (*Engraulis encrasicolus*) linked with a lower trophic level ecosystem model. Hydrobiologia 670: 141–163.

Purcell, J. E., 1992. Effects of predation by the scyphomedusan *Chrysaora quinquecirrha* on zooplankton populations in Chesapeake Bay, USA. Marine Ecology Progress Series 87: 65–65.

Sherr, B. F., E. B. Sherr, & T. Berman, 1983. Grazing, growth, and ammonium excretion rates of a heterotrophic microflagellate fed with four species of bacteria. Applied and Environmental Microbiology 45: 1196–1201.

Steele, J. H., & E. W. Henderson, 1992. The role of predation in plankton models. Journal of Plankton Research 14: 157–172.

Stoecker, D. K., & D. A. Egloff, 1987. Predation by *Acartia tonsa* Dana on planktonic ciliates and rotifers. Journal of Experimental Marine Biology and Ecology 110: 53–68.

Verity, P. G., 1985. Grazing, respiration, excretion, and growth rates of tintinnids. Limnology and Oceanography 30: 1268–1282.

Wang, S.-B., & E. D. Houde, 1995. Distribution, relative abundance, biomass and production of bay anchovy *Anchoa mitchilli* in the Chesapeake Bay. Marine Ecology Progress Series 27–38.

Chapter 4: Studying the trophic cascade concept in a model of the Chesapeake Bay planktonic ecosystem

Abstract

The trophic cascade, while an important concept in acknowledging the role of top predators, may not be actualized or may be dampened due to the complexity of ecosystems. A trophic cascade is hypothesized to occur in the planktonic ecosystem of the Chesapeake Bay, USA due to the loss of the gelatinous predator, *Chrysaora chesapeakei.* However, due to confounding factors, it is not clear that *C. chesapeakei* drives the changes observed in the lower food web. This study uses a 0-dimensional ecosystem model that contains representation of several zooplankton pools as well as bacteria and non-living organic matter. Perturbation experiments were conducted to study the effect of changing modeled *C. chesapeakei* (CHRY). Sensitivity experiments of the environmental and ecological parameters were conducted to understand the conditions that are important in driving the response. The change in CHRY had the potential to affect every state variable and throughflow but the response did not always conform to the trophic cascade concept and was highly dependent on the parameters. The parameters that were most important in varying the response were related to the energetics of the zooplankton and parameters related to alternative pathways of loss or gains of the state variables.

Introduction

The trophic cascade concept, although simple and having been in the ecological literature dating back to The Origin of Species, has important implications for understanding the controls on the structure and functioning of ecosystems (Hairston

et al., 1960; Pace et al., 1999; Paine, 1980; Terbough & Estes, 2010). Pressingly, the trophic cascade concept is of interest for fully understanding the ramifications of the loss of top predators (Terbough & Estes, 2010) as well as the suitability and effects of conservation efforts. In the quintessential trophic cascade, carnivores suppress herbivores, thus indirectly allowing plants to grow unimpeded by grazing (Hairston et al., 1960). The trophic cascade, as defined by early work from Hairston et al., 1960 and Carpenter et al., 1985, has two predictions that are of particular interest regarding cascading top-down control: first, that each trophic level of a food web is "inversely and directly related to trophic levels above and below it" (Brett & Goldman, 1997); second, that the control reaches down to primary producers. It should be noted that trophic cascades have not been well defined in the literature, often with different or vague usage (Polis et al., 2000; Ripple et al., 2016).

Although the trophic cascade concept is deeply ingrained in ecological thinking, "the extent and importance of trophic cascades in nature have been hotly debated" (Persson, 1999; Terbough & Estes, 2010). Some of the discussion questioned whether trophic cascades were a common ecological feature or a pattern relegated to certain, simplified systems that could be best represented by discrete trophic levels (e.g. lakes) (Polis et al., 2000; Polis & Strong, 1996). Currently, it is still not entirely clear what conditions result in a trophic cascade in nature (Persson, 1999; Power, 2000). The discussion has shifted to understanding the variables that control the strength of the trophic cascade (Power, 2000). The hypotheses include: resource

availability (productivity, nutrient availability), food webs that deviate from linear food chains (omnivory, recycling), predator and herbivore strength and efficiency, spatial heterogeneity (refugia for herbivores, external subsidy), and/or study duration (reviewed in Borer et al., 2005). Generally, there is conflicting evidence for the hypotheses and practically, many efforts at biomanipulation of predators using predictions from the trophic cascade concept have been unsuccessful, suggesting there is still work in order to fully understand the concept across systems

A trophic cascade has been hypothesized to have occurred in the Chesapeake Bay, USA (Testa et al., 2008), due to declines in populations of the gelatinous predator (Breitburg & Fulford, 2006), *Chrysaora chesapeakei* (the sea nettle), since the 1960s. Observations suggest the loss of the sea nettles releases predation pressure on the ctenophore, *Mnemiopsis leidyi*, which results in an undesirable ecosystem with low mesozooplankton (Feigenbaum & Kelly, 1994; Purcell & Decker, 2005) and high phytoplankton biomass (Kimmel et al., 2012; Testa et al., 2008). However, the Chesapeake Bay planktonic food web contains much complexity, with microzooplankton and microbial food webs. Therefore, it is not clear whether declines in the sea nettle and the trophic cascade are the actual cause of these changes in the lower food web as opposed to being caused by other confounding factors.

Trophic cascades, like all indirect effects, are complex to study and difficult to assess solely through experiment or observation. Mechanistic models are an ideal tool to look at the system holistically in order to manipulate the change in *C. chesapeakei* in

isolation to establish causal linkages. Therefore, this paper uses a 0-dimensional numerical ecosystem model to test the effect of changing *C. chesapeakei* on the Chesapeake Bay planktonic ecosystem. To understand the conditions of the response, we tested the effect under different predator forcing and environmental conditions, as well as ecosystem dynamics (differences in parameter choice).

Methods

To understand the effect of changes in the *Chrysaora* population in the Chesapeake pelagic ecosystem, *Chrysaora* press perturbation experiments (Bender et al., 1984) were conducted within a numerical ecosystem model. The model is of relatively high complexity, especially compared to previous theoretical work on trophic cascades (Oksanen et al., 1981; Pimm, 1979; Rosenzweig, 1973; Scheffer, 1991; Scheffer et al., 2000; Scheffer & Rinaldi, 2000), and was designed to represent the planktonic food web in the mesohaline region of the Chesapeake Bay for the summer. The nitrogen-based model contains 11 state variables, including four zooplankton compartments: small and large zooplankton (SZ and SZ, respectively) and two gelatinous predators, *Mnemiopsis* (MNE) and *Chrysaora* (CHRY). The model also contains inorganic nitrogen (NH4 and NO3) and labile and refractory organic detrital and dissolved pools (DET, DON, DETR and DONR). Additionally, there is a pool that represents free-living bacteria (B). The equations are fully described in Tay et al. (in prep), largely based on equations from Oguz et al. 2001, Keller and Hood 2011,

and Fasham et al. 1990. Physical processes are simply represented using a chemostat formulation to represent flow into and out of the mesohaline.

The perturbation experiments were conducted by holding environmental and ecological parameter values constant and only perturbing the value of the CHRY forcing by 1e-5 uM day^{-1}. Choosing to perturb the external CHRY forcing (as opposed to e.g. CHRY grazing rate) was based on the assumption that the differences in interannual *Chrysaora* populations are largely due environmental factors that affect their birth rate from the benthos (Calder, 1974; Cargo & King, 1990) and that *Chrysaora* may primarily reach the mainstem via transport from the tributaries (Breitberg & Burrell, 2014), which are external to the modeled region. Three metrics were calculated to describe the response of each state variable and throughflow to a change in CHRY for each perturbation experiment - the sign of the response (also referred to as the directional response) and two metrics of the magnitude of the response to a change in CHRY: $m_x = \frac{\Delta X}{\Delta\, CHRY}$, referred to as the slope and $m_{x,scaled} = \frac{CHRY}{X}\frac{\Delta X}{\Delta\, CHRY}$,, referred to as the scaled slope, where X represents a state variable or throughflow. To test the response under different conditions, the perturbation experiments were conducted for 5 levels of CHRY forcing, 11 years (1990-2000) of physical environmental conditions, and 100 parameter sets that were accepted to adequately describe the Chesapeake Bay pelagic ecosystem (Chapter 3) for a total of 5500 perturbation experiments.

In order to determine how the changes in state variables co-occurred for a given perturbation experiment, a machine learning algorithm, t-distributed Stochastic Neighbor Embedding (t-SNE), was used to visualize the responses of the MNE, LZ, SZ, and P for all of the experiments simultaneously. Additionally, to compare the response to that predicted by the trophic cascade concept, the direction of the response of the plankton state variables were grouped for each simulation (and this combined response is referred to as the "community response" or "CR" throughout this paper).

In order to understand the effect of individual environmental and ecological parameters on the ecosystem response to a change in CHRY, sensitivity experiments were performed. Each sensitivity experiment consisted of performing CHRY press perturbations at the base level of one parameter (base perturbation experiment) and at 50% increase or decrease of that given parameter (sensitivity perturbation experiment). For a given parameter, a set of sensitivity experiments were performed for 11 years, 100 parameter sets, and 1 CHRY forcing level in order to assess the sensitivity across a range of parameter and forcing combinations.

The difference between the base and sensitivity perturbation experiments were summarized to study the effect of the parameters on three responses: the change in the community response, the change in the directional response of each state variable, and the change in the magnitude of the response of each state variable. First, the

proportion of experiments that lead to a change in the CR due to the change in the parameter was calculated:

$$^{\Delta CR}\phi_j = \frac{\sum_{k=1}^{n_j} \Delta CR_{j,k}}{n_j},$$

where k is the index of the experiment for a total of n_j sensitivity experiments for parameter j and CRj, kis 1 if the community response changed and 0 if not.

Second, the proportion of the experiments that lead to a change in the directional response of each state variable due to the change in the parameter was calculated:

$$^{\Delta msign}\phi_{x,j} = \frac{\sum_{k=1}^{n_j} (sign(m_{x,j,k,sensitivity}) \; != sign(m_{x,j,k,base}))}{n_j}.$$

Additionally, the absolute change of the slope due to the change in the parameter was calculated:

$$| \Delta m_{x,j,k} | = | m_{x,j,k,sensitivity} - m_{x,j,k,base} |.$$

Both of the above metrics were also calculated for the scaled slope and follow the same form.

Thirdly, the proportion of experiments that lead to an increase in the absolute response of each state variable due to the change in the parameter (only for the sensitivity experiment in which the parameters were increased so as to not cancel out effects) was calculated:

$$^{increase}\phi_{x,j} = \frac{\sum_{k=1}^{n_j} (\Delta | m_{x,j,k} | > 0)}{n_j},$$

where

$$\Delta | m_{x,j,k} | = | m_{x,\ j,\ k,\ sensitivity} | - | m_{x,\ j,\ k,\ base} |$$

is the change in the absolute slope due to the change in the parameter j. Both of the above metrics were also calculated for the scaled slope and followed the same form.

Results

In order to determine the effect of changing *Chrysaora* biomass on the Chesapeake Bay ecosystem, 5500 perturbation experiments (increasing CHRY inflow) were run across 11 years, 5 levels of CHRY inflow, and 100 parameter sets. The direction of the response of every state variable and throughflow was variable, with the capacity to increase or decrease with an increase in CHRY depending on the conditions of the perturbation experiment (Fig. 4. 1). Some state variables and throughflows did not respond in some experiments, although this was less likely than an increase or decrease. State variables and throughflows mostly increased in a higher proportion of the experiments rather than decreased. The exception was MNE, NO3, and the throughflow through MNE, which decreased in a higher proportion of the experiments. NO3, SZ, and LZ were the state variables that were the least determined in that the experiments were split more evenly between increasing and

decreasing. Overall, the throughflows were generally more determined in their likelihood to increase than their respective state variable.

The magnitude of the response of each state variable, calculated as the absolute slope and absolute scaled slope, was variable, spanning several orders of magnitude for the suite of perturbation experiments (Fig. 4. 2). P and DONR had the largest absolute slopes of the state variables. The median and maximum absolute slopes were 0.79 and 114, respectively, for P and .95 and 117, respectively for DONR. DET had the smallest median and maximum absolute slopes of 2.5 e-03 and 17, respectively. However, MNE, LZ, and SZ had the largest absolute scaled slopes. The median and maximum absolute scaled slopes were 4.9e-3 and 51 for MNE, 2.4e-3 and 44 for LZ and 2.9e-3 and 11 for SZ. Assuming that there is linear change (which may not be completely appropriate), the absolute scaled slope can be interpreted as a percentage change: a 100% change in CHRY corresponds to between 0.49 to 5,100% change for MNE, 0.24 to 4,400% change for LZ, 0.29 to 1,100% change for SZ, and 0.17 to 2,000% change in P.

Similar to the biomass response, the magnitude change for each throughflow was also variable, depending on the perturbation experiment (Fig. 4. 2). NH4 and P throughflows had the largest median absolute slopes of 7.8e-2 and 8.1e-2, respectively. Whereas, LZ, DET, and SZ throughflows had the largest maximum absolute slope of all the throughflows (5.8, 2.9, and 1.8, respectively). The median absolute scaled slope was the largest for the throughflows through NH4 and LZ (2.6e-

3, 2.4e-3), corresponding to 0.26% and 0.24% change for a 100% change in CHRY. The largest maximum absolute scaled slope was the largest for the throughflows through MNE, LZ and SZ (51, 40, 10) corresponding to 5,100, 4,000, and 1,000 % for a 100% increase in CHRY.

In order to determine how the state variables co-varied, t-SNE was used to visualize the responses from all experiments simultaneously. The t-SNE did not reveal any clear clustering (Fig. 4. 3) and increases or decreases of one state variable did not correspond solely to an increase or decrease in another state variable (as would be predicted by the trophic cascade concept). Categorizing each response by the combined directional response of MNE, LZ, SZ, and P to the increase in CHRY resulted in 29 distinct "community responses" (CR; Fig. 4. 4). None of the CR resulted in no change for all of the state variables (i.e. CR of 0000). The CR realized in the most perturbation experiments were -+++, -+-+, ---+, --++, -++-. The t-SNE of the slopes suggested that the magnitude of the responses of the state variables were not related. For example, it was possible for P to respond strongly in experiments in which there was apparently small change in the MNE, LZ and SZ. However, the t-SNE of the scaled slopes suggested that the magnitude of the scaled responses were related (Fig. 4. 3). The proportional response of all the state variables tended to be strong in the same experiments.

Given the variability in the responses, sensitivity experiments were conducted to determine the effect of each ecological and environmental parameter on the response

of the individual state variables and the community response. All of the parameters had the capability to change the community response (e.g. change the direction of at least one state variable in at least one sensitivity experiment; Fig. 4. 5). Changes in the zooplankton maximum grazing, assimilation, and excretion rates, as well as grazing preferences caused a change in the CR in the highest proportion of their respective sensitivity experiments. e.g. Changing the maximum grazing parameter of LZ (maxLZgraze) changed the CR in 51% of the maxLZgraze sensitivity experiments. NO3 inflow, the most important of the environmental parameters, fish and phytoplankton-related parameters were of intermediate importance for changing the CR. Among the parameters of lowest importance, were parameters that affect refractory pools. Unexpectedly, CHRY assimilation of living and non -living food and CHRY mortality were among the least likely parameters to change the community response, changing the CR in less than 3% of their respective sensitivity experiments.

The capability of parameters to change the response was then determined for each state variable individually. MNE and LZ grazing and LZ assimilation were in the top 10 parameters for their capacity to change the direction of the response of MNE, LZ, SZ, and P to an increase in CHRY (Fig. 4. 6). Interestingly, these parameters also were in the top 10 parameters for changing the sign of all of the other model state variables. MNE excretion and SZ assimilation were also in the top 10 for MNE, LZ, SZ, and P. Largely, the parameters that were most likely to change the direction of

the MNE, LZ, SZ, and P were the parameters that elicited the strongest median response in those state variables. However, for other state variables, some parameters elicited strong change in the magnitude of the response but were not the most likely parameters to switch the sign of the response. LZ and SZ had the highest probability of switching signs in the sensitivity experiments, which corresponds to the high indeterminacy observed in the perturbation experiments.

In order to explore the effect of parameters on the strength of the response, the change in the absolute slopes were calculated. For the absolute slope, the parameters that elicited the most change in the magnitude of the response differed for each state variable, however, some general patterns emerged. The effect of CHRY on P, SZ, and MNE was reduced when the parameters that control the non-consumptive loss of each state variable was increased (e.g. p sinking, exudations, mortality, and excretion; Fig. 4. 7a). Additionally, the absolute slope was altered for SZ and LZ when their predators were altered. For LZ, increasing MNE grazing and assimilation could dampen the response of LZ to CHRY. Whereas, for SZ, increasing LZ natural mortality or fish predation could strengthen the response of SZ to CHRY.

The parameters that affected the absolute scaled slopes for MNE, LZ, SZ, and P were largely related to increasing CHRY biomass accumulation (Fig. 4. 7b). Increasing the value of parameters that increase CHRY (CHRY assimilation of living and non-living material and maximum grazing) led to stronger response in the plankton, whereas the increase of parameters that decrease CHRY (CHRY excretion and mortality rates)

resulted in a weaker response in the plankton. Furthermore, increased CHRY preference for detritus had the capability to reduce the response of the plankton to CHRY. Additionally, enhanced external nutrient or forcing had the capability to reduce the absolute scaled slope of the state variables to an increase in CHRY. Increases in both inorganic and organic nutrient sources, and inflow of P reduced the response of P. Similarly, increases in LZ and MNE forcing reduced the response of their respective state variables. Lastly, "cannibalism" parameters (LZ preference for LZ and SZ preference for SZ) were also important in dampening the response of the LZ and SZ, respectively, to CHRY.

Discussion

This paper used a 0-dimensional numerical ecosystem model to test the effect of changing modeled *C. chesapeakei* (CHRY) on the Chesapeake Bay planktonic ecosystem, with additional focus on the conditions that drive cascading responses. While complexity is thought to dampen trophic cascades (Polis et al., 2000; Polis & Strong, 1996), this work demonstrated that in a relatively complex ecosystem model, the change in CHRY had the potential to affect every state variable and throughflow (Fig. 4. 1). The change in CHRY had the largest proportional effect on MNE and the effect decreased down the food chain to P (Fig. 4. 2). This finding agrees with the "Bottom up-Top down hypothesis" which predicts that top-down forces are the strongest at the top of the food chain (Loreau, 2010; McQueen et al., 1986; McQueen et al., 1989; Persson, 1999). Additionally, it is well demonstrated that *Chrysaora spp.*

can affect zooplankton populations (Feigenbaum & Kelly, 1984; Purcell & Decker, 2005) and the results corroborate the finding that changing CHRY populations may affect P in the Chesapeake Bay (Testa et al., 2008), although the direction of the response is unclear.

The largest unscaled effect of changing CHRY was on DONR, P, and the throughflows through P and NH4 (Fig. 4. 2), which are ecosystem components that are not generally the primary focus of research related to top predators. As the largest storage pools, DONR and P have the capacity for the greatest change and may reflect a mechanism by which systems can be resilient to change. Previous work has found that *Chrysaora* and *Mnemiopsis* release high amounts of DOM (Condon et al., 2009; Condon et al., 2011) that shifts bacterial community composition (which is beyond the scope of this work). The increase of NH4 throughflow may be caused by the method used in this study of increasing CHRY through forcing. Indeed, predators have been noted as agents of nutrient transfer between spatially-separated systems (Schmitz et al., 2010; Vanni et al., 2006). Additionally, the increase in throughflow may represent a more general role of predators as maximizers of flow in ecosystems (Loreau, 1995). These effects on disparate parts of the ecosystem agree with the current understanding that top predators can have ramifying effects through food webs and that their role is broader than solely as "top-down" consumers (Terbough & Estes, 2010).

Although the change in CHRY could affect the plankton down to the level of phytoplankton, the response did not always align with that predicted by the trophic cascade concept (Fig. 4. 4), defined here as inverse relationships between adjacent trophic levels reaching phytoplankton (sensu Brett & Goldman, 1997; Carpenter et al., 1985; Hairston et al., 1960). While the second most frequent community response reflected mutualism between non-adjacent levels (-+-+), 28 other possible responses were also recorded. Our model contains a relatively high amount of ecological complexity, departing from the assumptions of the trophic cascade concept (HSS) and other trophic cascade models of simple 3-level chains (Pimm, 1979; Rosenzweig, 1973). More complex models that contain recycling, omnivory, and detrital subsidy (Attayde et al. 2010; Herendeen, 1995) have found similar responses - primarily that state variables could respond by either increasing or decreasing to perturbations in top predators. Complexity allows indirect effects to propagate along many different paths, leading to different responses than that predicted by one trophic chain. The great diversity in the system response underscores the problems with the trophic cascade concept (Polis et al., 2000; Polis & Strong, 1996).

Aside from model complexity, differences in parameter values alter the system's directional response to a change in the top predator. This highlights the result of previous work (Taucher & Oschlies, 2011; Yodzis, 1988) that the uncertainty in parameters leads to the inability to predict the direction that state variables will respond to a perturbation. While every ecological and environmental parameter had

the capacity to influence the community response to a change in CHRY inflow, the most important parameters were related to zooplankton growth and efficiency (MNE and LZ grazing, LZ and SZ assimilation, and MNE excretion; Fig. 4. 5). The importance of these parameters likely reflects the importance of the basic ecological principle of trophic efficiency (Hutchinson, 1941; Lindeman, 1942) in understanding how systems respond to changes in top predators (DeBruyn et al., 2007). These parameters influence the efficiency of the system to support top predators (Oksanen et al., 1981) as well as the paths of nutrient flow (Stibor et al., 2004). Additionally, LZ and SZ were the most sensitive of the state variables to parameter choice in the sensitivity experiments, suggesting they could be useful aggregate indicators of ecosystem function in modeling and observational studies (Dolbeth et al., 2012).

An array of other parameters were important in dictating the strength of the response of individual state variables to a change in CHRY. Parameters that affect CHRY biomass accumulation were important in modulating the proportional state variable response to CHRY (Fig. 4. 7b). CHRY biomass could be increased by increasing CHRY grazing or assimilation or by decreasing CHRY natural mortality or excretion. It is important to note that MNE and CHRY predation were modeled with linear functions, which may have allowed for particularly strong control over the system in this study and their classification as "keystone" predators in others (Libralato et al., 2006). The presence of keystone predators has been indicated as important for driving trophic cascades (Paine, 1980). Therefore, it is still an open

question whether other predators, with saturating functional responses, may stimulate the same community level effects (sensu Polis) as observed in this study.

The other suite of parameters that were important in modulating the state variable response to CHRY were those related to alternative pathways of loss or gains of the state variables. The unscaled response of P was strongly determined by non-grazing losses of P (e.g. increases in P sinking, P mortality or exudation would decrease the effect of CHRY on P; Fig. 4. 7a). Additionally, increasing self-cannibalism (lzpreflz and szprefsz) also reduced the effect of CHRY on LZ and SZ, respectively. Lzpreflz and szprefsz are parameters that simply parameterize food web complexity or diversity while retaining highly aggregated compartments and the result supports the idea that omnivory or complexity does dampen the magnitude of, but does not eliminate, top down control. The scaled responses of P, SZ, and MNE to a change in CHRY were dampened by external subsidy and nutrients, which is counter to theory (reviewed in Borer et al., 2005; Leroux & Loreau, 2008) but agrees with past experimental studies (Borer et al., 2005; Chase, 2003).

In conclusion, although complexity has called into question the importance of trophic cascades (Polis et al., 2000; Polis & Strong, 1996), this work demonstrates that changes in top gelatinous predators can still have effects that ramify through the food web. However, the great diversity in the system response underscores the problems with the simplicity of the trophic cascade concept. Both model complexity, which more closely reflects natural systems, as well as parameter uncertainty, which reflects

differences in process rate across and within systems, cause the system to respond in ways that are not readily predicted by the trophic cascade concept. Both complexity and uncertainty are challenges for ecologists making predictions as the earth undergoes large environmental change.

The results of this work suggest herbivore and predator energetics as well as alternate sources of loss and gains are important components in understanding the role of top predators (Borer et al., 2005; Shurin et al., 2002). It should be noted that the parameters that were deemed most important were dependent on the metric of change (direction, unscaled or scaled magnitude) and the state variable, highlighting the need for studies to clearly define their usage of the term "trophic cascade" (Polis et al., 2000; Ripple et al., 2016). This work highlights the need to include complexity and energetics in the development of new frameworks (Barbier & Loreau, 2019) to fully understand the trophic cascade and other patterns that emerge from perturbations through complex systems.

References

Attayde, J. L., E. H. van Nes, A. I. L. Araujo, G. Corso & M. Scheffer, 2010. Omnivory by planktivores stabilizes plankton dynamics, but may either promote or reduce algal biomass. Ecosystems 13: 410–420.

Barbier, M. & M. Loreau, 2019. Pyramids and cascades: A synthesis of food chain functioning and stability. Ecology Letters 22: 405–419.

Bender, E. A., T. J. Case & M. E. Gilpin, 1984. Perturbation experiments in community ecology: Theory and practice. Ecology 65: 1–13.

Borer, E.T., E.W. Seabloom, K.E. Anderson, C.A. Blanchette, B. Broitman, S.D. Cooper & B.S. Halpern, 2005. What determines the strength of a trophic cascade? Ecological Society of America 86: 528-537.

Breitburg, D. & R. Burrell, 2014. Predator-mediated landscape structure: seasonal patterns of spatial expansion and prey control by *Chrysaora quinquecirrha* and *Mnemiopsis leidyi.* Marine Ecology Progress Series 510: 183–200.

Breitburg, D. L. & R. S. Fulford, 2006. Oyster-sea nettle interdependence and altered control within the Chesapeake Bay ecosystem. Estuaries and Coasts 29: 776–784.

Brett, M. T. & C. R. Goldman, 1997. Consumer versus resource control in freshwater pelagic food webs. Science 275: 384–386.

Calder, D., 1974. Strobilation of the sea nettle, *Chrysaora quinquecirrha*, under field conditions. Biological Bulletin 146: 326–334.

Cargo, D. G. & D. R. King, 1990. Forecasting the abundance of the sea nettle, *Chrysaora quinquecirrha*, in the Chesapeake Bay. Estuaries 13: 486–491.

Carpenter, S. R., J. F. Kitchell & J. R. Hodgson, 1985. Cascading trophic interactions and lake productivity. BioScience 35: 634–639.

Chase, J. M., 2003. Strong and weak trophic cascades along a productivity gradient. Oikos 101: 187–195.

Condon, R. H., D. K. Steinberg & D. A. Bronk, 2009. Production of dissolved organic matter and inorganic nutrients by gelatinous zooplankton in the York River Estuary, Chesapeake Bay. Journal of Plankton Research 32: 153–170.

Condon, R.H., D. K. Steinberg, P.A. del Giorgio, T. C. Bouvier, D. A. Bronk, W. M. Graham & H.W. Ducklow, 2011. Jellyfish blooms result in a major microbial

respiratory sink of carbon in marine systems. Proceedings of the National Academy of Sciences 108: 10225–10230.

DeBruyn, A.M.H., K. S. McCann, J. C. Moore & D. R. Strong, 2006. An energetic framework for trophic control in Rooney. In N., K. S. McCann, & D. L. G. Noakes (eds), From Energetics to Ecosystems: The Dynamics and Structure of Ecological Systems. Springer, Netherlands: 65–85.

Dolbeth, M., M. Cusson, R. Sousa & M. A. Pardal, 2012. Secondary production as a tool for better understanding of aquatic ecosystems. Canadian Journal of Fisheries and Aquatic Sciences 69: 1230–1253.

Feigenbaum, D. & M. Kelly, 1984. Changes in the lower Chesapeake Bay food chain in presence of the sea nettle *Chrysaora quinquecirrha*. Marine Ecology Progress Series 19: 39–47.

Hairston, N.G., F.E. Smith & L.B. Slobodkin, 1960. Community structure, population control, and competition. The American Naturalist 94: 421–425.

Herendeen, R.A., 1995. A unified quantitative approach to trophic cascade and bottom-up: top-down hypotheses. Journal of Theoretical Biology 176: 13–26.

Kimmel, D. G., W. R. Boynton & M. R. Roman, 2012. Long-term decline in the calanoid copepod *Acartia tonsa* in central Chesapeake Bay, USA: An indirect effect of eutrophication? Estuarine, Coastal and Shelf Science 101: 76–85.

Leroux, S. J. & M. Loreau, 2008. Subsidy hypothesis and strength of trophic cascades across ecosystems: Subsidies and trophic cascades. Ecology Letters 11: 1147–1156.

Libralato, S., V. Christensen & D. Pauly, 2006. A method for identifying keystone species in food web models. Ecological Modelling 195: 153–171.

Lindeman, R., 1942. The trophic-dynamic aspect of ecology. Ecology 23: 399-417.

Loreau, M., 1995. Consumers as maximizers of matter and energy flow in ecosystems. The American Naturalist 145: 22–42.

Loreau, M., 2010. From populations to ecosystems: theoretical foundations for a new ecological synthesis. Princeton University Press, Princeton.

McQueen, D. J., M. R. S. Johannes, J. R. Post, T. J. Stewart & D. R. S. Lean, 1989. Bottom-up and top-down impacts on freshwater pelagic community structure. Ecological Monographs 59: 289–309.

McQueen, D. J., J. R. Post & E. L. Mills, 1986. Trophic relationships in freshwater pelagic ecosystems. Canadian Journal of Fisheries and Aquatic Sciences 43: 1571–1581.

Oksanen, L., S. D. Fretwell, J. Arruda & P. Niemela, 1981. Exploitation ecosystems in gradients of primary productivity. The American Naturalist 118: 240–261.

Pace, M. L., J. J. Cole, S. R. Carpenter & J. F. Kitchell, 1999. Trophic cascades revealed in diverse ecosystems. Trends in Ecology & Evolution 14: 483–488.

Paine, R. T., 1980. Food webs: Linkage, interaction strength and community infrastructure. Journal of Animal Ecology 49: 667–685.

Persson, L., 1999. Trophic cascades: Abiding heterogeneity and the trophic level concept at the end of the road. Oikos 85: 385.

Pimm, S. L., 1979. The structure of food webs. Theoretical Population Biology 16: 144–158.

Polis, G. A., A. L. Sears, G. R. Huxel, D. R. Strong & J. Maron, 2000. When is a trophic cascade a trophic cascade? Trends in Ecology & Evolution 15: 473–475.

Polis, G. A., & D. R. Strong, 1996. Food web complexity and community dynamics. The American Naturalist 147: 813–846.

Power, M. E., 2000. What enables trophic cascades? Commentary on Polis et al. Trends in Ecology and Evolution 15: 443–444.

Purcell, J. E., & M. B. Decker, 2005. Effects of climate on relative predation by scyphomedusae and ctenophores on copepods in Chesapeake Bay during 1987-2000. Limnology and Oceanography 50: 376–387.

Ripple, W. J., J. A. Estes, O. J. Schmitz, V. Constant, M. J. Kaylor, A. Lenz, J. L. Motley, K. E. Self, D. S. Taylor & C. Wolf, 2016. What is a trophic cascade? Trends in Ecology & Evolution 31: 842–849.

Rosenzweig, M. L., 1973. Evolution of the predator isocline. Evolution 27: 84–94.

Scheffer, M., 1991. Fish and nutrients interplay determines algal biomass: A minimal model. Oikos 62: 271.

Scheffer, M., & S. Rinaldi, 2000. Minimal models of top-down control of phytoplankton. Freshwater Biology 45: 265–283.

Scheffer, M., S. Rinaldi & Y. A. Kuznetsov, 2000. Effects of fish on plankton dynamics: a theoretical analysis. Canadian Journal of Fisheries and Aquatic Sciences 57: 1208-1219.

Schmitz, O. J., D. Hawlena & G. C. Trussell, 2010. Predator control of ecosystem nutrient dynamics: Predator control of ecosystem nutrient dynamics. Ecology Letters 13: 1199–1209.

Shurin, J. B., E. T. Borer, E. W. Seabloom, K. Anderson, C. A. Blanchette, B. Broitman, S. D. Cooper & B. S. Halpern, 2002. A cross-ecosystem comparison of the strength of trophic cascades: Strength of cascades. Ecology Letters 5: 785–791.

Stibor, H., O. Vadstein, S. Diehl, A. Gelzleichter, T. Hansen, F. Hantzsche, A. Katechakis, B. Lippert, K. Løseth, C. Peters, W. Roederer, M. Sandow, L. Sundt-Hansen & Y. Olsen, 2004. Copepods act as a switch between alternative trophic cascades in marine pelagic food webs: Trophic cascades in marine plankton. Ecology Letters 7: 321–328.

Taucher, J. & A. Oschlies, 2011. Can we predict the direction of marine primary production change under global warming? Geophysical Research Letters 38: L02603, doi: 10.1029/2010GL045934

Terborgh, J., & J. A. Estes (eds), 2010. Trophic cascades: predators, prey, and the changing dynamics of nature. Island Press, Washington DC.

Testa, J. M., W. M. Kemp, W. R. Boynton, & J. D. Hagy, 2008. Long-term changes in water quality and productivity in the Patuxent River Estuary: 1985 to 2003. Estuaries and Coasts 31: 1021–1037.

Vanni, M. J., A. M. Bowling, E. M. Dickman, R. S. Hale, K. A. Higgins, M. J. Horgan, L. B. Knoll, W. H. Renwick & R. A. Stein, 2006. Nutrient cycling by fish supports relatively more primary production as lake productivity increases. Ecology 87: 1696–1709.

Yodzis, P., 1988. The indeterminacy of ecological interactions as perceived through perturbation experiments. Ecology 69: 508–515.

Fig. 4. 1 Proportion of the simulated *Chrysaora* (CHRY) perturbation experiments in which each state variable (top panel) or throughflow (bottom panel) decreased (red), increased (teal) or had no response (grey) in response to increase in CHRY inflow

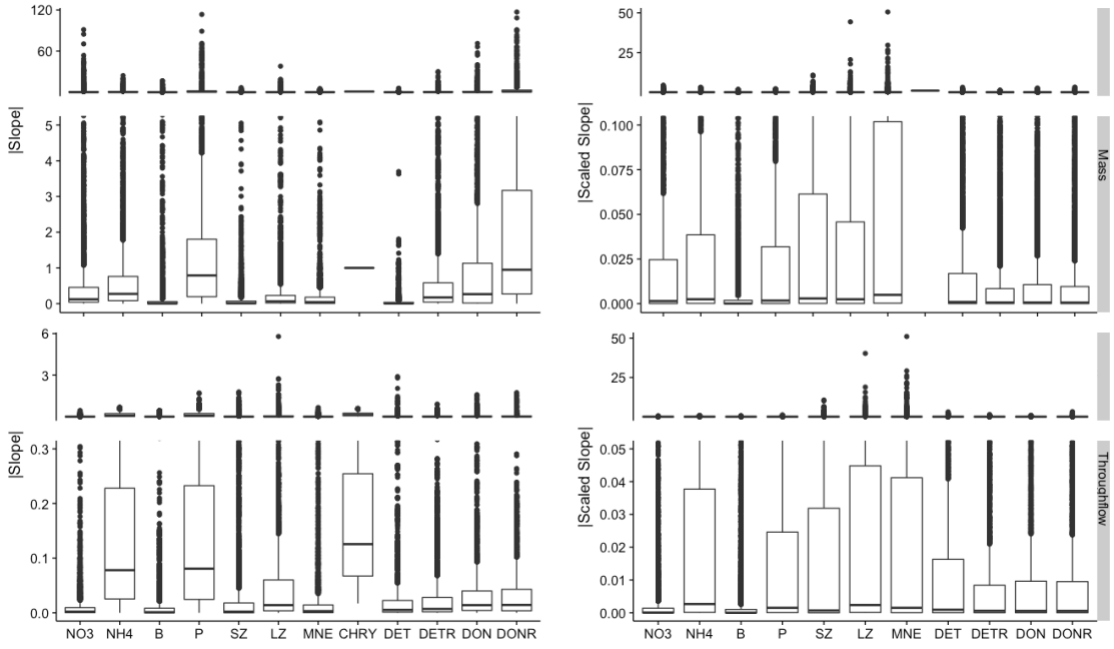

Fig. 4. 2 Absolute value of the response of each state variable (top panel) and throughflow (bottom panel) in response to increasing CHRY

Left column reports the absolute value of the slope and the right column reports the absolute value of the proportion slope. Note split axes and scale differences between panels.

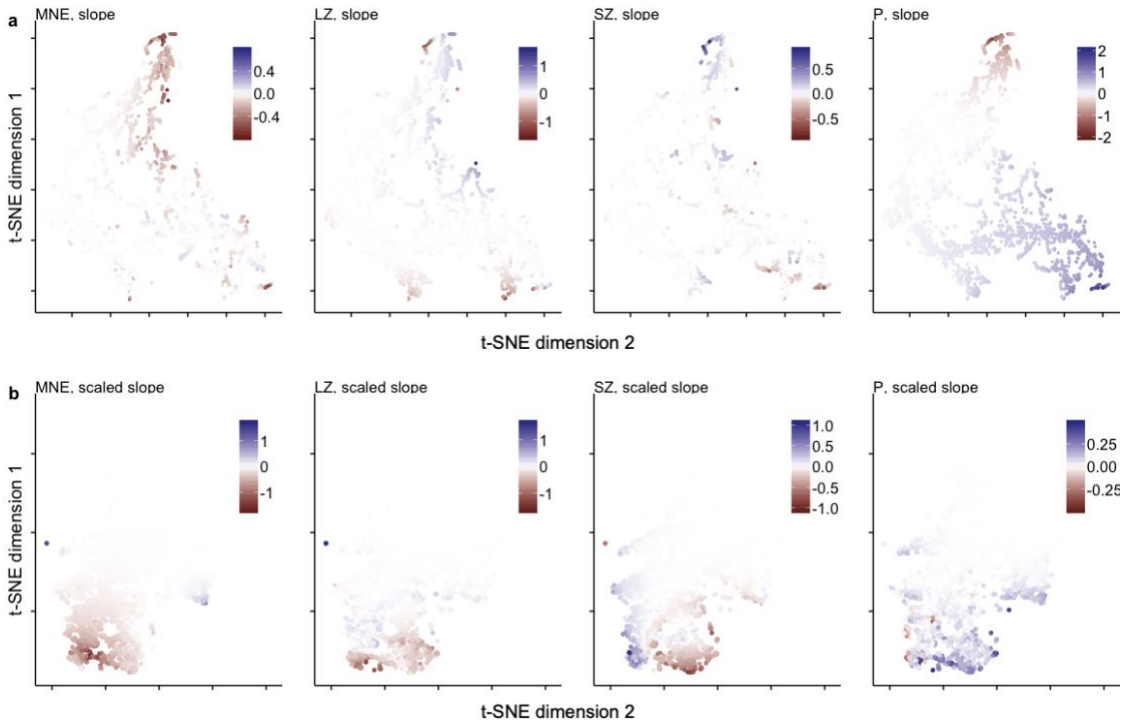

Fig. 4. 3 t-SNE visualization of the press perturbation experiments using the a) slope and b) scaled slope

Each panel reports the response of one state variable and each point represents the response for one perturbation experiment. The color represents the direction of the response of the state variable and the intensity of the color is the order of magnitude strength of the response. The axes have no meaning.

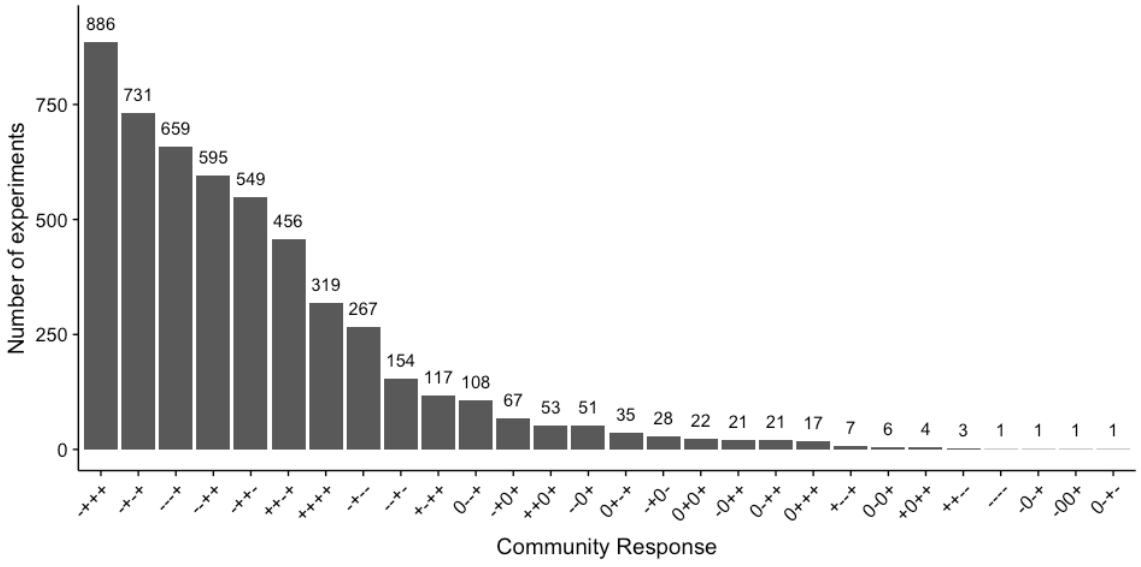

Fig. 4. 4 The number of simulated *Chrysaora* (CHRY) perturbation experiments that resulted in a given community response

The community response is defined as the combined directional response of MNE, LZ, SZ, and P in response to an increase in CHRY (e.g. ++++ represents that each state variable increased). Each experiment was run with a different set of environmental and ecological parameters.

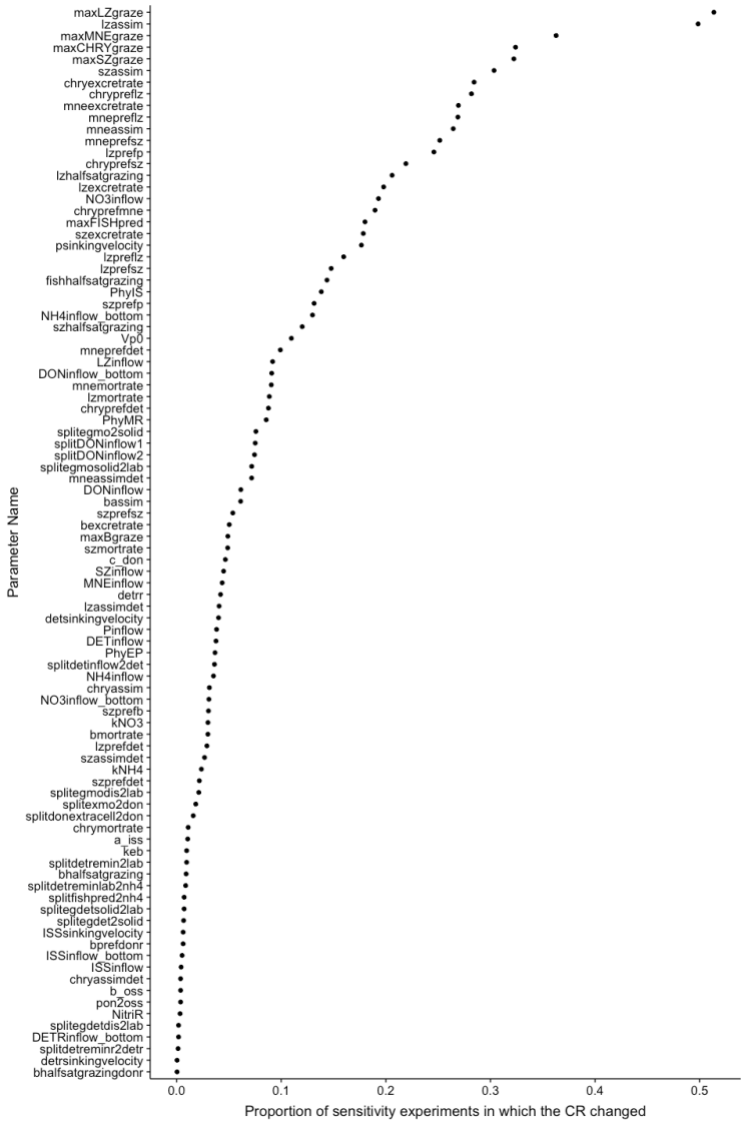

Fig. 4. 5 The proportion of sensitivity experiments in which the community response changed

The sensitivity experiments consisted of running simulated *Chrysaora (*CHRY) perturbation experiments for base levels of the given parameter and +/- 50% of that parameter for 11 years and 100 parameter sets. The community response is defined

as the combined directional response of MNE, LZ, SZ, and P in response to an increase in CHRY.

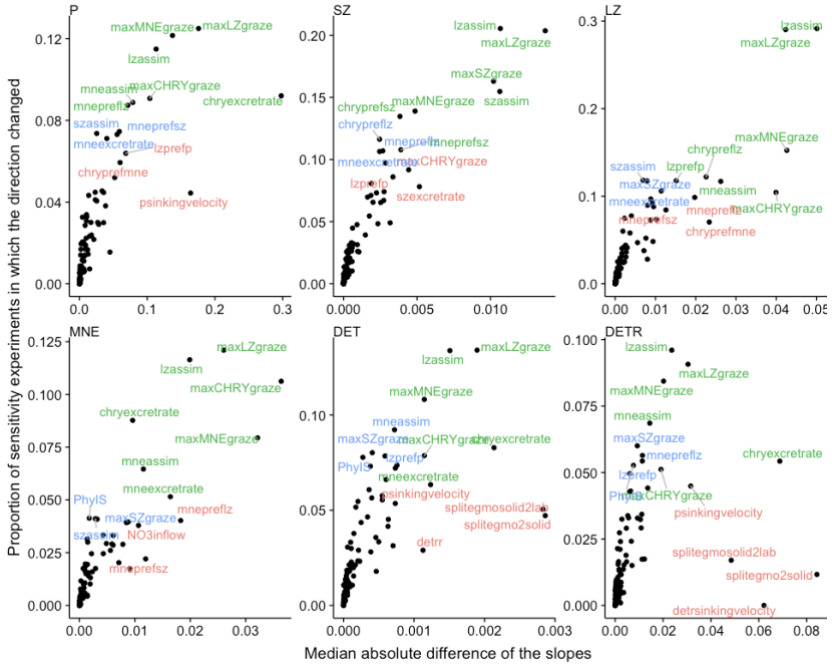

Fig. 4. 6 The proportion of experiments in which the directional response of a given state variable (panel) changed due to a change in the parameter versus the median of the absolute slopes

Each point represents the summary for the suite of sensitivity experiments for one parameter. Each panel represents one state variable. The 10 parameters that changed the highest proportion of experiments or with the greatest magnitude were labeled. Green, blue, and red denote that the parameter was in the top 10 parameters for its importance in changing both the proportion and magnitude, only the proportion, and only the magnitude, respectively.

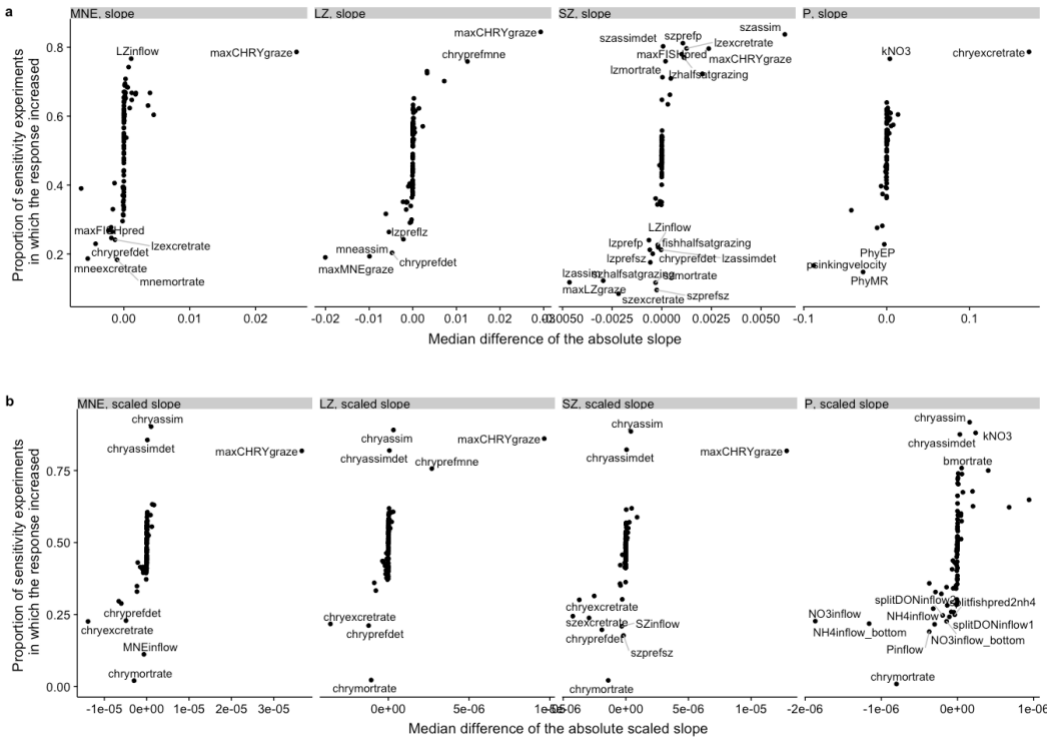

Fig. 4. 7 The proportion of sensitivity experiments that lead to an increase in the absolute a) slope and b) scaled slope when the parameter was increased by 50% versus the median value of the response

A proportion of 1 represents that all of the experiments resulted in an increase for a given state variable (panels), whereas 0 represents that all of the experiments led to a decrease in the magnitude of the response. The sensitivity experiments consisted of running simulated *Chrysaora (*CHRY) perturbation experiments for base levels of the given parameter and +/- 50% of that parameter for 11 years and 100 parameter sets. Parameters for which >= 75% of the experiments increased or decreased in the absolute response were labeled.

Chapter 5: Conclusion

The goals of this dissertation were to understand the previously undescribed high-frequency signal in a fixed-station, visual shore-based time series of *Chrysaora chesapeakei* (Chapter 2), to use a Bayesian data assimilation method to enhance objectivity in calibrating and formulating a mechanistic model to include jellyfish (Chapter 3), and using that model, to explore the trophic cascade concept triggered by jellyfish in the Chesapeake Bay (Chapter 4).

In Chapter 2, I analyzed a 4-year high-frequency time series of *C. chesapeakei* medusa counts collected using three sampling methods in the Choptank River, Chesapeake Bay. Medusae abundance was modeled by change points and was highly correlated between the sampling methods, suggesting that shore-based surveys are an inexpensive and effective method to collect information on jellyfish. The remaining signal was random, and indices of aggregation (fit to the Poisson distribution, Taylor's Power Law (TPL), and Morisita's Index) indicated that medusae were aggregated. TPL suggested that patches grew in the number of individuals as abundance increased. A simple conceptualization of where the time series sampled in space revealed that the upper bound of patch size was on the order of kilometers.

The finding that the high-frequency temporal variability reflects spatial patchiness of the sea nettles as they move into and out of the sampling region is not unexpected as many species of jellyfish exhibit patchiness at fine (1 to 10_2 m) to coarse (10_3-10_4 m) scales (reviewed in Hamner & Dawson, 2008). And while "spatial heterogeneity is scarcely a new or novel concept in ecology (Wiens, 2000)," there are still many

unknowns related to spatial patterns and the basic population ecology of *C. chesapeakei* (Shahrestani, 2018). As demonstrated in this study, understanding patchiness affects the ability to estimate abundance and to accurately detect demographic changes (Haury et al., 1978). Furthermore, patchiness has important implications for ecosystem dynamics as aggregations of organisms may have vastly different effects than predicted by their average abundance (reviewed in Wiens, 2000). Overall, this study suggests that more shore-based surveys, such as through a citizen science project, would help to gather more information on *C. chesapeakei*, which is needed to fully understand and predict the role of jellyfish in the Chesapeake Bay ecosystem.

In Chapter 3, I developed a 0-dimensional process-based model of the Chesapeake Bay mesohaline region that includes the additional complexity of jellyfish and the microbial food web. The ability to simulate zooplankton biomass was improved mainly by adding representation of refractory non-living organic materials, which is not generally included in aquatic ecosystem models. Although the purpose of this research was to develop this model, the main contribution of this chapter was in the use of a data assimilation method, Approximate Bayesian Computation (ABC - rejection method), to calibrate and guide the model's development. This more objective means of calibration highlighted inability for the model formulation to represent observations. However, the model error remaining after calibration was not solely due to inadequacies in model structure but also due to the cost function choice.

The dependence of the results of data assimilation on the cost function highlights the need for care when using cost functions. The Reliability Index (RI) chose parameters that resulted in better predictions than the squared percentage error (SPE). The RI is likely a more appropriate cost function, if calibrating over small-valued variables and/or if the uncertainty in the variables span orders of magnitude. However, in ABC, the outcome of the calibration is due the relationship between cost function and the prior parameter distribution, making it difficult to fully predict the appropriateness of a cost function. Some efforts have begun in automating the choice of cost functions (Fearnhead & Prangle, 2012). However, a simple and pragmatic recommendation is to apply different cost functions to determine the sensitivity to its choice in the calibration stage.

Besides the considerations related to calibration, this chapter underscores that other stages of the modeling process can benefit from continued improvements (Alexandrov et al., 2011; Jakeman et al., 2006). Further attention to the documentation of both model structure and the development processes would help researchers learn from and build on past work (Alexandrov et al., 2011; Benz et al., 2001; Benz & Knorrenschild, 1997; Crosier et al., 2003; Grimm et al., 2006; Hoch et al., 1998; Martinez-Moyano, 2012). Model documentation should focus on developing methods that are information rich, as well simple for developers to generate and for users to interpret. I suggest a visual adjacency matrix (Fig. 3. 1) to replace or supplement spaghetti or other network-like visualizations. The field may

also benefit from a central repository to store such model structures for ease of searching and comparison (Benz et al. 2001).

Documentation of the model development process is important for researchers to learn from the huge amount of currently undocumented expert knowledge but also for transparency. Generally, the models that are published are those that "work," so the many tested and rejected hypotheses are not available to the greater modeling community (Anderson & Mitra 2010; Franks, 2009). The form of such a development log may include the literature (models, experiments, and observations) reviewed, the processes (linkages or equations) or state variables that were tested, and the reasons features were or were not eventually incorporated into the model formulation. This documentation would help to save developers effort as well as to guide them in determining features that may be important in their models. Additionally, such documentation would improve transparency, allowing for assessment of the process by which a model is developed. Assessment of the process may be a more pragmatic means to assess model adequacy than testing of the final product (Ravetz, 1997, Jakeman et al., 2006).

Lastly, in Chapter 4, I used the model developed in the previous chapter, which represents several zooplankton pools as well as bacteria and non-living organic matter, to probe the trophic cascade concept. There has been much scientific debate regarding whether the trophic cascade is actualized due to the complexity of ecosystems, which would dampen top down effects. Simulation experiments

demonstrated that a change in modeled *C. chespeakei* (CHRY) had the potential to affect every state variable and throughflow, but that the response did not always conform to the trophic cascade concept. This finding demonstrates the importance of the trophic cascade concept in focusing attention on top predators (as opposed the historical focus on bottom-up processes), as well as, highlights that continued work is needed to more fully understand the roles of predators in structuring ecosystems.

This work contributes to that understanding by highlighting that the ecosystem response to a perturbation of the top predator was highly dependent on the ecological and environmental parameters. Every parameter could alter the response of the system, which may explain, in part, the confusion within the literature regarding the pervasiveness of the trophic cascade. That disparate features of the ecosystem can alter the system response emphasizes the importance of network and ecosystem perspectives. Analysis of static ecological networks have provided valuable insights into the importance of *C. chesapeakei* (Baird & Ulanowicz 1989), however, future work on a general understanding of how networks respond to perturbations is still needed (Barzel & Barabasi, 2013).

The most important parameters in altering the response of the ecosystem to the change in CHRY were those related to the energetics of the zooplankton and those related to loss or gains of state variables that were not related to the linear grazing food chain. Our findings largely agree with past work on the importance of herbivore and predator efficiency in generating strong cascading responses (Borer et al.,

2005). In fact, several new ideas have been proposed that frame the trophic cascade in a larger theory related to energetics (Barbier & Loreau, 2019; DeBruyn et al., 2007). However, because many ecological and environmental parameters were important in determining the response, combining energetics with the study of networks may be a fruitful path to more fully understanding how ecosystems respond to changes in top predators.

References

Alexandrov, G. A., D. Ames, G. Bellocchi, M. Bruen, N. Crout, M. Erechtchoukova, A. Hildebrandt, F. Hoffman, C. Jackisch, P. Khaiter, G. Mannina, T. Matsunaga, S. T. Purucker, M. Rivington & L. Samaniego, 2011. Technical assessment and evaluation of environmental models and software: Letter to the Editor. Environmental Modelling & Software 26: 328–336.

Anderson, T. R., & A. Mitra, 2010. Dysfunctionality in ecosystem models: An underrated pitfall?. Progress in Oceanography 84: 66–68.

Baird, D., & R. E. Ulanowicz, 1989. The Seasonal Dynamics of The Chesapeake Bay Ecosystem. Ecological Monographs 59: 329–364.

Barbier, M., & M. Loreau, 2019. Pyramids and cascades: a synthesis of food chain functioning and stability. Ecology Letters 22: 405–419.

Barzel, B., & A.-L. Barabási, 2013. Universality in network dynamics. Nature Physics 9: 673–681.

Benz, J., R. Hoch, & T. Legović, 2001. ECOBAS – modelling and documentation. Ecological Modelling 138: 3–15.

Benz, J. & M. Knorrenschild, 1997. Call for a common model documentation etiquette. Ecological Modelling 97: 141-143.

Borer, E.T., E.W. Seabloom, K.E. Anderson, C.A. Blanchette, B. Broitman, S.D. Cooper & B.S. Halpern, 2005. What determines the strength of a trophic cascade? Ecological Society of America 86: 528-537.

Crosier, S. J., M. F. Goodchild, L. L. Hill & T. R. Smith, 2003. Developing an infrastructure for sharing environmental models. Environment and Planning B: Planning and Design 30: 487–501.

DeBruyn, A. M. H., K. S. McCann, J. C. Moore & D. R. Strong, 2006. An energetic framework for trophic control in Rooney. In N., K. S. McCann, & D. L. G. Noakes (eds), From Energetics to Ecosystems: The Dynamics and Structure of Ecological Systems. Springer Netherlands: 65–85.

Fearnhead, P., & D. Prangle, 2012. Constructing summary statistics for approximate Bayesian computation: semi-automatic approximate Bayesian computation: Semi-automatic Approximate Bayesian Computation. Journal of the Royal Statistical Society: Series B (Statistical Methodology) 74: 419–474.

Franks, P. J. S., 2009. Planktonic ecosystem models: perplexing parameterizations and a failure to fail. Journal of Plankton Research 31: 1299–1306.

Grimm, V., U. Berger, F. Bastiansen, S. Eliassen, V. Ginot, J. Giske, J. Goss-Custard, T. Grand, S. K. Heinz, G. Huse, A. Huth, J. U. Jepsen, C. Jørgensen, W. M. Mooij, B. Müller, G. Pe'er, C. Piou, S. F. Railsback, A. M. Robbins, M. M. Robbins, E. Rossmanith, N. Rüger, E. Strand, S. Souissi, R. A. Stillman, R. Vabø, U. Visser & D. L. DeAngelis, 2006. A standard protocol for describing individual-based and agent-based models. Ecological Modelling 198: 115–126.

Hamner, W. M., & M. N. Dawson, 2008. A review and synthesis on the systematics and evolution of jellyfish blooms: advantageous aggregations and adaptive assemblages. Hydrobiologia 616: 161–191.

Haury, L. R., J. A. McGowan, & P. H. Wiebe, 1978. Patterns and processes in the time-space scales of plankton distributions spatial pattern in plankton communities. Plenum Press, N.Y.: 277–327.

Hoch, R., T. Gabele, & J. Benz, 1998. Towards a standard for documentation of mathematical models in ecology. Ecological Modelling 113: 3–12.

Jakeman, A. J., R. A. Letcher, & J. P. Norton, 2006. Ten iterative steps in development and evaluation of environmental models. Environmental Modelling & Software 21: 602–614.

Martinez-Moyano, I. J., 2012. Documentation for model transparency. System Dynamics Review 28: 199–208.

Ravetz, J.R., 1997. Integrated Environmental Assessment Forum: Developing Guidelines for ''Good Practice''. Darmstadt University of Technology, ULYSSES WP-97e1, ULYSSES Project.

Shahrestani, S., 2018. Spatial and temporal dynamics of the Chesapeake Bay sea nettle. Doctoral dissertation, University of Maryland, College Park, USA.

Wiens, J. A., 2000. Ecological heterogeneity: an ontogeny of concepts and approaches. In Hutchings, M.J., John, E.A. & A.J.A. Stewart (eds), The Ecological Consequences of Environmental Heterogeneity. Blackwell Science, Oxford: 9–31.